



## UvA-DARE (Digital Academic Repository)

### Multi-modality radiotherapy in cervical cancer

*Impact on the 3D dose distribution*

van Heerden, L.E.

**Publication date**

2019

**Document Version**

Final published version

**License**

Other

[Link to publication](#)

**Citation for published version (APA):**

van Heerden, L. E. (2019). *Multi-modality radiotherapy in cervical cancer: Impact on the 3D dose distribution*.

**General rights**

It is not permitted to download or to forward/distribute the text or part of it without the consent of the author(s) and/or copyright holder(s), other than for strictly personal, individual use, unless the work is under an open content license (like Creative Commons).

**Disclaimer/Complaints regulations**

If you believe that digital publication of certain material infringes any of your rights or (privacy) interests, please let the Library know, stating your reasons. In case of a legitimate complaint, the Library will make the material inaccessible and/or remove it from the website. Please Ask the Library: <https://uba.uva.nl/en/contact>, or a letter to: Library of the University of Amsterdam, Secretariat, Singel 425, 1012 WP Amsterdam, The Netherlands. You will be contacted as soon as possible.

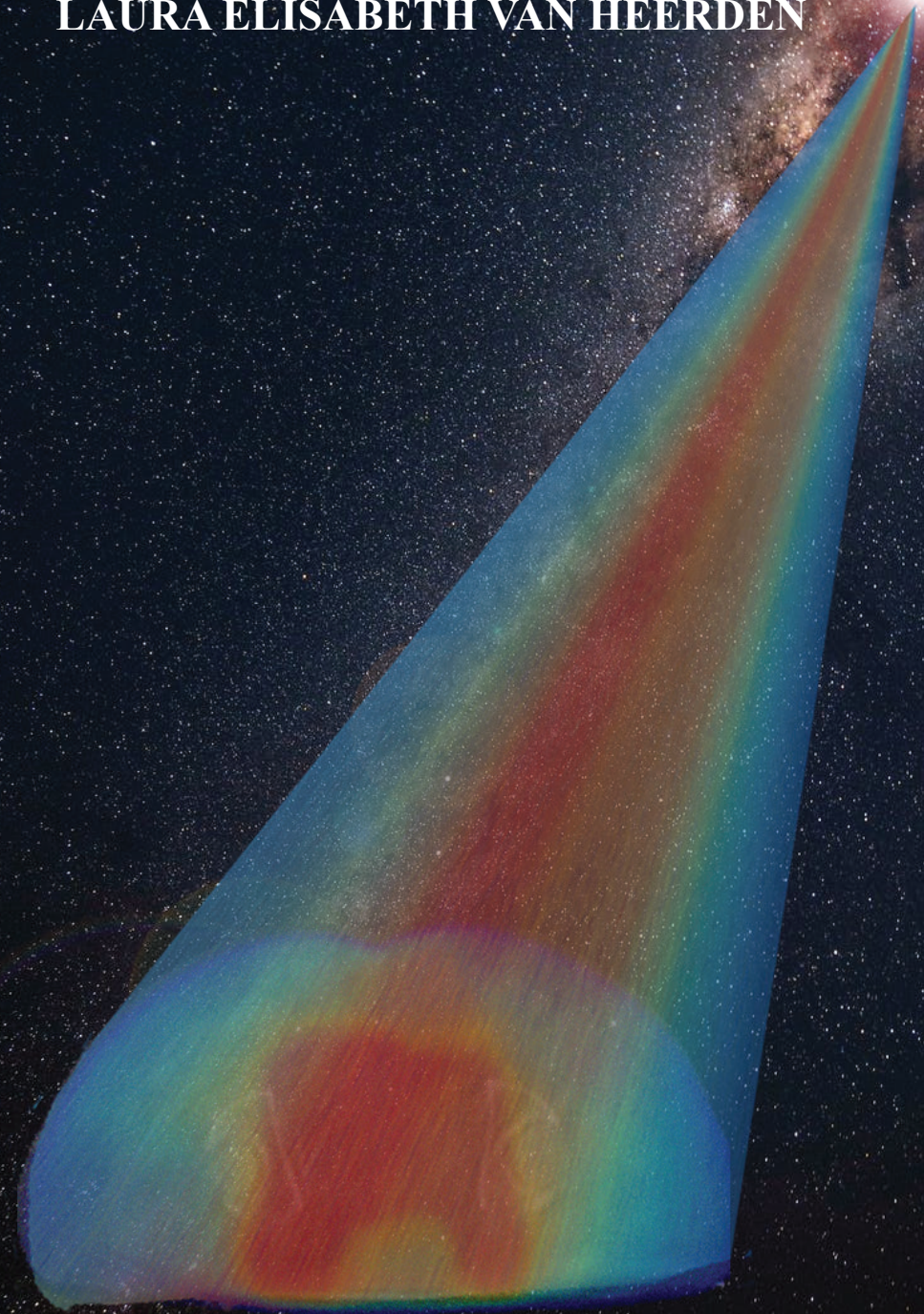


# MULTI-MODALITY RADIOTHERAPY IN CERVICAL CANCER: IMPACT ON THE 3D DOSE DISTRIBUTION

LAURA ELISABETH VAN HEERDEN

MULTI-MODALITY RADIOTHERAPY IN CERVICAL CANCER: IMPACT ON THE 3D DOSE DISTRIBUTION

LAURA ELISABETH VAN HEERDEN





Multi-modality radiotherapy in cervical cancer:  
impact on the 3D dose distribution

Laura Elisabeth van Heerden



Source image: Philippe Donn

Printed by: Ipskamp Printing B.V., Enschede

ISBN: 978-94-028-1518-4

© Copyright: Laura Elisabeth van Heerden, Amsterdam, 2019.

All rights reserved, no part of this thesis may be reproduced or transmitted in any form or by any means without permission of the author.



MULTI-MODALITY RADIOTHERAPY IN CERVICAL CANCER:  
IMPACT ON THE 3D DOSE DISTRIBUTION

ACADEMISCH PROEFSCHRIFT

ter verkrijging van de graad van doctor

aan de Universiteit van Amsterdam

op gezag van de Rector Magnificus

prof. dr. ir. K.I.J. Maex

ten overstaan van een door het College voor Promoties ingestelde commissie,

in het openbaar te verdedigen in de Agnietenkapel

op donderdag 6 juni 2019, te 12:00 uur

door Laura Elisabeth van Heerden

geboren te Amsterdam

**Promotiecommissie:**

Promotor(es)	prof. dr. C.R.N. Rasch	AMC-UvA
Copromotor(es):	dr. B.R. Pieters dr. A. Bel	AMC-UvA AMC-UvA
Overige leden:	prof. dr. L.J.A. Stalpers prof. dr. ir. A.J. Nederveen prof. dr. ir. J. Sonke dr. R.A. Nout dr. ir. I.K.K. Kolkman-Deurloo prof. dr. U.A. van der Heide	AMC-UvA AMC-UvA AMC-UvA Universiteit Leiden Erasmus Universiteit Rotterdam Universiteit Leiden
Faculteit der Geneeskunde		



# Multi-modality radiotherapy in cervical cancer: impact on the 3D dose distribution

## Table of contents

<b>Chapter 1</b>	General introduction	7
<b>Chapter 2</b>	Quantification of image distortions on the Utrecht interstitial CT/MR brachytherapy applicator at 3 T MRI	21
<b>Chapter 3</b>	Image distortions on the Utrecht Interstitial CT/MR brachytherapy applicator at 3 T MRI and their dosimetric impact	39
<b>Chapter 4</b>	Structure-based deformable image registration: added value for dose accumulation of external beam radiotherapy and brachytherapy in cervical cancer	57
<b>Chapter 5</b>	Role of deformable image registration for dose accumulation of adaptive external beam radiation therapy and brachytherapy in cervical cancer	75
<b>Chapter 6</b>	Dose warping uncertainties for the accumulated rectal wall dose in cervical cancer brachytherapy	95
<b>Chapter 7</b>	General discussion	113
<b>Summary</b>		125
<b>Samenvatting</b>		129
<b>Addendum</b>	List of publications	133
	PhD portfolio	135
	Curriculum vitae	140
	Dankwoord	141





# Chapter 1

General Introduction

## Cervical cancer

The uterine cervix is the lower part of the uterus (Fig. 1). The vaginal cavity and the uterine cavity are connected by the cervical canal, which is located between the bladder and rectum. For natural human fertilization, sperm must travel through the cervical canal to reach an egg cell after sexual intercourse.

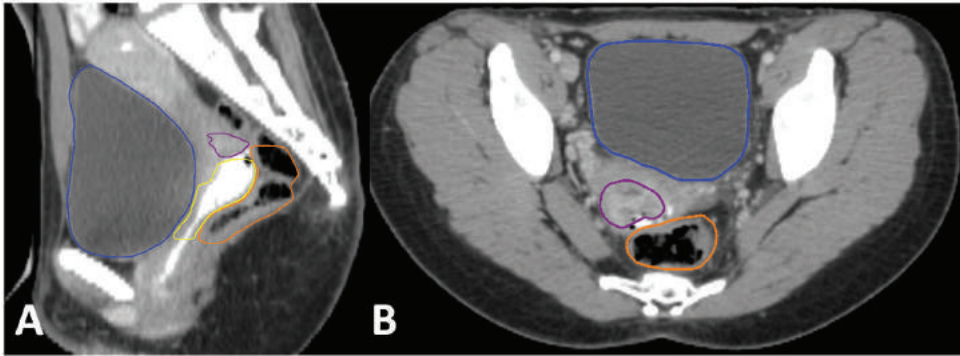


**Fig. 1** Sagittal (A) and transversal (B) computed tomography (CT) scan showing the anatomy of a cervical cancer patient with the cervix and tumor (purple), vagina (yellow), bladder (blue) and rectum (orange).

### *Epidemiology*

Cervical cancer is the fourth most common cancer in women with an estimated 528,000 new cases in 2012. Mortality was 266,000 worldwide in 2012. In the Netherlands cervical cancer is the sixth most common cancer with 708 new cases in 2015.<sup>1</sup>

The primary cause of cervical cancer is infection with the sexually-transmitted human papillomavirus (HPV). Although most infections do not lead to cancer, certain high-risk oncogenic HPV strains (HPV-16 and HPV-18) are responsible for 70% of HPV-caused cervical cancer cases.<sup>2</sup> The world health organization recommends cervical screening and HPV vaccination for women at a young age. In the Netherlands, preventative screening consists of cytology screening every 5 years for women between 30 and 60, and since 2011, HPV vaccination for girls at the age of 13. Smoking, long-term use of oral contraceptives, sexual intercourse at a young age and multiple sexual partners are also risk factors for cervical cancer.

In the last decades, treatment of cervical cancer has improved due to advancements in surgical methods, chemotherapy and radiotherapy delivery techniques. In high-income econ-



omy countries, the combination of therapeutic improvements, preventative screening and vaccination programs have led to decreased mortality.<sup>3</sup> The treatment protocol for cervical cancer varies per region, due to a disparity in available treatment options. In the Netherlands the three-year overall survival rate is 73%.<sup>1</sup> Less developed regions of the world such as India or Africa show lower survival rates.

Preventative screening and vaccination programs, which have contributed to increased survival, are also not offered in all countries. Globally, mortality due to cervical cancer varies from 2 in 100,000 in Western Europe to more than 20 per 100,000 in Africa. 85% of the new cases and 90% of the deaths occur in less developed countries.<sup>4</sup>

### ***Tumor staging***

Cervical cancer tumors are staged according to the staging system of the Federation of Gynaecology and Obstetrics (FIGO).<sup>5</sup> Tumor extent is evaluated with a physical examination by the physician to determine the clinical visibility and can be followed by imaging studies.<sup>6</sup> In the last decades, staging has benefited from improved imaging methods. Magnetic resonance imaging (MRI) provides superior soft-tissue contrast compared to other imaging methods such as ultrasound and computed tomography (CT). MR imaging is therefore better suitable to determine the tumor extent as well as parametrial infiltration and vaginal extension.<sup>7,8</sup> Lymph nodes and distal diseases can be evaluated with <sup>18</sup>F FDG positron emission tomography (PET)-CT scans. This technique combines CT imaging with PET to measure the uptake of the radionuclide 18-fluorodeoxyglucose (<sup>18</sup>F FDG).<sup>9</sup>

Tumors are discerned into early and locally advanced lesions. Early stage cervical tumors, classified as FIGO stage IB1 and IIA1, are clinically visible but limited to the cervix, or have a limited extension (tumor size <4 cm) outside the cervix, and no parametrial invasion. For locally advanced cervix carcinoma (FIGO stage IB2 and IIA2-IVA), the tumor is clinically visible and extending substantially (>4 cm) outside the cervix, or with an invasion into the parametria, lower third of the vagina, into the pelvic wall or the neighboring organs. If the cancer has spread to the lymph nodes and other distant organs, the cancer is classified as FIGO IVb.

### ***Treatment of cervical cancer***

For early stage tumors the treatment usually consists of surgical excision. Locally advanced carcinoma is treated with a combination of cisplatin chemotherapy and radiotherapy. Irradiation is delivered as external beam radiotherapy and complemented with a brachytherapy boost to the tumor area.<sup>10,11</sup> This thesis will focus on the radiotherapy for locally advanced cervical cancer.

## **Radiotherapy**

Radiotherapy is the delivery of radiation dose to a lesion, mostly to treat cancer. Lethal DNA damage is induced by the ionizing radiation to establish cell kill. For cervical cancer high-energy photons (1-25 MeV) are used. The treatment chain for radiotherapy consists of pre-treatment imaging, delineation of the target volumes and organs, treatment planning and radiation delivery in multiple treatment fractions. Imaging plays an important role. Treatment planning is based on the pretreatment imaging and on the delineations. For treatment delivery, image guidance techniques are used to verify the position of the patient and the resemblance of the daily anatomy to the anatomy on the planning image.

### ***External beam radiation treatment***

For external beam radiation therapy, the radiation is typically delivered by 23-28 daily fractions over a course of 5-6 weeks. Before the start of the radiation treatment, CT scans are acquired for treatment planning. On these scans the target regions and organs at risk (OARs) are delineated (Fig. 2, A). In cervical cancer, the target volume consists of the whole cervix and uterus. Organs at risk include the bladder, rectum, bowel and vagina.<sup>12</sup> Radiation oncologists have to increase the target volume with a margin to ensure that the tumor is sufficiently irradiated, in case of microscopic spread of the disease and geometric misalignment of the patient on the treatment device. As a consequence, tissue near the cervix may also be affected by the radiation leading to urinary, bowel and sexual problems. Based on the anatomy visible on the planning image, a treatment plan containing the treatment field positions and planned dose distribution (Fig. 2, B) is created using a treatment planning system. Considerations during treatment planning are obtaining sufficient tumor dose coverage and maximizing OAR sparing.

A linear accelerator (linac) is used to generate the radiation (Fig. 3). A cone beam computed tomography (CBCT) system is mounted on the linear accelerator. Before irradiation, steps are taken to verify the patient position. When the planning CT is acquired, three tattoos are placed on the skin with semi-permanent ink using lasers. In the treatment room, a laser system is attached in the same configuration as on the CT scanner to the linear accelerator and CBCT system. The gravitational center of the three markers, the patient isocenter, is aligned to that of the planning CT to achieve a reproducible treatment set-up. However, variation of the anatomy and target movement is substantial for cervical patients, due to bladder filling and gastrointestinal activity.<sup>13</sup> Therefore, while the patient is on the treatment table, CBCT scans are acquired to evaluate the anatomy on the day of treatment. At the Academic Medical Center (AMC) in Amsterdam, patients are treated using adaptive radia-

tion therapy to compensate for such daily target motion.<sup>14</sup> A library of plans fitting different target shapes and positions is created. Prior to irradiation the plan that best fits the anatomy of that day is selected based on the pretreatment CBCT.

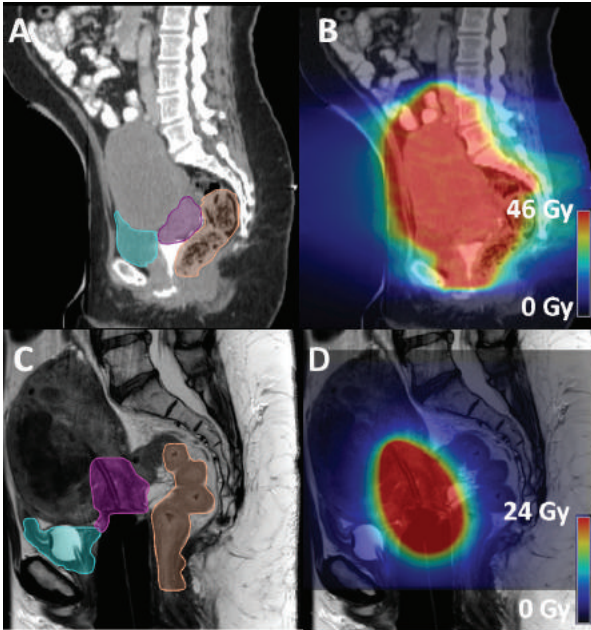


**Fig. 2.** A,C: Sagittal view of a patient CT (A) and MRI (C) used for EBRT (A) and brachytherapy (C) planning with the target (purple/pink), rectum (orange) and bladder (blue).

The brachytherapy planning MRI is acquired with the applicator in situ. B, D: color wash of the EBRT dose planned with volumetric arc therapy on the CT (B) and the planned brachytherapy dose on the MRI (D).

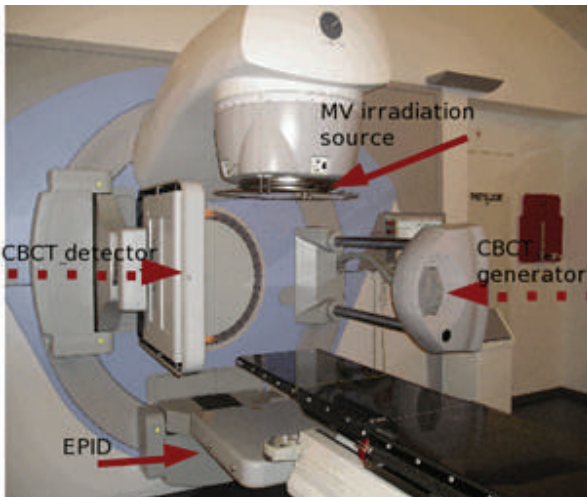


**Fig. 3** The Elekta Synergy® linear accelerator (Elekta, Crawley, UK) equipped with a (kV) Cone Beam CT (CBCT). Images of a patient (positioned on the black couch) can be obtained by the CBCT. Acquisition requires a gantry rotation (> 180°). The EPID (electronic portal imaging device) can be used to check the geometry and dose of the radiation beam.

### ***Brachytherapy***

In accordance with international guidelines, at our institute EBRT is followed by a brachytherapy boost to the tumor area in one or two applications. The patient is placed under full anesthesia with epidural regional anesthesia for postoperative pain control. The applicator used in this thesis is the Utrecht interstitial CT/MR applicator. The applicator is inserted under ultrasound guidance into the uterus, and if indicated interstitial needles are used to obtain a full coverage of the tumor or to lower the dose to the OARs. For dose delivery, the applicator is attached to the brachytherapy afterloader (Fig. 4), which is used to guide a radioactive source through the target volume. The source will move along the irradiation path in a stepwise manner. Dwell positions are defined where the stepping source will stop for a defined period of time (the dwell time).

Prior to brachytherapy delivery a planning MRI using a field strength of 1.0 T / 1.5 T is acquired and a brachytherapy delivery plan is created (Fig. 2 C, D).<sup>15,16</sup> The applicator geometry as it appears on the MRI scan is reconstructed. Target volumes at high, intermediate and low risk of recurrent disease are defined, as well as OAR such as the bladder and rectum. Optimization of the brachytherapy plan is performed manually by varying the dwell times to achieve sufficient tumor coverage and low OAR doses.

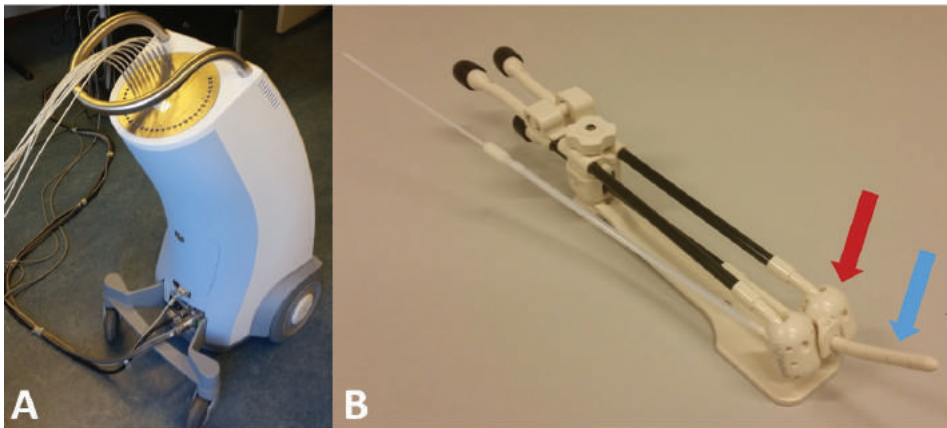


**Fig. 4** A) The remote Flexitron® afterloader system (Elekta Brachytherapy, Veenendaal, The Netherlands) used for brachytherapy delivery. B) The Utrecht brachytherapy applicator with the intrauterine device (blue arrow) and the ovoids (red arrow) and a plastic needle. The applicator can be attached to the afterloader using the transfer tubes.



At the AMC, the brachytherapy dose is delivered in 24 hours using Pulsed dose rate (PDR) brachytherapy in 1Gy pulses every hour with a high dose rate of 12Gy per hour or more. High-dose rate (HDR) brachytherapy, where the dose is delivered continuously, is also frequently used. PDR brachytherapy provides a radiobiological advantage in terms of late tissue effects over HDR brachytherapy. However, this has not been reflected by a difference in late radiation toxicities between the two techniques in clinical trials.<sup>17,18</sup> To calculate the total EBRT and brachytherapy (BT) dose, the physical dose (46 Gy for EBRT, 24 Gy for BT to the target) is converted to the radiobiologically equivalent dose in 2 Gy fractions ( $Gy_{EQD2}$ ) using the linear-quadratic model, and then summated. The total dose from both radiotherapy modalities to the target should be 85-90  $Gy_{EQD2}$ .<sup>19,20</sup>

### Challenges in multimodality radiotherapy for cervical cancer

For cervical cancer patients, the radiation treatment has proven to be highly effective, leading to improved long-term survival.<sup>21</sup> However, the radiation may cause damage to the healthy tissues, with the most common issues being late side effects of the bladder, rectum and bowel.<sup>22,23</sup> The main challenge in cervical cancer radiotherapy is therefore to reduce the total dose from EBRT and BT to organs at risk while maintaining a high tumor control.

Accurate calculation of the combined dose from EBRT and BT is vital to assess toxicity and tumor control. Yet, calculation of the total delivered dose from EBRT and BT is problematic, since there are many uncertainties in the estimated delivered dose distributions.<sup>15,24</sup> Sources of uncertainty in the delivered dose include delineation errors, organ motion, positioning errors and image distortions. At the start of the research documented in this thesis, standard practice was MR imaging at a field strength of 1.0 or 1.5 T. Higher field strength MRI offers increased signal to noise ratio. With the advent of 3 T MR imaging techniques, definition of the tumor volumes may become more accurate, thereby potentially minimizing OAR doses.<sup>25</sup> However, at higher field strengths image distortions due to main magnetic field inhomogeneity become larger, which may lead to differences between the planned and delivered dose distributions.

Another source of uncertainty in the delivered dose is the dose accumulation method. According to the recommendations of the International Commission on Radiation Units and Measurements (ICRU), it is necessary to calculate cumulative dose volume histogram (DVH) parameters of EBRT and multiple BT applications in  $Gy_{EQD2}$ .<sup>26</sup> Using their method, for OARs the assumption is that the same volume receives the highest dose from each BT application. For the cumulative OAR dose from EBRT and BT it is assumed that the EBRT dose near the BT boost is uniform and equal to the prescription dose. In EBRT, organs

are partly inside the target volume, due to a margin applied around the target volume to compensate for geometrical and delineation uncertainties. In current practice, this margin can be as large as 13 mm in the anterior-posterior direction,<sup>13</sup> but planned EBRT dose distributions are becoming increasingly conformal. It is therefore important to monitor the cumulative 3D dose distributions from EBRT and brachytherapy.

Moreover, at the time of brachytherapy planning, the delivered dose from EBRT and earlier BT applications may differ from the planned dose due to anatomical changes. For both brachytherapy and EBRT, there is considerable anatomical variation over the course of the treatment due to organ motion and, in the case of brachytherapy, the presence of the brachytherapy applicator. The applicator which is placed during brachytherapy will change the anatomy as compared to the anatomy during EBRT. Bladder filling has a large effect on the shape and the position of the target volume,<sup>27,28</sup> and therefore patients at the AMC are instructed to have a full bladder for each EBRT fraction. In practice, however, the bladder size varies over the whole EBRT treatment. Variation due to organ movement and applicator insertion is not taken into account when evaluating the combined effect of the total radiation treatment.

To account for anatomical changes, deformable image registration can be used to register images acquired at each step in the treatment. Deformable image registration is a method to find the deformation vector field that maps points in one (3D) image to the corresponding points in another (3D) image. The doses can be deformed with the resulting deformation vector field and subsequently summed to obtain the estimated cumulative 3D dose distribution. Estimation of the cumulative DVH parameters may be improved by calculating the 3D cumulative dose distribution delivered by EBRT and all BT applications using deformable image registration. However, deformable image registrations may suffer from low accuracy, for example in the case of large organ deformations. It is still unclear how uncertainties related to deformable image registration may impact the accumulated dose.<sup>29</sup>

### **Objective and outline of this thesis**

The topic of research of this thesis is the impact of uncertainties on the cumulative 3D dose distribution in multimodality radiotherapy for cervical cancer. Specifically, the dosimetric implications of imaging uncertainties and accumulation uncertainties will be addressed. We present multiple studies investigating the combined dose of external beam radiotherapy and brachytherapy, addressing the feasibility of brachytherapy planning at 3 T MRI, as well as the accuracy and clinical impact of dose accumulation with deformable image registration.

In the **second chapter** we present an MR-only method to quantify image distortions due to main magnetic field inhomogeneity at 3 T MRI on the brachytherapy applicator used in our institute for cervical cancer patients. Our measurements were performed in a phantom and in four patients. In the **third chapter**, we used the same method to quantify the image distortions for ten patients, as well as the dosimetric impact for the target, bladder and rectum. In **chapter 4**, the role of deformable image registration for the accumulated dose from EBRT is investigated, by accumulating the planned EBRT and brachytherapy dose. Since planned dose may vary from the delivered dose, in **chapter 5** the delivered EBRT dose is accumulated to the planned BT dose, to investigate if the delivered EBRT dose is uniform near the planned BT boost. **Chapter 6** describes uncertainties related to dose accumulation from multiple brachytherapy applications with deformable image registration. In the Discussion (**chapter 7**) we will discuss the dosimetric implications of imaging and accumulation uncertainties and consider possible future research. Finally, the work will be summarized in both English and Dutch in **chapter 8**.

## References

- [1] The Netherlands Cancer Registry <http://www.cijfersoverkanker.nl/> (accessed January 4, 2018).
- [2] Braaten KP, Laufer MR. Human Papillomavirus (HPV), HPV-Related Disease, and the HPV Vaccine. *Rev Obstet Gynecol* 2008;1:2–10.
- [3] LaVigne AW, Triedman SA, Randall TC, Trimble EL, Viswanathan AN. Cervical cancer in low and middle income countries: Addressing barriers to radiotherapy delivery. *Gynecol Oncol Reports* 2017;22:16–20.
- [4] Globocan 2012- Cancer fact sheets n.d. <http://globocan.iarc.fr/Default.aspx> (accessed January 4, 2018).
- [5] Denny L, Quinn M. FIGO Cancer Report 2015. *Int J Gynecol Obstet* 2015;131:S75.
- [6] Greco A, Mason P, Leung AW, Dische S, McIndoe GA, Anderson MC. Staging of carcinoma of the uterine cervix: MRI-surgical correlation. *Clin Radiol* 1989;40:401–5.
- [7] de Boer P, Adam JA, Buist MR, van de Vijver MJ, Rasch CR, Stoker J, et al. Role of MRI in detecting involvement of the uterine internal os in uterine cervical cancer: systematic review of diagnostic test accuracy. *Eur J Radiol* 2013;82:e422-8.
- [8] Kataoka M, Kido A, Koyama T, Isoda H, Umeoka S, Tamai K, et al. MRI of the female pelvis at 3T compared to 1.5T: Evaluation on high-resolution T2-weighted and HASTE images. *J Magn Reson Imaging* 2007;25:527–34.
- [9] Singh AK, Grigsby PW, Dehdashti F, Herzog TJ, Siegel BA. FDG-PET lymph node staging and survival of patients with FIGO stage IIIb cervical carcinoma. *Int J Radiat Oncol Biol Phys* 2003;56:489–93.
- [10] Al-Mansour Z, Verschraegen C. Locally advanced cervical cancer: what is the standard of care? *Curr Opin Oncol* 2010;22:503–12.
- [11] Bermudez A, Bhatla N, Leung E. Cancer of the cervix uteri. *Int J Gynaecol Obstet* 2015;131 Suppl:S88-95.
- [12] Lim K, Small W, Portelance L, Creutzberg C, Jürgenliemk-Schulz IM, Mundt A, et al. Consensus Guidelines for Delineation of Clinical Target Volume for Intensity-Modulated Pelvic Radiotherapy for the Definitive Treatment of Cervix Cancer. *Int J Radiat Oncol* 2011;79:348–55.
- [13] van de Schoot AJAJ, de Boer P, Visser J, Stalpers LJA, Rasch CRN, Bel A. Dosimetric advantages of a clinical daily adaptive plan selection strategy compared with a non-adaptive strategy in cervical cancer radiation therapy. *Acta Oncol* 2017;56:667–74.
- [14] Lutkenhaus LJ, Visser J, de Jong R, Hulshof MCCM, Bel A. Evaluation of delivered dose for a clinical daily adaptive plan selection strategy for bladder cancer radiotherapy. *Radiother Oncol* 2015;116:51–6.
- [15] Kirisits C, Rivard MJ, Baltas D, Ballester F, De Brabandere M, van der Laarse R, et al. Review of clinical brachytherapy uncertainties: analysis guidelines of



- GEC-ESTRO and the AAPM. *Radiother Oncol* 2014;110:199–212.
- [16] Dimopoulos JCA, Petrow P, Tanderup K, Petric P, Berger D, Kirisits C, et al. Recommendations from Gynaecological (GYN) GEC-ESTRO Working Group (IV): Basic principles and parameters for MR imaging within the frame of image based adaptive cervix cancer brachytherapy. *Radiother Oncol* 2012;103:113–22.
- [17] Kumar P, Sharma DN, Kumar S, Gandhi AK, Rath GK, Kumar Julka P. Pulsed-dose-rate vs. high-dose-rate intracavitary radiotherapy for locally advanced carcinoma of cervix: A prospective randomized study 2016.
- [18] Visser AG, van den Aardweg GJM, Levendag PC. Pulsed dose rate and fractionated high dose rate brachytherapy: Choice of brachytherapy schedules to replace low dose rate treatments. *Int J Radiat Oncol* 1996;34:497–505.
- [19] Dale E, Hellebust TP, Skjønberg A, Høgberg T, Olsen DR. Modeling normal tissue complication probability from repetitive computed tomography scans during fractionated high-dose-rate brachytherapy and external beam radiotherapy of the uterine cervix. *Int J Radiat Oncol* 2000;47:963–71.
- [20] Pötter R, Haie-Meder C, Van Limbergen E, Barillot I, De Brabandere M, Dimopoulos J, et al. Recommendations from gynaecological (GYN) GEC ESTRO working group (II): concepts and terms in 3D image-based treatment planning in cervix cancer brachytherapy-3D dose volume parameters and aspects of 3D image-based anatomy, radiation physics, radiobiology. *Radiother Oncol* 2006;78:67–77.
- [21] Waggoner SE. Cervical cancer. *Lancet* 2003;361:2217–25.
- [22] Georg P, Pötter R, Georg D, Lang S, Dimopoulos JCA, Sturdza AE, et al. Dose effect relationship for late side effects of the rectum and urinary bladder in magnetic resonance image-guided adaptive cervix cancer brachytherapy. *Int J Radiat Oncol Biol Phys* 2012;82:653–7.
- [23] Michalski JM, Gay H, Jackson A, Tucker SL, Deasy JO. Radiation dose-volume effects in radiation-induced rectal injury. *Int J Radiat Oncol Biol Phys* 2010;76:S123–9.
- [24] Nesvacil N, Tanderup K, Lindegaard JC, Pötter R, Kirisits C. Can reduction of uncertainties in cervix cancer brachytherapy potentially improve clinical outcome? *Radiother Oncol* 2016;120:390–6.
- [25] van de Schoot AJAJ, de Boer P, Buist MR, Stoker J, Bleeker MCG, Stalpers LJA, et al. Quantification of delineation errors of the gross tumor volume on magnetic resonance imaging in uterine cervical cancer using pathology data and deformation correction. *Acta Oncol* 2015;54:224–31.
- [26] International Commission on Radiation Units and Measurements. Prescribing, Recording, and Reporting Brachytherapy for Cancer of the Cervix (ICRU report 89). vol. 13. 2013.
- [27] Ahmad R, Hoogeman MS, Bondar M, Dhawtal V, Quint S, De Pree I, et al. Increasing treatment accuracy for cervical cancer patients using correlations between bladder-filling change and cervix-uterus displacements: proof of principle. *Radio-*

- ther Oncol 2011;98:340–6.
- [28] Bondar L, Hoogeman M, Mens JW, Dhawtal G, de Pree I, Ahmad R, et al. Toward an individualized target motion management for IMRT of cervical cancer based on model-predicted cervix-uterus shape and position. *Radiother Oncol* 2011;99:240–5.
- [29] Wognum S, Heethuis SE, Rosario T, Hoogeman MS, Bel A. Validation of deformable image registration algorithms on CT images of ex vivo porcine bladders with fiducial markers. *Med Phys* 2014;41:071916.







# Chapter 2

## Quantification of image distortions on the Utrecht Interstitial CT/MR brachytherapy applicator at 3 T MRI

L.E. van Heerden<sup>1</sup>, O.J. Gurney-Champion<sup>1,2</sup>, Z. van Kesteren<sup>1</sup>,  
A.C. Houweling<sup>1</sup>, C. Koedooder<sup>1</sup>, C.R.N. Rasch<sup>1</sup>, B.R. Pieters<sup>1</sup>, A. Bel<sup>1</sup>.

<sup>1</sup>Department of Radiation Oncology, Amsterdam UMC, University of Amsterdam, location AMC, Meibergdreef 9, 1105 AZ Amsterdam, The Netherlands

<sup>2</sup>Department of Radiology, Amsterdam UMC, University of Amsterdam, location AMC, Meibergdreef 9, 1105 AZ Amsterdam, The Netherlands

Published in: *Brachytherapy* 2016;15:118–26.

## **Abstract**

### ***Purpose***

To quantify distortions on magnetic resonance (MR) images of the Utrecht Interstitial CT/MR applicator at a field strength of 3 T using an MRI-only method.

### ***Materials and methods***

An MR-compatible phantom suspending the applicator in water was built and imaged on a Philips Ingenia 3 T MRI scanner. A map of the magnetic field ( $B_0$ ) was calculated from multi-echo images and used to quantify the field inhomogeneity. The expected displacements of the applicator could be quantified using the measured field inhomogeneity and sequence bandwidth. Additionally, two scans were acquired using opposing readout gradients. These scans were rigidly matched and their displacement was compared to the expected displacements from the  $B_0$  map.

These same methods were applied in four patients. By rigid matching of the scans acquired with opposing readout direction the applicator displacement due to image distortion from  $B_0$  inhomogeneity as well as patient movement and organ deformation was determined.

### ***Results***

According to the  $B_0$  map, the displacement on the intrauterine device of the plastic brachytherapy applicator was  $<0.4$  mm for both the phantom and patients. Displacements obtained by the opposing readout method were  $\leq 0.8$  mm for each patient with a mean  $\pm$  standard deviation over the patients of  $0.3 \pm 0.1$  mm.

### ***Conclusion***

The results of our study indicate that the  $B_0$  method agrees with the opposing readout method. Displacements caused by magnetic field inhomogeneity on 3 T MRI were small compared to displacements due to patient movement and organ deformation.

## Introduction

Magnetic resonance imaging (MRI) is increasingly used in brachytherapy treatment planning since it offers soft tissue contrast that is superior to CT and thus allows the delivered dose to be better adapted towards organ-at-risk (OAR) sparing.<sup>1,2</sup> Susceptibility variations, which are introduced by the patient itself and the brachytherapy applicator, will lead to inhomogeneity of the main magnetic field ( $B_0$ ) resulting in image distortions. Such distortions increase with field strength. MRI for application in brachytherapy is typically performed at  $B_0 \leq 1.5$  T because image distortions caused by inhomogeneity of  $B_0$  are considered acceptable at these low field strengths.<sup>3</sup>

There has been an increasing interest in 3 T MRI<sup>4</sup> because it leads to a higher signal-to-noise ratio. For gynecological cancers, this may improve the delineation of, in particular, the uterine cervix and macroscopic tumor regions.<sup>5</sup> Higher field strengths also provide the opportunity to obtain functional images, such as diffusion weighted MRI, for improved tumor delineation.<sup>6</sup>

With increasing field strength and the associated lower scanning bandwidth the susceptibility induced image distortions become more pronounced.<sup>7</sup> Geometric uncertainties near the applicator could lead to an incorrect reconstruction of the applicator, which leads to uncertainties in the dose distribution and the delivery of unintended dose to the OARs.<sup>8</sup> Thus, there is a clear need to investigate the magnitude of distortions caused by 3 T MRI scanners in order to determine whether images acquired with high field scanners could be used for brachytherapy treatment planning.

In previous research by Kim et al.<sup>9</sup> the distortion of a titanium applicator at 3 T was investigated by registering MR images with CT images for a phantom and patients using an artifact favorable  $T_1$ -weighted MRI sequence. They found that the distortion at the tip of the applicator was less than  $1.5 \pm 0.5$  mm (average  $\pm$  standard deviation). To our knowledge there is currently no study that uses MR-only methods, which can be applied for any sequence, to quantify the distortion on a plastic applicator at 3 T.

The aim of the present study is therefore to quantify image distortion on the Utrecht Interstitial CT/MR tandem/ovoid applicator<sup>10</sup> (Elekta Brachytherapy, Veenendaal, The Netherlands) at 3 T MRI using a method which determines displacements independently of the used clinical MRI sequence, in order to explore the feasibility of 3 T MRI for brachytherapy for cervical cancer.

## Materials & Methods

### *Applicator*

The investigated Utrecht Interstitial CT/MR compatible tandem/ovoid applicator<sup>10</sup> (Elekta Brachytherapy, Veenendaal, The Netherlands), for short the Utrecht applicator, is widely used for the treatment of cervical cancer and provides the option to place needles parallel to the tandem using dedicated needle holes in the ovoids. The applicator set is made of polyphenylsulfone, while the intrauterine device (IUD) and ovoid tubes contain a glass fiber. The adjustable fixation mechanism contains titanium, which is always outside the patient's body.

### *Phantom & Patients*

A water-filled MR-compatible phantom of 40x40x30 cm<sup>3</sup> was developed (Fig. 1) in which the Utrecht applicator was mounted in a similar orientation as during treatment with respect to the main magnetic field. The phantom design was based on designs described previously by Haack et al.<sup>3</sup> and Kim et al.<sup>9</sup>. The Utrecht applicator was suspended in the center of the phantom in order to minimize potential distortions caused by the phantom material.

In addition we quantified the distortions in vivo for four cervical cancer patients with the Utrecht applicator in situ. As part of patient specific quality assurance additional MR scans were added to the standard clinical MRI protocol for brachytherapy planning. The patients, FIGO stage (IIA-IIIB), received treatment consisting of a combination of external beam radiation therapy on the pelvis and para-aortic area combined with (MRI-guided) pulsed-dose rate brachytherapy.

### *Displacements due to $B_0$ inhomogeneity*

$B_0$  inhomogeneity is a local variation in the main magnetic field and is associated with artifacts and image distortions.  $B_0$  inhomogeneity can cause misinterpretation of the spatial encoding, which leads to distortion in the images. The magnitude of distortions is inversely dependent on the scanning bandwidth of the MRI sequence, and is generally most pronounced in-plane in the readout direction of the MR image.<sup>7</sup> Reversing the readout direction will also reverse the direction of the distortion (Fig. 2).



**Fig. 1** The MR-compatible phantom in which the Utrecht applicator is suspended.

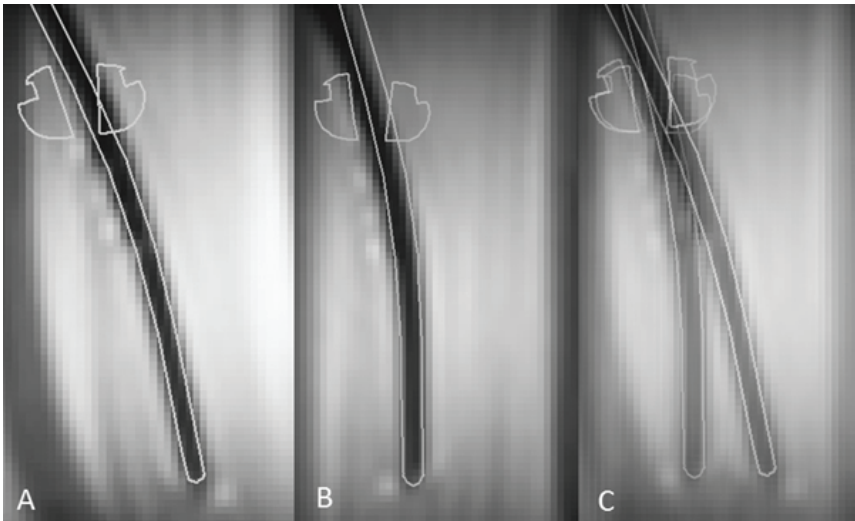


**Fig. 2** Example of deformations occurring at low scanning bandwidth (63.1 Hz). Sagittal scans showing the reconstructed applicator for scans with opposing readout directions (A, anterior-posterior; B, posterior-anterior) in a phantom. The anterior-posterior direction is from left to right in these images. In C the overlay of A and B is shown.

### 3 T MRI

In this study, the magnitude of the distortions was determined with an MRI-only technique, i.e. without matching to an undistorted CT. Validation using a CT has the disadvantages that 1) in the phantom markers are necessary as a reference system, which will introduce additional artifacts, 2) an additional CT scan of the patients with the applicator in situ has to be performed, and 3) an additional error is introduced due to registration between CT and MRI. Therefore, a dual approach was used to evaluate distortions near the Utrecht applicator for the clinical MRI protocol. First, the applicator displacement due to local magnetic field inhomogeneity was determined by measuring a  $B_0$  field map, a map of the variation in the main magnetic field ( $\Delta B_0$ ) at different spatial locations. Secondly, the results from the  $B_0$  map were compared to displacements obtained using a clinical MRI sequence, with opposing readout directions. This method was previously described in a study by Gurney-Champion et al.<sup>11</sup>

Since the extent of the distortions depends inversely on the scanning bandwidth, the displacements are expected to be rather small for the clinically used MR protocol which has a bandwidth of  $>300$  Hz. To further investigate the relationship between bandwidth and displacement, and compare the opposing readout method to the  $B_0$  field map method, we also performed measurements with varying low readout bandwidth. Therefore, images were acquired with an Echo Planar Imaging (EPI) readout as a way to obtain a low bandwidth. EPI, a rapid MRI technique, is used widely in functional MRI research.<sup>12-14</sup>

The MR images of the phantom and patients were all acquired on an Ingenia 3 T MRI scanner (Philips Healthcare, Best, The Netherlands). The MR acquisition parameters for the phantom experiments are summarized in Table 1, for the patients in Table 2. The field of view was chosen to include the intrauterine device (IUD) from the ovoids to the tip. For both phantom and patients, multi-echo images including magnitude and phase images were acquired, from which the  $B_0$  field map was calculated. The field of view for these measurements also included the ovoids.

In the phantom, sagittal scans at varying low scanning bandwidth (18.4 Hz, 33.3 Hz and 63.1 Hz) were acquired. To further increase the artifact no shimming was applied for the low bandwidth scans. For both the phantom and the patients, the MRI protocol included  $T_2$ -weighted Turbo Spin Echo (TSE) images, which are used in the clinical protocol for brachytherapy treatment planning, acquired using a scanning bandwidth of 311 Hz. For each of the mentioned bandwidths, two scans were obtained successively using opposing readout directions (anterior-posterior and vice versa). For the TSE images the standard shimming was applied in both the phantom and the patients (Table 2).

**Table 1** MR acquisition parameters for the phantom measurements. TE: Echo time, TR: Repetition time.

MRI sequence type	Acquired voxel size (mm <sup>3</sup> )	Bandwidth (Hz/pixel)	TR (ms)	TE (ms)	Scanning time (min)	Scan direction	Image Volume Voxel size (mm <sup>3</sup> )
B <sub>0</sub>	0.8x0.8x1.5	1200	17	4	<2	Transversal	0.8x0.8x1.5
EPI	4.3x1.5x1.5	18.4	3000	20	<3	Sagittal	4.3x1.3x1.3
EPI	4.3x2.0x2.0	33.3	3000	20	<3	Sagittal	4.3x1.3x1.3
EPI	4.3x2.5x2.5	63.1	3000	20	<3	Sagittal	4.3x1.3x1.3
T <sub>2</sub> W TSE	0.7x0.8x3.3	311	3000	40	<5	Transversal	0.7x0.7x3.3

**Table 2** MR acquisition parameters for the patient measurements. TE: Echo time, TR: Repetition time.

MRI sequence type	Acquired voxel size (mm <sup>3</sup> )	Bandwidth (Hz/pixel)	TR (ms)	TE (ms)	Scanning time (min)	Scan direction	Image Volume Voxel size (mm <sup>3</sup> )
B <sub>0</sub>	0.8x0.8x1.5	1200	17	4	<2	Transversal	0.8x0.8x1.5
T <sub>2</sub> W TSE	0.7x0.8x3.3	311	3000	40	<5	Transversal	0.7x0.7x3.3

### *Analysis of distortions: B<sub>0</sub> field map method*

The magnitude and phase images from the multi-echo images were used to calculate a B<sub>0</sub> field. Analysis was performed in Mathematica (Wolfram Research, USA) using the DTI-tools toolbox.<sup>15</sup> With the B<sub>0</sub> field map the displacement along the length of the IUD could be calculated for any MRI sequence, thus providing a sequence-independent measure of image distortions.

The magnitude and phase data was cropped around the Utrecht applicator. The intensity values in the signal void of the Utrecht applicator were set to zero using a mask, since any signal coming from this area is noise. Voxels within the signal void were selected for the mask by setting a cutoff value on the magnitude data.

The B<sub>0</sub> field map was calculated from the acquired phase images according to Jezzard et al.<sup>7:</sup>

$$\Delta B_0 = \Delta\theta / (2 \pi \gamma \Delta TE) \quad (1)$$

with  $\Delta B_0$  the magnetic field inhomogeneity,  $\Delta\theta$  the phase difference between the echoes,  $\gamma$  the gyromagnetic ratio, and  $\Delta TE$  the time between the echoes. The measured phase is the true phase modulo  $2\pi$  constrained to the interval  $(-\pi, \pi]$ . To become continuous the phase data first required unwrapping<sup>16</sup>.



Next, the  $B_0$  field difference was translated into the expected signal displacement for any given sequence using the bandwidth and pixel size of that sequence, where displacement = pixel size \*  $\Delta B_0$  / pixel bandwidth. For the phantom the displacement was calculated for the low bandwidths of 18.4 Hz, 33.3 Hz and 63.1 Hz, while for both the phantom and patients the displacement was calculated for the clinically used bandwidth of 311 Hz.

The displacement estimated from the  $B_0$  map is determined by averaging the values over a region of interest of 20 x 20 pixels around the applicator cross section. This was repeated for all slices along the length of the IUD.

The displacements were also calculated from the  $B_0$  map for a region of interest volume containing the whole IUD and the ovoids for the phantom and the patients.

### ***Analysis of distortions: Opposing readout direction***

The displacement can also be determined by obtaining two scans using opposing readout directions as distortions occur primarily in this direction.<sup>7</sup> Next, these scans were rigidly matched per slice to determine the applicator displacement.

For the phantom measurements acquired at a scanning bandwidth of 18.4 Hz, 33.3 Hz, 63.1 Hz and 311 Hz and the patient measurements acquired at 311 Hz, manual rigid registration was performed (VelocityAI, Velocity Medical Solutions, Atlanta, GA, United States) on each transversal slice to obtain the displacement of the Utrecht applicator cross section along the length of the IUD. Translations were only allowed in the readout direction. The rigid match was visually assessed by inverting the gray values of one image and shifting the image until there were no black/white transitions visible in the readout direction. The reproducibility in the measured displacement was determined by performing the match on each slice ten times and calculating the mean and standard deviation.

### ***Data analysis***

We determined the displacement on the IUD both by matching cross sections at the same position and by calculating it from the  $B_0$  map. The separate steps of both procedures are schematically shown in Fig. 3. The calculated displacement from the  $B_0$  map was compared to the opposing readout method to verify whether the  $B_0$  field map can be used to calculate the displacement.

The displacements on the IUD and the ovoids was determined by calculating the mean and the standard deviation of the distribution of calculated displacements.

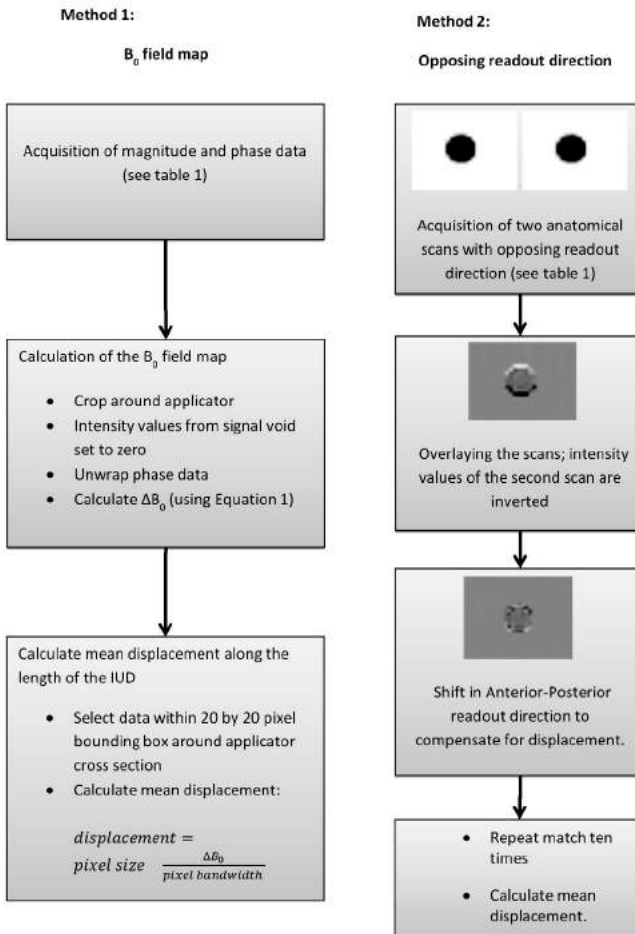


**Fig. 3** Flowchart of the analysis of the data, according to the B<sub>0</sub> field map method (left), and the opposing readout method (right).

## Results

### *Phantom*

The displacements in the IUD that were found using MRI sequences with low bandwidth EPI-readout scans (18.4 Hz, 33.3 Hz, 63.1 Hz) are presented in Fig. 4. For 63.1 Hz, the maximum displacement of the IUD according to calculations from the B<sub>0</sub> map was  $6.3 \pm 0.2$  mm near the tip, and  $0.8 \pm 0.1$  mm near the ovoids. The maximum and minimum displacement found with the opposing readout method was  $5.6 \pm 0.3$  mm (mean  $\pm$  standard deviation) and  $1.1 \pm 0.1$  mm, respectively.

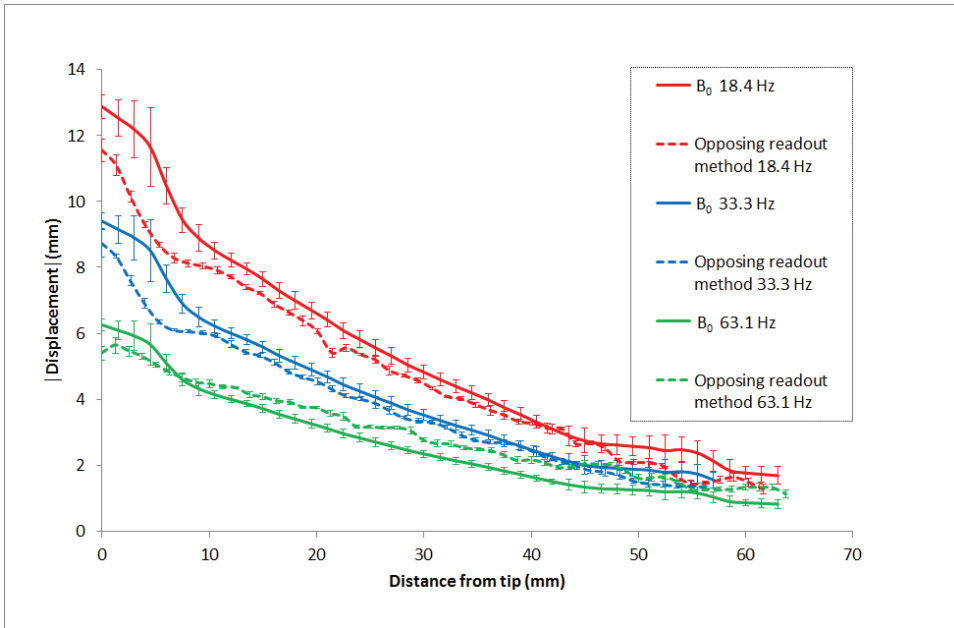


**Fig. 4** Absolute displacement along the length of the IUD measured in the phantom, calculated from the  $B_0$  field map (solid) or obtained with the opposing readout method (dashed), for scans acquired with different bandwidths (18.4 Hz, 33.3 Hz and 63.3 Hz). The error bar for the  $B_0$  field map method is the standard deviation of the values within the selection box around the cross section of the applicator; the error bar for the opposing readout method is the standard deviation over ten repeated measurements.

The displacement calculated with the  $B_0$  map was larger than the displacement obtained with the opposing readout method. The difference between the  $B_0$  map calculations and the opposing readout direction method was within the pixel size (1.3 mm) of the MRI sequences with EPI readout for 94% of the measured values. Between 30 mm from the tip up to the ovoids the difference was smaller than the pixel size for all the measured values. Between 30 mm up to the tip, the percentage of measured displacements with a difference larger than the pixel size increased for 18.4 Hz and 33.3 Hz; the percentage was respectively 18% and 14%. For 63.1 Hz the difference was always smaller than the pixel size.

By acquiring the transversal  $T_2$ -weighted scan with a bandwidth of 311 Hz as used in the clinical protocol we found that the displacement in the phantom was maximally 0.4 mm according to the  $B_0$  map, and 0.3 mm according to the opposing readout method (Fig. 5). For a region of interest containing the IUD and the ovoids the mean displacement calculated

from the  $B_0$  map was  $0.05 \pm 0.06$  mm (Fig. 6). Within this volume, all calculated displacements were smaller than 0.7 mm.

### ***Patients***

The displacements on the IUD found for the patients are presented in Fig. 5. Calculations from the  $B_0$  map showed that the maximum displacement on the TSE images due to local magnetic field inhomogeneity varied between  $0.2 \pm 0.1$  mm (patient 2) and  $0.4 \pm 0.03$  mm (patient 3). The maximum absolute displacement in the anterior-posterior direction obtained using the opposing readout method varied between  $0.3 \pm 0.03$  mm (patient 3) and  $0.8 \pm 0.08$  mm (patient 1). The average displacement over all patients for the whole IUD was  $0.3 \pm 0.1$  mm.

The displacements on the IUD and the ovoids for the patients are presented in Fig. 6. The mean displacement varied between  $-0.07 \pm 0.13$  mm and  $0.03 \pm 0.19$  mm. For all patients, the displacements within the volume were smaller than 0.7 mm for 99% of the measured values.

### **Discussion**

The present study is the first to quantify image distortions on a plastic applicator caused by magnetic field inhomogeneity at 3 T MRI using MR-only methods. These methods comprised 1) measuring a map of the  $B_0$  inhomogeneity and calculating the displacements, and 2) matching the cross section of the IUD on scans acquired using opposing readout directions. According to the  $B_0$  field map method, the displacement of the Utrecht applicator in the phantom and in the patients was smaller than the pixel size used in our clinical scanning protocols. The results of our study therefore suggest that accurate reconstruction of this Utrecht applicator can be performed at 3 T MRI in our clinical practice.

With the  $B_0$  map method we present a sequence-independent method to estimate distortions due to susceptibility artifacts. Along with the opposing readout method, both provide a valuable tool for quality assurance to monitor the potential distortions of MR images in clinical practice.

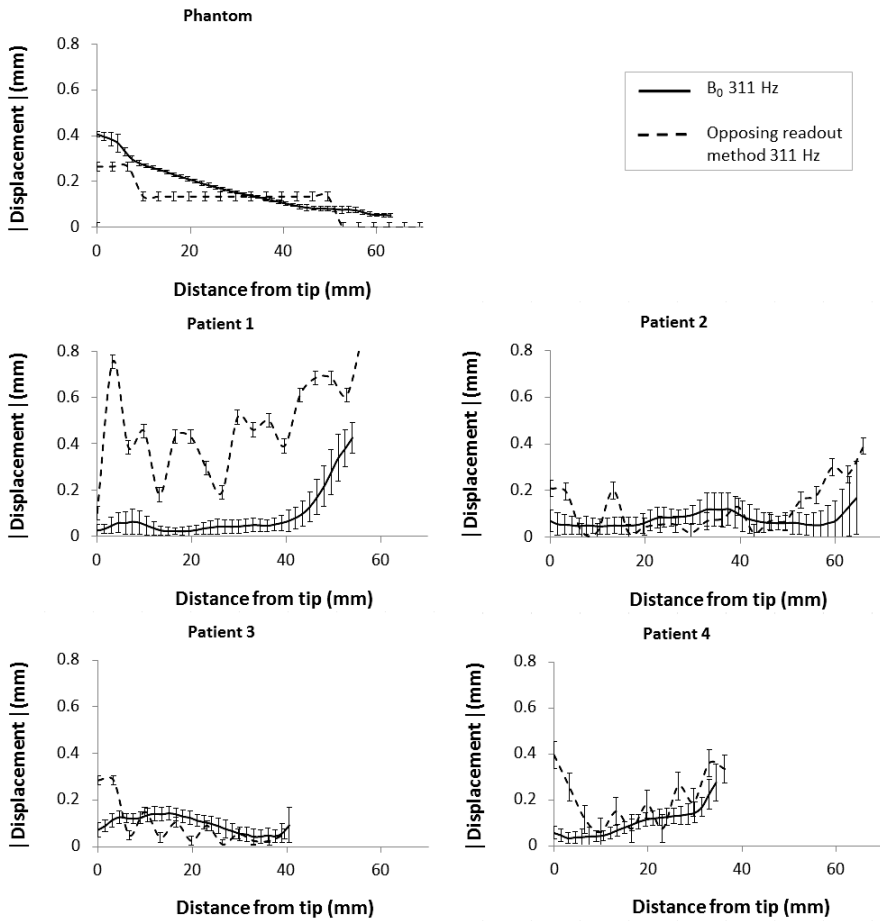


**Fig. 5** Absolute displacement along the length of the IUD calculated from the  $B_0$  field map (solid) or obtained with the opposing readout method (dashed), for scans acquired with the clinically used bandwidth (311 Hz), for the phantom and four patients. The error bar for the  $B_0$  field map method is the standard deviation of the values within the selection box around the cross section of the applicator; the error bar for the opposing readout method is the standard deviation over ten repeated measurements.

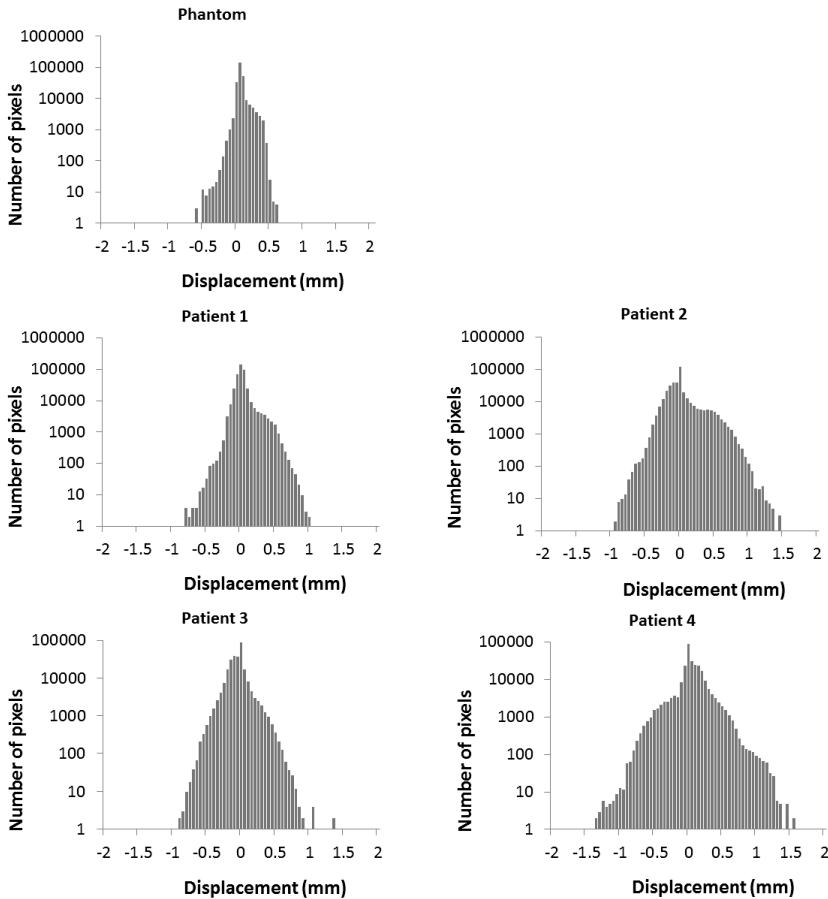


**Fig. 6** Histogram of displacements calculated from the  $B_0$  field on the IUD and the ovoids for the phantom and for four patients. The number of pixels is plotted on the y-axis on a logarithmic scale.

Both methods presented in this study gave consistent results for the displacements along the IUD. The displacements found for the clinical  $T_2$  weighted scans were smaller than the voxel size, and verification scans of the phantom at low bandwidth show that the difference between the two methods was less than the pixel size for 94% of the measured displacements. Near the tip the difference in measured displacement increased up to 2 mm maximally at 18.4 Hz. In the phantom, the cause of this difference was most likely the poor image quality at lower bandwidth. This made the matching more difficult, especially for measurements at such low bandwidths as 18.4 Hz. Therefore, displacements found with the opposing readout method at 33.3 Hz and 63.1 Hz will be more consistent with the true displacement than at 18.4 Hz, as was confirmed by the  $B_0$  map.

In the patients it could be expected that the displacement predicted by the opposing readout method was larger than predicted by the  $B_0$  map, since the displacements measured by rigid matching could include motion artifacts caused by patient movement in between the scans, typically 4-5 minutes. This effect was clear for patient 1 but less pronounced for the other patients. During the treatment, filling of the bladder and rectum will contribute to the applicator displacement.<sup>17</sup> Although considerable organ deformation and patient movement can occur during brachytherapy, the effect on the dose is minor.<sup>18</sup> Quantifying the displacement due to patient induced deformations separately was beyond the scope of the present study. Another cause of the differences between the two methods could be the large field of view and air-to-tissue transitions in the pelvic region, which introduce additional susceptibility artifacts.

Previous research by Haack et al.<sup>19</sup>, who investigated the potential of  $B_0$  field map correction to reduce geometrical distortion for diffusion weighted MRI at 3 T with the applicator in situ, found a significant residual error of 2.9 mm at the IUD center. In our study the  $B_0$  field map method and the opposing readout direction method also gave different results for MR-sequences with comparable scanning bandwidth (<100 Hz). According to the  $B_0$  field map acquired in the patients, the displacements of the Utrecht applicator at a bandwidth of 63.1 Hz, which could be considered a typical bandwidth for functional imaging, would be as high as 6.2 mm. Functional imaging, typically acquired using low scanning bandwidths, should therefore be implemented in brachytherapy treatment planning with caution.

Previous studies<sup>3,9</sup> investigated for specific MR protocols the displacement of a brachytherapy applicator by matching the distorted MR image to a CT image. Kim et al.<sup>9</sup> found maximum displacements of 1.5 mm at the tip of a titanium applicator on 3 T. The present MR-only method resulted in displacements smaller than 0.7 mm in a plastic applicator according to the  $B_0$  map method, which is less than the voxel size. The main cause of this discrepancy was most likely the difference in applicator material, as titanium will lead to higher susceptibility variations. Also, a different MR-protocol with a higher bandwidth (>600 Hz) was used.

In the aforementioned studies,<sup>3,9</sup> the use of markers as a reference system was necessary, which introduced additional artifacts. Because we determined the displacement using MR-only methods, there was no need to perform an additional CT scan of the patients with the applicator in situ.

Only four patients were included in the present study. This study could therefore not take into account inter-patient variation in patient movement,  $B_0$  inhomogeneity, and applicator orientation within the patient. We plan to include more patients in the future. However, in



the phantom we were able to show in a controlled environment that the distortion of the applicator using the clinical MRI sequence was small, and the limited patient data showed that it was in the same range in vivo.

Another limitation of this study is that the distortion was only investigated with the opposing readout method on the IUD and not on the ovoids. We concentrated on the small cross section of the IUD because the distortion of the large cross section of the ovoids made it difficult to perform an overall satisfying match. The distortion on the IUD and the ovoids was investigated using only the  $B_0$  map method and the calculated displacements were found to be smaller than the pixel resolution for all values in the phantom, and in the patients for 99% of the measured values.

Furthermore, distortions were only investigated using a single applicator, and the applicator used in the phantom was limited to a single angle for the IUD and ovoids. A different configuration of the applicator IUD and ovoids might influence the magnetic field, causing different distortions.

Tanderup et al.<sup>20</sup> investigated the impact of random and systematic errors in applicator reconstruction on DVH parameters. The applicator was translated and rotated to mimic the uncertainty in applicator reconstruction, after which the dose was recalculated. By deriving a population based estimate of the delivered dose versus the expected dose, they found 1 mm of applicator displacement in the anterior posterior direction resulted in a 5% difference for rectum and bladder  $D_{2\text{cm}^3}$ . The difference in  $D_{90}$  of the GTV (Gross Tumor Volume) and  $CTV_{\text{HR}}$  (High-Risk Clinical Target Volume) was found to be less than 2% for 1 mm shifts. Since the applicator displacement found in the present study was smaller than 1 mm, we expect that the dosimetric implications of our findings will be limited.

## Conclusion

The displacement of the IUD of a plastic brachytherapy applicator at 3 T due to magnetic field inhomogeneity was found to be less than 0.4 mm based on the  $B_0$  method. The results of our study indicate that for the Utrecht applicator patient movement has a larger impact on treatment uncertainty than susceptibility artifacts.

## Acknowledgements

This work was funded by Elekta Brachytherapy (II 250008). The authors would like to thank Jan Sijbrands for the phantom construction.

## References

- [1] Dimopoulos JCA, Petrow P, Tanderup K, Petric P, Berger D, Kirisits C, et al. Recommendations from Gynaecological (GYN) GEC-ESTRO Working Group (IV): Basic principles and parameters for MR imaging within the frame of image based adaptive cervix cancer brachytherapy. *Radiother Oncol* 2012;103:113–22.
- [2] Dinkla AM, Pieters BR, Koedooder K, van Wieringen N, van der Laarse R, van der Grient JN, et al. Improved tumour control probability with MRI-based prostate brachytherapy treatment planning. *Acta Oncol* 2013;52:658–65.
- [3] Haack S, Nielsen SK, Lindegaard JC, Gelineck J, Tanderup K. Applicator reconstruction in MRI 3D image-based dose planning of brachytherapy for cervical cancer. *Radiother Oncol* 2009;91:187–93.
- [4] Kharofa J, Morrow N, Kelly T, Rownd J, Paulson E, Rader J, et al. 3-T MRI-based adaptive brachytherapy for cervix cancer: Treatment technique and initial clinical outcomes. *Brachytherapy* 2014;13:319–25.
- [5] Kataoka M, Kido A, Koyama T, Isoda H, Umeoka S, Tamai K, et al. MRI of the female pelvis at 3T compared to 1.5T: Evaluation on high-resolution T2-weighted and HASTE images. *J Magn Reson Imaging* 2007;25:527–34.
- [6] Kallehauge JF, Tanderup K, Haack S, Nielsen T, Muren LP, Fokdal L, et al. Apparent Diffusion Coefficient (ADC) as a quantitative parameter in diffusion weighted MR imaging in gynecologic cancer: Dependence on b-values used. *Acta Oncol* 2010;49:1017–22.
- [7] Jezzard P, Balaban RS. Correction for geometric distortion in echo planar images from B(o) field variations. *Magn Reson Med* 1995;34:65–73.
- [8] De Leeuw AAC, Moerland MA, Nomden C, Tersteeg RHA, Roesink JM, Jürgenliemk-Schulz IM. Applicator reconstruction and applicator shifts in 3D MR-based PDR brachytherapy of cervical cancer. *Radiother Oncol* 2009;93:341–6.
- [9] Kim Y, Muruganandham M, Modrick JM, Bayouth JE. Evaluation of artifacts and distortions of titanium applicators on 3.0-tesla MRI: Feasibility of titanium applicators in MRI-guided brachytherapy for gynecological cancer. *Int J Radiat Oncol Biol Phys* 2011;80:947–55.
- [10] Nomden CN, de Leeuw AAC, Moerland MA, Roesink JM, Tersteeg RJHA, Jürgenliemk-Schulz IM. Clinical Use of the Utrecht Applicator for Combined Intracavitary/Interstitial Brachytherapy Treatment in Locally Advanced Cervical Cancer. *Int J Radiat Oncol* 2012;82:1424–30.
- [11] Gurney-Champion OJ, Lens E, van der Horst A, Houweling AC, Klaassen R, van Hooft JE, et al. Visibility and artifacts of gold fiducial markers used for image guided radiation therapy of pancreatic cancer on MRI. *Med Phys* 2015;42:2638–47.
- [12] Koyama T, Togashi K. Functional MR imaging of the female pelvis. *J Magn Reson Imaging* 2007;25:1101–12.

- [13] Nakayama T, Yoshimitsu K, Irie H, Aibe H, Tajima T, Nishie A, et al. Diffusion-weighted echo-planar MR imaging and ADC mapping in the differential diagnosis of ovarian cystic masses: Usefulness of detecting keratinoid substances in mature cystic teratomas. *J Magn Reson Imaging* 2005;22:271–8.
- [14] Shen S-H, Chiou Y-Y, Wang J-H, Yen M-S, Lee R-C, Lai C-R, et al. Diffusion-weighted single-shot echo-planar imaging with parallel technique in assessment of endometrial cancer. *AJR Am J Roentgenol* 2008;190:481–8.
- [15] Froeling M, Nederveen AJ, Heijtel DFR, Lataster A, Bos C, Nicolay K, et al. Diffusion-tensor MRI reveals the complex muscle architecture of the human forearm. *J Magn Reson Imaging* 2012;36:237–48.
- [16] Herráez MA, Burton DR, Lator MJ, Gdeisat MA. Fast two-dimensional phase-unwrapping algorithm based on sorting by reliability following a noncontinuous path. *Appl Opt* 2002;41:7437–44.
- [17] Hellebust TP, Dale E, Skjønsberg A, Olsen DR. Inter fraction variations in rectum and bladder volumes and dose distributions during high dose rate brachytherapy treatment of the uterine cervix investigated by repetitive CT-examinations. *Radiother Oncol* 2001;60:273–80.
- [18] Lang S, Nesvacil N, Kirisits C, Georg P, Dimopoulos JCA, Federico M, et al. Uncertainty analysis for 3D image-based cervix cancer brachytherapy by repetitive MR imaging: Assessment of DVH-variations between two HDR fractions within one applicator insertion and their clinical relevance. *Radiother Oncol* 2013;107:26–31.
- [19] Haack S, Kallehauge JF, Jespersen SN, Lindegaard JC, Tanderup K, Pedersen EM. Correction of diffusion-weighted magnetic resonance imaging for brachytherapy of locally advanced cervical cancer. *Acta Oncol* 2014;53:1073–8.
- [20] Tanderup K, Hellebust TP, Lang S, Granfeldt J, Pötter R, Lindegaard JC, et al. Consequences of random and systematic reconstruction uncertainties in 3D image based brachytherapy in cervical cancer. *Radiother Oncol* 2008;89:156–63.



# Chapter 3

Image distortions on a plastic interstitial CT/MR brachytherapy applicator at 3 T MRI and their dosimetric impact

L.E. van Heerden<sup>1</sup>, O.J. Gurney-Champion<sup>1,2</sup>, Z. van Kesteren<sup>1</sup>,  
A.C. Houweling<sup>1</sup>, C. Koedooder<sup>1</sup>, C.R.N. Rasch<sup>1</sup>, B.R. Pieters<sup>1</sup>, A. Bel<sup>1</sup>.

<sup>1</sup>Department of Radiation Oncology, Amsterdam UMC, University of Amsterdam, location AMC, Meibergdreef 9, 1105 AZ Amsterdam, The Netherlands

<sup>2</sup>Department of Radiology, Amsterdam UMC, University of Amsterdam, location AMC, Meibergdreef 9, 1105 AZ Amsterdam, The Netherlands

Published in: International Journal of Radiation Oncology\*Biology\*Physics  
2017;99:710-8

## **Abstract**

### ***Purpose***

To quantify magnetic resonance image (MRI) distortions on a plastic intracavitary/interstitial applicator with plastic needles at a field strength of 3 T and to determine the dosimetric impact, using patient data.

### ***Methods and Materials***

For eleven cervical cancer patients, our clinical MRI protocol was extended with three scans. From the first scan, a multi-echo acquisition, a map of the magnetic field ( $B_0$ ) was calculated and used to quantify the field inhomogeneity. The expected displacements of the applicator were quantified for the clinical sequence using the measured field inhomogeneity and the clinical sequence's bandwidth. The second and third scan were our routine clinical sequence (duration: <5 min each), acquired consecutively using opposing readout directions. The displacement of the applicator between these scans is approximately twice the displacement due to  $B_0$  inhomogeneity. The impact of the displacement on the dose was determined by reconstructing the applicator on both scans. The applicator was then shifted and rotated the same distance as the observed displacement to create a worst-case scenario (i.e. twice the actual displacement due to  $B_0$  inhomogeneity). Next, the dose to 98%/90% ( $D_{98}/D_{90}$ ) of the clinical target volume at high risk ( $CTV_{HR}$ ) as well as the dose to the most irradiated 2 cm<sup>3</sup> ( $D_{2cm^3}$ ) for bladder and rectum was calculated for the original plan as well as the shifted plan.

### ***Results***

For a volume of interest containing the intrauterine device and the ovoids the 95<sup>th</sup> percentile of the absolute displacement ranged between 0.2 and 0.75 mm, over all patients. For all patients, the difference in  $D_{98}/D_{90}$  in the opposing readout scans with the original plan was at most 4.7/4.3%. For  $D_{2cm^3}$  of bladder/rectum, the difference was at most 6.0/6.3%.

### ***Conclusions***

The dosimetric impact of distortions on this plastic applicator with plastic needles is limited. Applicator reconstruction for brachytherapy planning purposes is feasible at 3 T MRI.

## Introduction

Concurrent radiotherapy and chemotherapy is the standard treatment for locally-advanced cervical cancer. Radiotherapy typically combines external beam radiotherapy with a brachytherapy (BT) boost to the tumor area using an intracavitary/interstitial applicator. Magnetic resonance imaging (MRI) is increasingly used for BT planning, since soft tissue contrast on MR images is superior to computed tomography (CT). The improved visibility can be employed to improve target definition<sup>1,2</sup> and to better adapt the planned dose towards organ-at-risk (OAR) sparing.<sup>3,4</sup> Susceptibility variations introduced by the patient and the BT applicator will lead to inhomogeneity of the main magnetic field ( $B_0$ ), resulting in image distortions. These distortions increase at higher field strength.<sup>5</sup> For BT applications, MRI is typically performed at  $B_0 \leq 1.5\text{T}$  since at these field strengths image distortions due to  $B_0$  inhomogeneity are considered acceptable.<sup>6</sup>

There has been an increasing interest in the use of 3 T MRI for gynecological cancers.<sup>7-9</sup> The higher signal-to-noise ratio may improve the delineation of, in particular, the uterine cervix and macroscopic tumor regions.<sup>10</sup> With increasing field strength and the associated lower scanning bandwidth, susceptibility induced image distortions become more pronounced.<sup>5</sup> Geometric uncertainties near the applicator could lead to incorrect reconstruction of the applicator, resulting in uncertainties in the dose distribution and delivery of unintended dose to the OARs.<sup>11</sup> Thus, there is a clear need to investigate the magnitude of these distortions for 3 T MRI, as well as the effect on the dose parameters, in order to determine whether MR images acquired with high field scanners could safely be used for BT planning.

The dosimetric impact of geometrical uncertainties for the reconstruction of plastic tandem/ring applicators was investigated by Tanderup et al.<sup>12</sup>, and for titanium tandem/ovoid applicators by Schindel et al.<sup>13</sup> In both studies, the applicator was translated and rotated to mimic the uncertainty in applicator reconstruction, after which the dose was recalculated. It was demonstrated that errors of a few mm could lead to large deviations in dose volume histogram (DVH) parameters used in BT planning. The image distortion of a titanium applicator was already investigated for specific MR protocols at 3 T MRI by matching the distorted MR image to CT images.<sup>14</sup> In our previous study, an MRI-only method was introduced to investigate image distortions on the Utrecht interstitial CT/MR applicator.<sup>15</sup> For a tungsten brachytherapy applicator in a phantom, image distortions were already quantified at 1.5 T using only MRI.<sup>16</sup> An MRI-only method as compared to a CT-based method provides the advantage that no additional CT scan of the patients with the applicator in situ has to be performed, and no additional error is introduced due to registration between CT and MRI.

In our previous study, we have tested the MRI-only method in a phantom and demonstrated the in vivo feasibility for 4 patients.<sup>15</sup> Interpatient variation in patient movement and  $B_0$  inhomogeneity were not taken into account. Moreover, the orientation of the applicator varies per patient, which will affect the results.<sup>17</sup> In our present study image distortions on the Utrecht interstitial CT/MR applicator<sup>18</sup> (Elekta Brachytherapy, Veenendaal, The Netherlands) were investigated in vivo for a substantial patient dataset. We therefore consider this study to be a valuable contribution to the rather limited literature regarding the dosimetric impact of brachytherapy applicator image distortions at 3 T MRI, since our study both quantifies image distortions at 3 T MRI, and investigates how these image distortions affect planned DVH parameters.

The aim of this study is to quantify in vivo the image distortion on the Utrecht applicator using an MRI-only method, and to determine the impact on brachytherapy dosimetry.

## Methods & Materials

### *Applicator*

The investigated Utrecht interstitial CT/MR applicator<sup>18</sup> provides the option to place needles parallel to the intrauterine device (IUD) using dedicated needle holes in the ovoids. The IUD, ovoids and the needles are made of the plastic polyphenylsulfone, while the IUD and the ovoid tubes contain a glass fiber (Fig. 1). The adjustable fixation mechanism, which is always outside the patient's body, contains titanium. The IUD has a thickness of 4 mm and a bending angle of 15/30°. Each ovoid (sizes: 15, 20, 25 or 30 mm) contains three to five needle holes in a 15/25° angle.

### *Patients*

Eleven consecutive patients treated for locally-advanced cervical carcinoma (FIGO stages IIA-IIIB) were investigated in this study. Tanderup et al. showed that the DVH difference is small for applicator displacements under 1 mm.<sup>12</sup> A sample size analysis (standard deviation  $\sigma=0.75$  mm) revealed that to detect a difference of 1 mm, at least 9 patients had to be analyzed to obtain statistical power of 80% or more at a 5% significance level. The value  $\sigma=0.75$  mm is a conservative estimate based on the results of our previous study.<sup>15</sup>



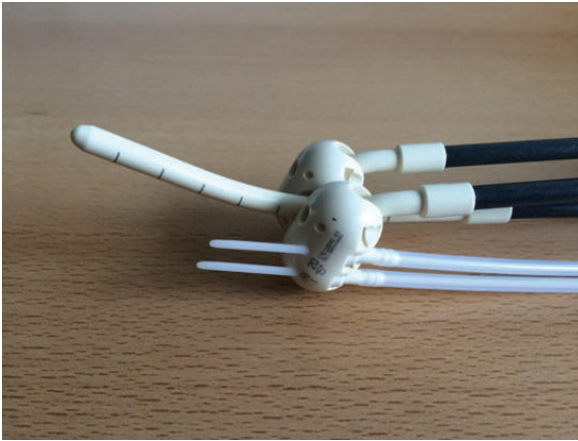


**Fig. 1** Photographic image of the Utrecht interstitial CT/MR applicator showing the intrauterine device (IUD) and the ovoids.

Patients were irradiated with external beam radiotherapy using volumetric modulated arc therapy (VMAT), receiving 46 Gy in daily fractions of 2 Gy. Following VMAT, all patients received a pulsed-dose rate (PDR) BT boost in two applications. MR images were acquired of all patients for BT planning purposes. For either application 1 or 2, the standard clinical MRI protocol for BT planning was extended with additional MR scans, as part of our local patient-specific quality assurance protocol.

A dose of 18 Gy in pulse doses of 0.75 Gy every hour using an Iridium-192 source (18.5-74 MBq) was planned to the clinical target volume at high risk ( $CTV_{HR}$ ). The mean (range) of the  $CTV_{HR}$  volume over all patients was 37 (11-74)  $cm^3$ . Planning was performed using Oncentra® Brachy 4.5 (Elekta AB, Stockholm, Sweden). Planning aims for the target include a  $D_{90}$  (total dose planned to 90% of the target) from VMAT and BT of 85-90  $Gy_{EQD2}$ . In bladder/rectum the dose to the most irradiated 2  $cm^3$  ( $D_{2cm^3}$ ) had to be less than 80/65  $Gy_{EQD2}$ . Radiobiological equivalent doses were calculated using LQ-model based equations with an  $\alpha/\beta$  value of 10 Gy for tumor and 3 Gy for late OAR toxicity and a 1.5 h repair half-time.<sup>19,20</sup>

The BT dose was planned using a library for applicator reconstruction after which the plan was manually optimized.

### **3 T magnetic resonance imaging**

In this study, the magnitude of the distortions was determined with MRI-only techniques along the lines of previous studies of our group.<sup>15,17,21</sup> To evaluate image distortions near the applicator, displacements due to local magnetic field inhomogeneity were determined for the clinical MRI protocol. This was achieved by obtaining a  $B_0$  field map, a map of the magnetic field inhomogeneity at different spatial locations, for a volume of interest containing

the IUD and ovoids.  $B_0$  inhomogeneity can cause misinterpretation of the spatial encoding, which leads to distortion in the images. The magnitude of distortions is inversely dependent on the scanning bandwidth of the MRI sequence, and is generally most pronounced in-plane in the readout direction of the MR image.<sup>5</sup>

To determine the dosimetric impact of the image distortions, the applicator was reconstructed on two scans with opposing readout directions, using the clinical plan as a starting point. Since distortions occur primarily in the readout direction, the applicator will appear to be shifted in this direction on both scans. In a previous study the displacement on the IUD was determined both by matching cross sections at the same position on opposing readout images and by calculating it from the  $B_0$  field map.<sup>15</sup> Displacements quantified with the  $B_0$  field map were shown to be consistent with displacements obtained by rigid registration of opposing readout scans.

The MR images of the patients were all acquired on an Ingenia 3 T MRI scanner (Philips Healthcare, Best, The Netherlands). The MRI protocol included  $T_2$ -weighted Turbo Spin Echo (TSE) acquisitions with a scanning bandwidth of 311 Hz. These scans were used for BT treatment planning. The MR acquisition parameters of the additional scans are summarized in Table 1. Multi-echo spoiled gradient echo images (number of echoes: 6) including magnitude and phase images were acquired, from which the  $B_0$  field map was calculated. Next, two additional  $T_2$ -weighted TSE scans were obtained consecutively, using opposing readout directions (anterior-posterior and vice versa). For both the multi-echo acquisition and the two scans with opposing readout directions, the field of view was chosen to include the IUD from the ovoids to the tip. For all acquisitions shimming was applied over the entire field of view.

**Table 1** MR acquisition parameters for the additional MR scans, which were added to the standard clinical MRI protocol for BT planning. The scan direction was transversal in all cases.

MRI sequence type	Acquired voxel size (mm <sup>3</sup> )	Bandwidth (Hz/pixel)	TR (ms)	TE (ms)	Scanning time (min)	Reconstructed voxel size (mm <sup>3</sup> )	Field of view (mm <sup>3</sup> )
$B_0$	0.8x0.8x1.5	1200	17	4	<2	0.8x0.8x1.5	296x296x150
$T_2$ W TSE	0.7x0.8x3.3	311	3000	40	<5	0.7x0.7x3.3	239x239x76

***Analysis of distortions***

The phase images from two consecutive echoes from the multi-echo acquisitions were used to calculate a  $B_0$  field map. Analysis was performed in Mathematica (Version 8.0, Wolfram Research, USA) using the DTItools toolbox.<sup>22</sup>

The magnitude and phase data were cropped around the applicator. Voxels within the applicator were masked, since only noise could be obtained from that volume.

The  $B_0$  field map was calculated from the acquired phase images according to Jezzard et al.<sup>5</sup>:

$$\Delta B_0 = \Delta\theta / ( 2 \pi \gamma \Delta TE ) \tag{1}$$

with  $\Delta B_0$  the magnetic field inhomogeneity,  $\Delta\theta$  the phase difference between the echoes,  $\gamma$  the gyromagnetic ratio, and  $\Delta TE$  the time between the echoes. The measured phase is the true phase, modulo  $2\pi$ , constrained to the interval  $(-\pi, \pi]$ . Since the phase data was not yet continuous, it first had to be unwrapped.<sup>23</sup>

The  $\Delta B_0$  field difference was translated into the expected signal displacement for any given sequence using the bandwidth and pixel size of that sequence, where displacement= pixel size\* $\Delta B_0$  / pixel bandwidth.<sup>15</sup> For each patient, a box-shaped volume of interest was selected so that it exactly covered the whole IUD and the ovoids (Fig. 2). Since the orientation of the applicator could vary between patients, the size and shape of the selected volume of interest also varied. The expected displacement on the  $T_2$ -weighted TSE images was then calculated using the  $\Delta B_0$  of the voxels and the bandwidth of the  $T_2$ -weighted TSE sequence.

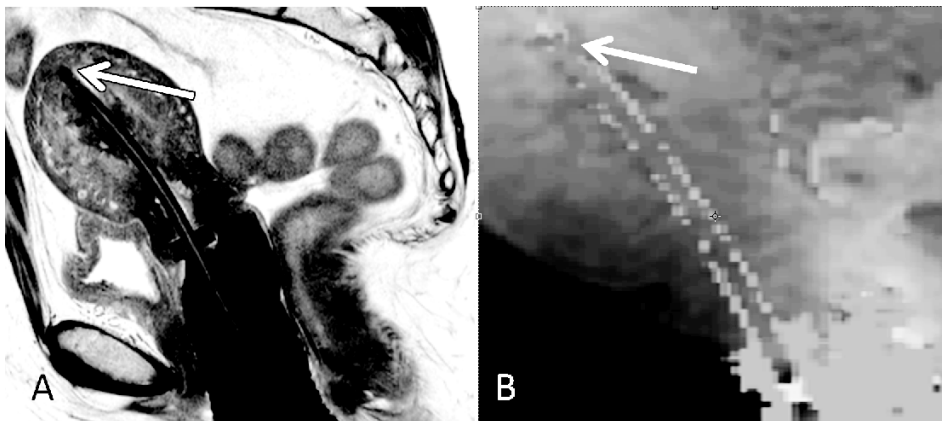


**Fig. 2** A) Sagittal  $T_2$ -weighted MR image with the applicator in situ. The arrow indicates the tip of the IUD, B) Map of the  $B_0$  inhomogeneity, zoomed in on the applicator.

### ***Impact of image distortion on DVH parameters***

To investigate the dosimetric impact of the image distortion, the applicator was reconstructed on scans acquired with opposing readout directions. On each scan the applicator will appear to be shifted in the readout direction and the shift necessary to realign the applicator is actually two times the displacement caused by  $B_0$  inhomogeneity. Since this method overestimates the displacement of the applicator, we are evaluating a worst-case scenario.

We visualized the reconstructed applicator from the clinical BT plan on the transversal scan with the same read-out direction ( $MR_{ref}$ ) as the transversal scan used for planning ( $MR_{planning}$ ). Both these scans were acquired with the same scanning parameters. However, the time difference between  $MR_{planning}$  and the scan with opposing readout direction ( $MR_{opposing}$ ) was >15 min. In an earlier study, DVH differences due to anatomical variation were found to be negligible in HDR brachytherapy for an irradiation interval of 50 min.<sup>24</sup> From this we conclude that on an even shorter time scale of <15 min variation of the anatomy has a minimal effect on the DVH parameters. Still, the scan was repeated just before acquiring  $MR_{opposing}$  to minimize the effect of patient motion. Despite the larger time interval between  $MR_{planning}$  and  $MR_{ref}$  the applicator reconstruction for  $MR_{planning}$  did not have to be modified for  $MR_{ref}$ . Next,  $MR_{ref}$  was registered with the opposing readout scan ( $MR_{opposing}$ ). The registration was based on the bony anatomy. Using the applicator library, the applicator was translated and rotated to fit the geometry on  $MR_{opposing}$ , resulting in a shifted plan. The loading of the applicator of the original plan was also used for the shifted plan. The delineations of the target and OAR volumes, including bladder and rectum, that were made on  $MR_{planning}$  were not altered. For the original plan and the shifted plan, the doses to 98% ( $D_{98}$ ) and 90% ( $D_{90}$ ) of the volume of the  $CTV_{HR}$  were evaluated. Next,  $D_{2cm^3}$  for bladder and rectum were calculated. DVH parameters calculated using the new applicator reconstruction were compared to the DVH parameters from the original plan.

### ***Data analysis***

For every patient, the 25<sup>th</sup>, 50<sup>th</sup>, 75<sup>th</sup> and 95<sup>th</sup> percentiles of the displacements in the volume containing the IUD and the ovoids, were calculated from the  $B_0$  field map. Also, over all patients the average percentage of voxels within the volume with displacements smaller than the imaging voxel size (0.7 mm) was determined. The difference (dose from shifted plan–dose from original plan) over one BT application of 24 x 0.75 Gy was calculated for  $D_{98}$  and  $D_{90}$  of  $CTV_{HR}$ , and  $D_{2cm^3}$  of the bladder and rectum. For all patients, the 25<sup>th</sup>, 50<sup>th</sup>, 75<sup>th</sup> and 100<sup>th</sup> percentiles of the DVH difference were calculated.

## Results

### *Quantification of displacements*

The displacements on the IUD and the ovoids calculated with the  $B_0$  field map are presented in Fig. 3. Over all patients, the 95<sup>th</sup> percentile of absolute displacements in a volume of interest containing the IUD and ovoids varied between 0.2 mm and 0.75 mm. Averaged over all patients, 98% of the calculated displacements within the volume were smaller than the resolution of the MR images (0.7 mm).

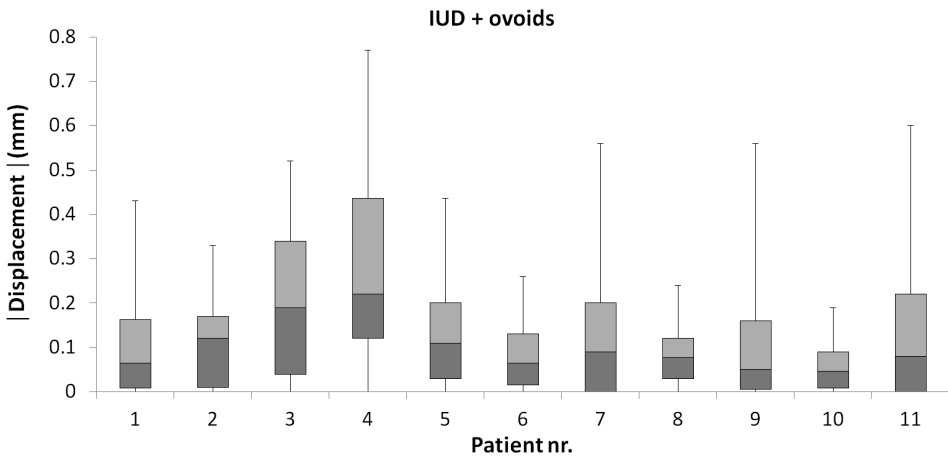


**Fig. 3** Boxplot of the absolute displacements on the IUD and ovoids calculated with the  $B_0$  field map for all patients, with the median and the 25th and 75th percentile for all patients. The whiskers show the minimum and the 95th percentile.

### *Impact of image distortions on DVH parameters*

The original treatment plan was compared to the shifted treatment plan by looking at the dose to the  $CTV_{HR}$ , and the bladder and rectum (Fig. 4). For  $CTV_{HR}$ , the difference (dose from shifted plan – dose from original plan) in  $D_{98}$  varied between -3.3 – 4.7% (-0.8 – 1.1 Gy). The difference in  $D_{90}$  varied between -4.3 – 3.0% (-1.0 – 0.7 Gy). Thus, the dose to the target was at least 95.7% of the original planned dose. The difference range for  $D_{2cm^3}$  was -6.4 – 3.1% (-1.5 – 0.7 Gy) for the bladder and -2.6 – 6.3% (-0.6 – 1.5 Gy) for the rectum (Fig. 5), meaning that the dose to the OARs was at most 106% of the original planned dose in the rectum. Over all patients, the absolute difference was less than 6.4% for all DVH parameters, and ranged between 0 – 4.7% for  $D_{98} CTV_{HR}$ , 0 – 4.3% for  $D_{90} CTV_{HR}$ , 0 – 6.0% for  $D_{2cm^3}$  bladder and 0 – 6.3% or the  $D_{2cm^3}$  rectum (Fig. 5).



## Discussion

The present study is the first to quantify the dosimetric implications of image distortions caused by magnetic field inhomogeneity at 3 T MRI using patient scans. Using an MRI-only method, we found that displacements of the applicator on  $T_2$ -weighted TSE scans were small ( $<0.75$  mm) and that the dosimetric impact was limited. The results of our study therefore indicate that accurate reconstruction of this plastic applicator with plastic needles can be performed at 3 T MRI in clinical practice.

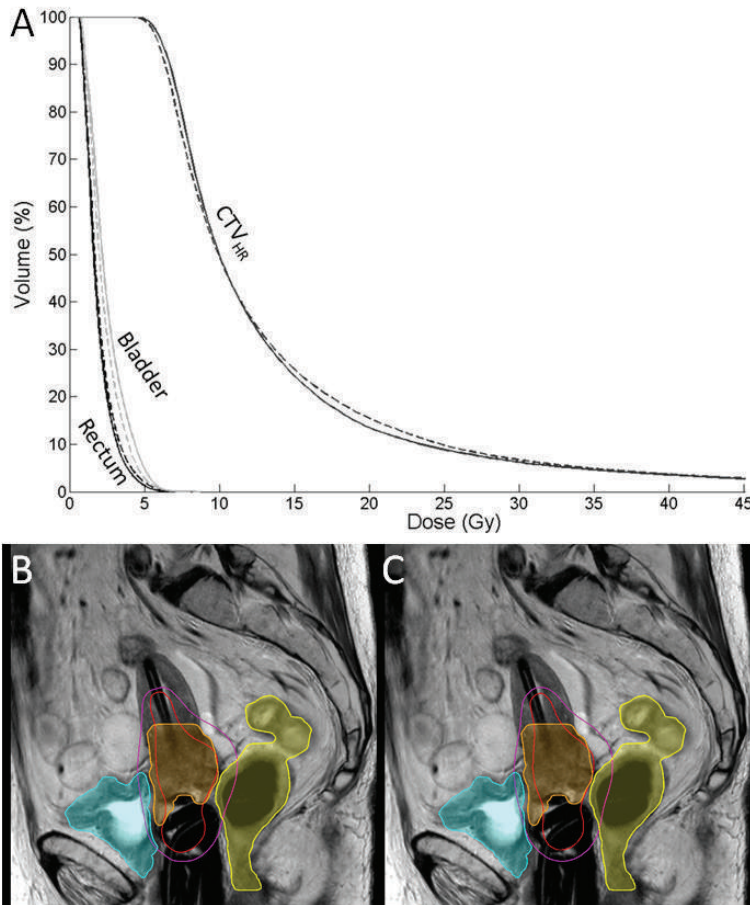


**Fig. 4** A) Example of a dose volume histogram for CTV<sub>HR</sub>, bladder and rectum. The dose was calculated using the original plan (solid) and the plan for which the applicator was shifted (dashed). This is the DVH of the patient with the largest absolute differences between the two plans. B) Sagittal planning MR image of the same patient with the 80% (pink) and 150% (red) isodose lines of the original plan and C) the shifted plan, with the bladder (yellow), rectum (blue) and CTV<sub>HR</sub> (orange).

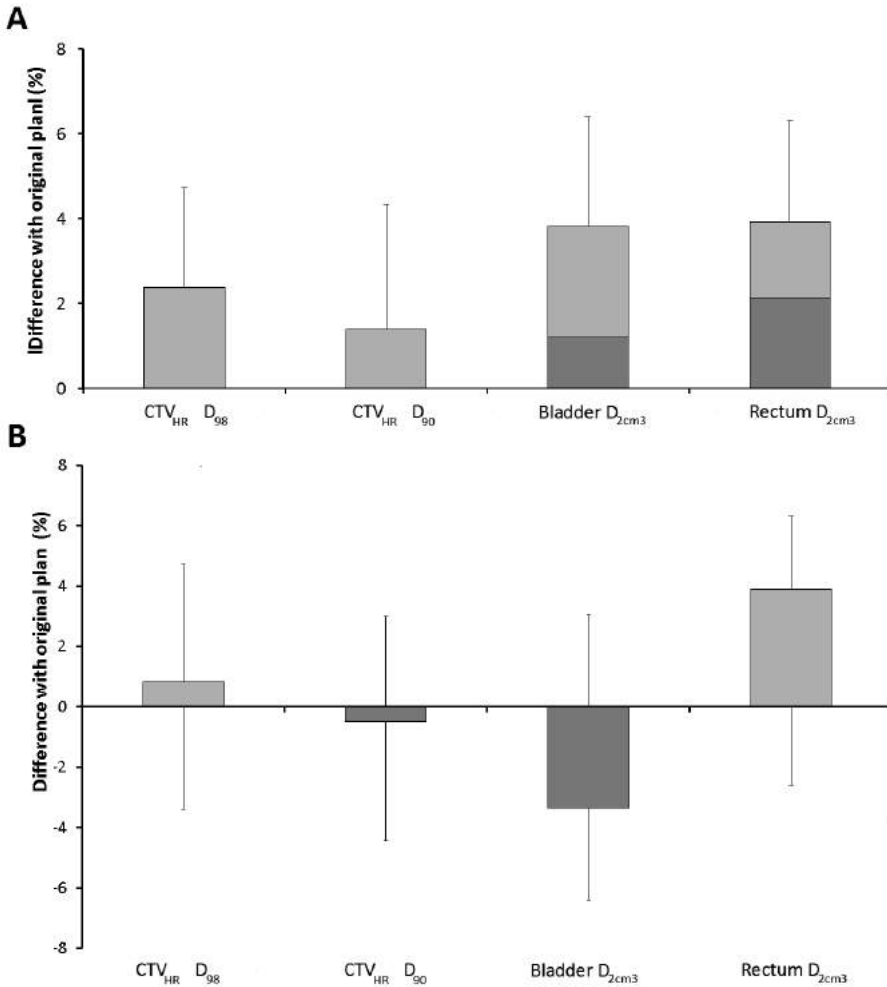


**Fig. 5** A) Boxplot of the absolute difference, and B) the relative difference of the DVH parameters from the original planned dose for all patients, with the median and the 25th and 75th percentile. The whiskers are the minimum and 100th percentile.

For each patient, 95% percent of the voxels within the volume of interest had displacements <0.75 mm. The ovoids were included within the volume of interest, so the range of displacements reported in the results also applies to the ovoids. Averaged over all patients, 98% of the calculated displacements was smaller than the resolution of the MR image (<0.7 mm). The displacements calculated with the in vivo B<sub>0</sub> field maps were comparable to the



displacement found in our previous study in the phantom and the small patient set ( $n=4$ ).<sup>15</sup> In an earlier study, Kim et al. found displacements up to 1.5 mm at the tip of the applicator.<sup>14</sup> However, in their study a titanium applicator was considered, which will lead to higher susceptibility differences as compared to a plastic applicator. In our current study a plastic applicator with plastic needles was evaluated, which resulted in smaller displacements.

To determine the impact of the image distortion, scans acquired with opposing readout direction were used to reconstruct the applicator, and the DVH parameters for the  $CTV_{HR}$  and the bladder and rectum were recalculated with the corresponding shift. With this method, we evaluated a worst-case scenario, since the displacement is overestimated with a factor two. It was not possible to separate the impact of the ovoids and the IUD on the DVH parameters, since the applicator was repositioned on  $MR_{opposing}$  based on the appearance of the whole applicator.

There are several uncertainties related to BT planning which may lead to a difference between planned and delivered dose. The implications of these uncertainties for the delivered dose and the clinical outcome were already investigated in multiple studies.<sup>12,13,25-27</sup> As shown by Nesvacil et al.<sup>26</sup>, random dosimetric uncertainty due to intra- and interfraction anatomical variation is in the order of 10% for  $D_{90}$  of the  $CTV_{HR}$  and 20% for the  $D_{2cm3}$  of the OAR. Image distortions on the planning images, as investigated in this study, lead to systematic dose errors persistent during the whole treatment. The uncertainty in applicator reconstruction resulting from the image distortions leads to a systematic dose error of at the most 4.7% for  $D_{98}$ , and 6.3% for the OAR.

The dose variation we found is in agreement with the study of Tanderup et al.<sup>12</sup>, who reported the mean DVH difference per mm of applicator displacement over 20 patients. They found that 1 mm of applicator displacement in the anterior-posterior direction resulted in a mean difference of 5% for bladder and rectum  $D_{2cm3}$ , while the mean difference in  $D_{90}$  of the  $CTV_{HR}$  was found to be less than 2% for 1 mm displacements. In their study, 10% was considered an acceptable deviation from the planned DVH parameters, which means a delivered dose of >90% of the planned dose to the target and <110% for the OAR. In our study, the dose to the target was, even for the worst case, at least 95.3% of the planned target dose, and for the OAR this was at most 106%. The effect on the total treatment dose from EBRT and BT was small, since the decrease in target dose ( $D_{98}/D_{90}$ ) was <1.1 Gy, and the increase in OAR  $D_{2cm3}$  was <1.5 Gy. Thus, our results show in a definite way that 3 T MRI can be used for applicator reconstruction.



A limitation of our study is that two scans with opposing readout direction are used, instead of an undistorted and a distorted image. As indicated, the shift that is necessary to realign the applicator is actually two times the displacement caused by  $B_0$  inhomogeneity. We chose not to shift the applicator only half as far as necessary. By shifting the applicator with only half the observed shift, the location of the applicator could not be verified using the available images and this could lead to additional errors being introduced. Our method will lead to an overestimation of the impact on the dose. Since the displacement caused by  $B_0$  inhomogeneity is twice as small as the shift necessary to realign the applicator and dose fall-off around the applicator is proportional to  $1/r$  for a line-source<sup>28</sup>, the actual dosimetric impact will not be close to 6.3% but 2-3%. Near the ovoids the geometry of the applicator is not exactly like a line source, and the fall-off is better modeled as  $1/r^2$ . The dosimetric impact would be even smaller in that area.

Another limitation of our study is that the opposing readout images do not only reflect distortions solely due to  $B_0$  inhomogeneity. The displacements could also reflect patient movement in between the scans, with a time between the scans of typically 4-5 minutes. However, on these short time frames dose variations due to patient movement and organ filling can be considered negligible.<sup>29</sup> The referenced study investigated HDR brachytherapy, but the results also apply to PDR brachytherapy.<sup>26</sup>

## Conclusion

For the plastic Utrecht Interstitial CT/MR applicator displacements are small in vivo for the MR sequence under consideration. The dosimetric impact to the DVH parameters of  $CTV_{HR}$  and bladder and rectum is limited (<6.3%). For this plastic applicator with plastic needles, applicator reconstruction for BT planning purposes is feasible at 3 T MRI.

## Acknowledgements

This work was funded by Elekta Brachytherapy (II 250008).

## References

- [1] Hegazy N, Pötter R, Kirisits C, Berger D, Federico M, Sturdza A, et al. High-risk clinical target volume delineation in CT-guided cervical cancer brachytherapy: Impact of information from FIGO stage with or without systematic inclusion of 3D documentation of clinical gynecological examination. *Acta Oncol* 2013;52:1345–52.
- [2] Krempien RC, Daeuber S, Hensley FW, Wannenmacher M, Harms W. Image fusion of CT and MRI data enables improved target volume definition in 3D-brachytherapy treatment planning. *Brachytherapy* 2003;2:164–71.
- [3] Dimopoulos JCA, Petrow P, Tanderup K, Petric P, Berger D, Kirisits C, et al. Recommendations from Gynaecological (GYN) GEC-ESTRO Working Group (IV): Basic principles and parameters for MR imaging within the frame of image based adaptive cervix cancer brachytherapy. *Radiother Oncol* 2012;103:113–22.
- [4] Dinkla AM, Pieters BR, Koedoodeer K, van Wieringen N, van der Laarse R, van der Grient JN, et al. Improved tumour control probability with MRI-based prostate brachytherapy treatment planning. *Acta Oncol* 2013;52:658–65.
- [5] Jezzard P, Balaban RS. Correction for geometric distortion in echo planar images from B(0) field variations. *Magn Reson Med* 1995;34:65–73.
- [6] Haack S, Nielsen SK, Lindegaard JC, Gelineck J, Tanderup K. Applicator reconstruction in MRI 3D image-based dose planning of brachytherapy for cervical cancer. *Radiother Oncol* 2009;91:187–93.
- [7] Dempsey C, Arm J, Best L, Govindarajulu G, Capp A, O'Brien P. Optimal single 3T MR imaging sequence for HDR brachytherapy of cervical cancer. *J Contemp Brachytherapy* 2014;6:3–9.
- [8] Han K, Croke J, Foltz W, Metser U, Xie J, Shek T, et al. A prospective study of DWI, DCE-MRI and FDG PET imaging for target delineation in brachytherapy for cervical cancer. *Radiother Oncol* 2016;120:519–25.
- [9] Kharofa J, Morrow N, Kelly T, Rownd J, Paulson E, Rader J, et al. 3-T MRI-based adaptive brachytherapy for cervix cancer: Treatment technique and initial clinical outcomes. *Brachytherapy* 2014;13:319–25.
- [10] Kataoka M, Kido A, Koyama T, Isoda H, Umeoka S, Tamai K, et al. MRI of the female pelvis at 3T compared to 1.5T: Evaluation on high-resolution T2-weighted and HASTE images. *J Magn Reson Imaging* 2007;25:527–34.
- [11] De Leeuw AAC, Moerland MA, Nomden C, Tersteeg RHA, Roesink JM, Jürgenliemk-Schulz IM. Applicator reconstruction and applicator shifts in 3D MR-based PDR brachytherapy of cervical cancer. *Radiother Oncol* 2009;93:341–6.
- [12] Tanderup K, Hellebust TP, Lang S, Granfeldt J, Pötter R, Lindegaard JC, et al. Consequences of random and systematic reconstruction uncertainties in 3D image based brachytherapy in cervical cancer. *Radiother Oncol* 2008;89:156–63.
- [13] Schindel J, Zhang W, Bhatia SK, Sun W, Kim Y. Dosimetric impacts of applicator

- displacements and applicator reconstruction-uncertainties on 3D image-guided brachytherapy for cervical cancer. *J Contemp Brachytherapy* 2013;5:250–7.
- [14] Kim Y, Muruganandham M, Modrick JM, Bayouth JE. Evaluation of artifacts and distortions of titanium applicators on 3.0-tesla MRI: Feasibility of titanium applicators in MRI-guided brachytherapy for gynecological cancer. *Int J Radiat Oncol Biol Phys* 2011;80:947–55.
- [15] van Heerden LE, Gurney-Champion OJ, van Kesteren Z, Houweling AC, Koedooder C, Rasch CRN, et al. Quantification of image distortions on the Utrecht interstitial CT/MR brachytherapy applicator at 3T MRI. *Brachytherapy* 2016;15:118–26.
- [16] Soliman AS, Elzibak A, Easton H, Kim JY, Han DY, Safigholi H, et al. Quantitative MRI assessment of a novel direction modulated brachytherapy tandem applicator for cervical cancer at 1.5T. *Radiother Oncol* 2016;120:500–6.
- [17] Gurney-Champion OJ, Bruins Slot T, Lens E, van der Horst A, Klaassen R, van Laarhoven HWM, et al. Quantitative assessment of biliary stent artifacts on MR images: Potential implications for target delineation in radiotherapy. *Med Phys* 2016;43:5603–15.
- [18] Nomden CN, de Leeuw AAC, Moerland MA, Roesink JM, Tersteeg RJHA, Jürgenliemk-Schulz IM. Clinical Use of the Utrecht Applicator for Combined Intracavitary/Interstitial Brachytherapy Treatment in Locally Advanced Cervical Cancer. *Int J Radiat Oncol* 2012;82:1424–30.
- [19] Pötter R, Haie-Meder C, Van Limbergen E, Barillot I, De Brabandere M, Dimopoulos J, et al. Recommendations from gynaecological (GYN) GEC ESTRO working group (II): concepts and terms in 3D image-based treatment planning in cervix cancer brachytherapy-3D dose volume parameters and aspects of 3D image-based anatomy, radiation physics, radiobiology. *Radiother Oncol* 2006;78:67–77.
- [20] International Commission on Radiation Units and Measurements. Prescribing, Recording, and Reporting Brachytherapy for Cancer of the Cervix (ICRU report 89). vol. 13. 2013.
- [21] Gurney-Champion OJ, Lens E, van der Horst A, Houweling AC, Klaassen R, van Hooft JE, et al. Visibility and artifacts of gold fiducial markers used for image guided radiation therapy of pancreatic cancer on MRI. *Med Phys* 2015;42:2638–47.
- [22] Froeling M, Nederveen AJ, Heijtel DFR, Lataster A, Bos C, Nicolay K, et al. Diffusion-tensor MRI reveals the complex muscle architecture of the human forearm. *J Magn Reson Imaging* 2012;36:237–48.
- [23] Herráez MA, Burton DR, Lalor MJ, Gdeisat MA. Fast two-dimensional phase-unwrapping algorithm based on sorting by reliability following a noncontinuous path. *Appl Opt* 2002;41:7437–44.
- [24] Nomden CN, de Leeuw AAC, Roesink JM, Tersteeg RJHA, Westerveld H, Jürgenliemk-Schulz IM. Intra-fraction uncertainties of MRI guided brachytherapy

- in patients with cervical cancer. *Radiother Oncol* 2014;112:217–20.
- [25] Kirisits C, Rivard MJ, Baltas D, Ballester F, De Brabandere M, van der Laarse R, et al. Review of clinical brachytherapy uncertainties: analysis guidelines of GEC-ESTRO and the AAPM. *Radiother Oncol* 2014;110:199–212.
- [26] Nesvacil N, Tanderup K, Hellebust TP, De Leeuw A, Lang S, Mohamed S, et al. A multicentre comparison of the dosimetric impact of inter- and intra-fractional anatomical variations in fractionated cervix cancer brachytherapy. *Radiother Oncol* 2013;107:20–5.
- [27] Nesvacil N, Tanderup K, Lindegaard JC, Pötter R, Kirisits C. Can reduction of uncertainties in cervix cancer brachytherapy potentially improve clinical outcome? *Radiother Oncol* 2016;120:390–6.
- [28] Bevelacqua JJ. Appendix II: Basic Source Geometries and Attenuation Relationships. *Contemp. Heal. Phys. Probl. Solut.* 2nd ed., Weinheim, Germany: Wiley-VCH Verlag GmbH & Co. KGaA; 2009, p. 368–75.
- [29] Nomden CN, de Leeuw AAC, Roesink JM, Tersteeg RJHA, Westerveld H, Jürgenliemk-Schulz IM. Intra-fraction uncertainties of MRI guided brachytherapy in patients with cervical cancer. *Radiother Oncol* 2014;112:217–20.





# Chapter 4

Structure-based deformable image registration: added value for dose accumulation of external beam radiotherapy and brachytherapy in cervical cancer

L.E. van Heerden, A.C. Houweling, C. Koedooder, Z. van Kesteren, N. van Wieringen, C.R.N. Rasch, B.R. Pieters, A. Bel.

Department of Radiation Oncology, Amsterdam UMC, University of Amsterdam, location AMC, Meibergdreef 9, 1105 AZ Amsterdam, The Netherlands

Published in: Radiotherapy and Oncology 2017;123:319-324

## **Abstract**

### ***Purpose***

Structure-based deformable image registration (DIR) can be used to calculate accumulated brachytherapy (BT) and external-beam radiation therapy (EBRT) dose-volume histogram (DVH) parameters in cervical cancer. Since direct parameter addition does not take dose non-uniformity into account, the added value of DIR over addition methods was investigated for bladder and rectum.

### ***Materials and Methods***

For twelve patients (EBRT:46 Gy, EBRT+BT: $D_{90}$  85-90 Gy<sub>EQD2</sub> in equivalent dose in 2 Gy fractions) the EBRT planning CT and BT planning MRI were registered using DIR. Affected lymph nodes, located far from the BT boost region, received an EBRT boost (9.2 Gy) not contributing to the BT boost dose. Cumulative bladder/rectum  $D_{2\text{cm}^3}/D_{1\text{cm}^3}$  were calculated and compared to direct addition methods, assuming uniform EBRT doses (UD), or overlapping high dose volumes (OHD).

### ***Results***

Between the three methods, the maximum differences in the cumulative DVH parameters were 3.2 Gy<sub>EQD2</sub> (bladder) and 3.3 Gy<sub>EQD2</sub> (rectum). The difference between DIR and UD was <1.8 Gy<sub>EQD2</sub> for both organs.

### ***Conclusions***

The UD method provides a better estimate of  $D_{2\text{cm}^3}/D_{1\text{cm}^3}$  than the OHD method. There is no added value of DIR since differences with direct addition methods are clinically insignificant. EBRT dose distributions can be considered uniform in bladder and rectum for the evaluated dose parameters.



## Introduction

For locally-advanced cervical cancer, concurrent radiotherapy and chemotherapy is the standard of care. The radiation treatment typically combines external beam radiotherapy (EBRT) with a brachytherapy (BT) boost to the tumor area using an intracavitary/interstitial applicator. The recommended EBRT dose to the target is 45-50 Gy in 1.8-2.0 Gy/fraction<sup>1</sup>, with a BT boost up to a total dose of at least 90 Gy<sub>EQD2</sub>, expressed as equivalent dose in 2 Gy fractions (EQD2), to 70% of the clinical target volume (CTV) at high risk. To spare the bladder and rectum, the minimum cumulative dose from EBRT and BT, to the most irradiated 2 cm<sup>3</sup> (D<sub>2cm3</sub>) should not exceed 90 Gy<sub>EQD2</sub> and 75 Gy<sub>EQD2</sub> for these organs respectively.

According to GEC-ESTRO recommendations, a straightforward summation of the EBRT prescription dose and the BT DVH parameters is adequate to predict toxicity in the organs-at-risk (OARs). The underlying assumption of this so-called uniform dose (UD) method, is that the EBRT dose to the OARs can be considered as uniform and equal to the prescription dose.<sup>2</sup> However, intensity-modulated radiotherapy (IMRT) and volumetric-modulated arc therapy (VMAT) are used increasingly to create highly conformal dose distributions, resulting in non-uniform EBRT dose distributions in the OARs (Fig. 1, left panel). Alternatively, a number of previous investigations evaluated cumulative doses by assuming overlapping high dose volumes for both treatments,<sup>3,4</sup> denoted as the OHD method, the worst-case scenario. Since the UD/OHD methods do not take non-uniformity in OAR doses into account, this may cause the cumulative D<sub>2cm3</sub> and D<sub>1cm3</sub> to be underestimated/overestimated at the time of BT planning. It may therefore be preferable to sum the 3D dose distributions instead.

3D doses can be accumulated by matching the planning images of EBRT and BT (CT and/or MR). Accumulated doses for cervical cancer patients were previously evaluated by registering the planning images using rigid registration.<sup>3,5</sup> However, the accuracy of the cumulative DVH parameters using rigid registration is limited since organ deformations due to the applicator and/or rectum/bladder filling are not considered. As a possible solution, several deformable image registration (DIR) algorithms have been investigated.<sup>3,4,6,7</sup> Planning images of EBRT and brachytherapy in gynecological cancer were registered for dose warping with deformable image matching. These studies compare cumulative DVH parameters calculated using DIR with either the UD or the OHD method.

Deformable matching is often based on image intensity values,<sup>3,4,6,7</sup> but this remains challenging and may lead to physically impossible solutions.<sup>4,7,8</sup> Structure-based DIR requires organ delineation but reduces the influence of different imaging modalities. Since the ob-

jective of structure-based DIR is to decrease the distance between points on the moving and reference contours, it is most reliable near the structure edges, making DIR most suitable for hollow organs like bladder and rectum. Several studies show that structure-based matching performs better than intensity-based matching in the bladder<sup>8-11</sup> and rectum.<sup>11</sup>

Jamema et al.<sup>8</sup> performed 3D dose addition of multiple BT fractions in cervical cancer using intensity-based DIR and compared this to structure-based DIR. They reported that intensity-based DIR may underestimate doses due to implausible DIR. Andersen et al.<sup>12</sup> used a structure-based, biomechanical DIR algorithm to compare cumulative DVH parameters in the bladder to the UD method for fractionated BT. However, there is currently no study exploring the added value of structure-based DIR to the UD/OHD methods for dose accumulation of EBRT/BT doses in both bladder and rectum.

The aim of the present study is therefore to investigate accumulated BT and EBRT 3D doses by calculating cumulative DVH parameters in the bladder and rectum using structure-based DIR and compare this to the uniform dose method and the overlapping high dose method.

## Materials and Methods

### *Patients and treatment*

Twelve consecutive patients treated for locally-advanced cervical carcinoma (FIGO stages IIA-IIIB) were investigated in this study. Patients were irradiated using VMAT, receiving 46 Gy in daily fractions of 2 Gy. Two patients received an additional simultaneous-integrated boost (SIB) of 0.4 Gy per fraction to affected lymph nodes in the common iliac region. These nodes were located in the region between the aortic bifurcation and above the internal/external iliac, and the dose to these nodes will not contribute to the BT boost region. For the VMAT and VMAT+SIB plan the same bladder and rectum dose constraints were considered during plan evaluation. The CTV consists of gross tumor volume (GTV), cervix, parametrium, corpus-uterus and the upper part of the vagina, expanded with a 10 mm isotropic margin. The planning target volume (PTV) consisted of the CTV with an 8 mm margin including the lymph nodes. The planning aims for EBRT stated that  $\geq 99\%$  of the PTV should receive  $\geq 95\%$  of the prescription dose, with a conformity index ( $V_{95}/\text{PTV volume}$ )  $< 1.35$ . A hotspot criterion was used for bladder and rectum ( $D_{1\text{cm}^3} < 103\%$  of the prescription dose). The dose fall-off region from 45-22.5 Gy was aimed to be  $< 1.2$  cm.

All patients received a pulsed-dose rate BT boost. A dose of 24 Gy in pulse doses of 1 Gy every hour was delivered to the high-risk CTV (CTV<sub>HR</sub>). The radiotherapy techniques are described in Table 1, while typical EBRT and BT dose distributions are shown in Fig. 1. The BT dose was planned with the applicator in situ, using a library for applicator reconstruction, after which the plan was manually optimized. On the CT and MRI scans, the total bladder volume was delineated and the rectum was delineated from the rectosigmoid junction to the level of the anal sphincter. For EBRT, patients were instructed to have a full bladder daily, while a catheter was inserted for BT. Bladder and rectum volumes at the time of EBRT and BT are described in Table 2.

**Table 1** Radiotherapy techniques for EBRT and PDR BT

	External Beam Radiation Therapy	Brachytherapy
Treatment type	VMAT	PDR
Treatment planning system	Oncentra 4.3 (Elekta AB, Stockholm, Sweden)	Oncentra Brachy 4.5 (Elekta AB, Stockholm, Sweden)
Dose calculation algorithm	Collapsed Cone using CT HU values	Based on the TG-43 formalism
Imaging	CT images	T <sub>2</sub> -weighted Turbo Spin Echo MRI
Scanner specification	LightSpeed RT16 (GE, WI, USA)	Ingenia 3 T (Philips Healthcare, Best, The Netherlands)
Imaging resolution (mm <sup>3</sup> )	1.2 x 1.2 x 3	0.7 x 0.7 x 3.3
Dose calculation grid size (mm <sup>3</sup> )	3 x 3 x 3	1 x 1 x 1
Planning aims	PTV V <sub>95</sub> ≥ 99% Bladder V <sub>45Gy</sub> < 40%; Rectum V <sub>40Gy</sub> < 70%; Bladder + Rectum D <sub>1cm<sup>3</sup></sub> < 103%	CTV <sub>HR</sub> D <sub>90</sub> 85-90 Gy <sub>EQD2</sub> Bladder / rectum D <sub>2cm<sup>3</sup></sub> < 80/65 Gy <sub>EQD2</sub>

PTV: planning target volume;

CTV: clinical target volume at high risk;

D<sub>90</sub>: dose received by 90% of the volume;

V<sub>95</sub>: the percentage of the volume receiving ≥ 95% of the prescription dose;

V<sub>45Gy</sub> / V<sub>40Gy</sub>: the percentage of the volume receiving ≥ 45/40 Gy;

D<sub>2cm<sup>3</sup></sub> / D<sub>1cm<sup>3</sup></sub>: dose to the most irradiated 2 cm<sup>3</sup> / 1 cm<sup>3</sup>)



**Table 2** The mean and the range over all patients of the bladder and rectum volume at the time of external beam radiation therapy (EBRT) and brachytherapy (BT), and the difference between the EBRT and BT volumes.

	<b>Bladder Mean (Range)</b>	<b>Rectum Mean (Range)</b>
<b>EBRT volume (cm<sup>3</sup>)</b>	299 (115;564)	100 (29;167)
<b>BT volume (cm<sup>3</sup>)</b>	85 (59;196)	51 (28;82)
<b>EBRT – BT Volume difference (cm<sup>3</sup>)</b>	222 (39;465)	59 (6;129)

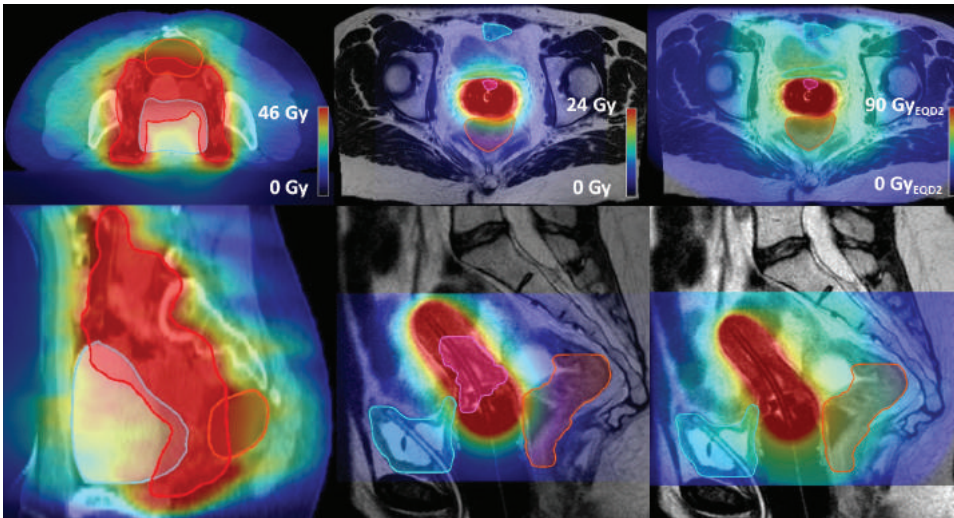


**Fig. 1** Axial and sagittal view of a patient CT/MRI with a color wash of the planned VMAT/BT dose and the accumulated dose from EBRT and BT. The EBRT dose is not uniform in proximity of the bladder/rectum walls (blue/orange) closest to the target.

***Study-specific image preparation***

The EBRT and BT doses were converted to EQD<sub>2</sub> on a voxel-by-voxel level (Matlab R2014b, Mathworks Inc., MA), using LQ-model based equations with an  $\alpha/\beta$  value of 3 Gy for late OAR toxicity and a 1.5 hour repair half-time.<sup>2,13</sup>

***Deformable image registration***

The Feature-Based Deformable Registration (FBDR) tool, available in a research version of Oncentra Brachy (Elekta Brachytherapy, Veenendaal, The Netherlands) was used for struc-

ture-based DIR with the EBRT CT as the reference frame. The DIR algorithm in the FBDR tool is directly derived from the symmetric unidirectional thin plate spline robust point matching algorithm.<sup>14-16</sup> A symmetric DIR method has the advantage that the change of anatomy is independent of the order in which images are registered.<sup>17</sup> Delineated structures were converted to 3D surface meshes, and a mapping was established to propagate elements on the primary (EBRT) reference surface to the secondary (BT) surface. For each patient, we performed two registrations for bladder and rectum separately to improve the quality of each registration in the proximity of the evaluated organ.

### ***Dose accumulation***

For both organ-specific matches, the deformation field obtained with DIR was used to inversely map the EBRT dose distribution and organ contour to the frame of reference of the BT dose distribution. Finally, the propagated EBRT/BT doses were summed to create the accumulated dose (Fig. 1, right panel).

### ***DIR accuracy***

The Dice Similarity Coefficient (DSC)<sup>18</sup> was used to compare the propagated and reference contours. DSC quantifies the spatial overlap of the matched bladder and rectum. Additionally, the surface distance error (SDE) was determined for every voxel of each bladder/rectum, which is the Euclidean distance between the reference and propagated contours.<sup>10,19</sup> Mean DSC and range over all patients were calculated. The 25<sup>th</sup>, 50<sup>th</sup>, 75<sup>th</sup> and 95<sup>th</sup> percentile of the SDEs were computed for all bladders/rectums. Finally the percentage of points with an SDE < 3 mm (the EBRT dose grid resolution) was calculated.

### ***Data analysis***

Bladder and rectum  $D_{2\text{cm}^3}/D_{1\text{cm}^3}$  were acquired for the three dose accumulation methods (Fig. 2) using VelocityAI (version 3.1.0, Velocity Medical, GA). For the DIR method,  $D_{2\text{cm}^3}/D_{1\text{cm}^3}$  were calculated from the accumulated dose distributions for both rectum and bladder. For the UD method, the cumulative  $D_{2\text{cm}^3}/D_{1\text{cm}^3}$  were calculated by adding the prescription dose of 46 Gy to  $D_{2\text{cm}^3}/D_{1\text{cm}^3}$  from the BT boost. For the OHD method, a summation of  $D_{2\text{cm}^3}/D_{1\text{cm}^3}$  from EBRT and the BT boost was performed. For the three methods, the mean and range of  $D_{2\text{cm}^3}/D_{1\text{cm}^3}$  of bladder and rectum were calculated over all patients.

## Results

### Cumulative DVH parameters

The mean and range of  $D_{2\text{cm}^3}/D_{1\text{cm}^3}$  was calculated for bladder and rectum (Table 3). For the bladder, maximum absolute differences in  $D_{2\text{cm}^3}/D_{1\text{cm}^3}$  were 1.8/1.1  $\text{Gy}_{\text{EQD2}}$  (UD vs. DIR), and 3.2/3.3  $\text{Gy}_{\text{EQD2}}$  (OHD vs. DIR). In the rectum, maximum absolute differences were 1.7/1.6  $\text{Gy}_{\text{EQD2}}$  (UD vs. DIR) and 2.2/2.3  $\text{Gy}_{\text{EQD2}}$  (OHD vs. DIR). Individual patient results can be found in Fig. 3.

### DIR accuracy

The bladder DSC, averaged over all patients, was 0.98 (0.97-0.99). The average rectum DSC was 0.94 (0.89-0.98).

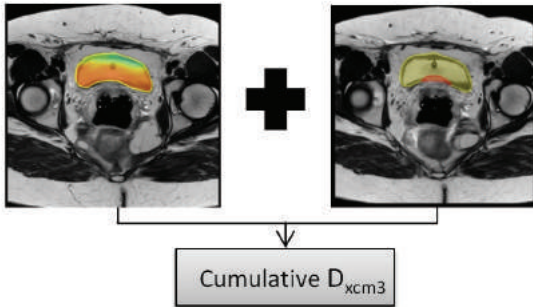
For the bladder, the average 95<sup>th</sup> percentile of the SDE was 1.3 mm (0.7-1.5 mm), ranging between 0.7-1.5 mm. For the rectum, the average 95<sup>th</sup> percentile of the SDE over all patients was 3.5 mm (1.0-6.4 mm). Individual patient results are shown in Fig 4.

Averaged over all patients, bladder/rectum structures had SDE values < 3 mm for 98%/87% of the points. In Fig. 5, visualization is presented of the rectum match for patient 3 (DSC = 0.89, 95<sup>th</sup> percentile = 6.4 mm) and patient 10 (DSC = 0.95, 95<sup>th</sup> percentile = 3.7 mm).

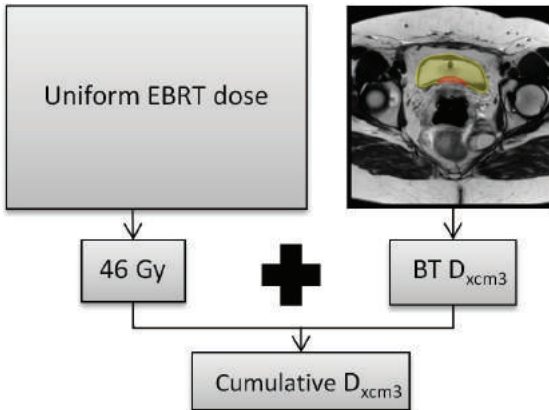
**Table 3** The mean and the range over all patients of the planned cumulative  $D_{2\text{cm}^3}$  and  $D_{1\text{cm}^3}$  calculated with the DIR method, UD and OHD method, and the difference  $\Delta D_{2\text{cm}^3}$  and  $\Delta D_{1\text{cm}^3}$  with the DIR method, in bladder and rectum.

Bladder			
Method	DIR Mean (Range)	Uniform dose Mean (Range)	Overlapping high dose Mean (Range)
$D_{2\text{cm}^3}(\text{Gy}_{\text{EQD2}})$	69.8 (58.1;81.1)	69.7(56.6;80.9)	71.6 (59.9;84.0)
$\Delta D_{2\text{cm}^3}(\text{Gy}_{\text{EQD2}})$	-	0.1(-1.8;-1.5)	-1.8 (-3.2;-1.0)
$D_{1\text{cm}^3}(\text{Gy}_{\text{EQD2}})$	73.6 (60.5;84.2)	73.4(59.4;84.0)	75.6 (63.0;87.6)
$\Delta D_{1\text{cm}^3}(\text{Gy}_{\text{EQD2}})$	-	0.2(-0.8;1.1)	-2.0 (-3.3;-0.9)
Rectum			
Method	DIR Mean (Range)	Uniform dose Mean (Range)	Overlapping high dose Mean (Range)
$D_{2\text{cm}^3}(\text{Gy}_{\text{EQD2}})$	59.6 (51.6;67.4)	60.0 (50.6;68.6)	60.7 (53.0;69.2)
$\Delta D_{2\text{cm}^3}(\text{Gy}_{\text{EQD2}})$	-	-0.4 (-1.7;1.1)	-1.1 (-2.2;-0.6)
$D_{1\text{cm}^3}(\text{Gy}_{\text{EQD2}})$	62.1 (52.0;71.8)	62.4 (51.0;72.0)	63.4 (53.8;73.8)
$\Delta D_{1\text{cm}^3}(\text{Gy}_{\text{EQD2}})$	-	-0.3 (-1.6;0.9)	-1.3 (-2.3;-0.6)

**A 3D dose addition with DIR**



**B Uniform Dose**



**C Overlapping High Dose volumes**

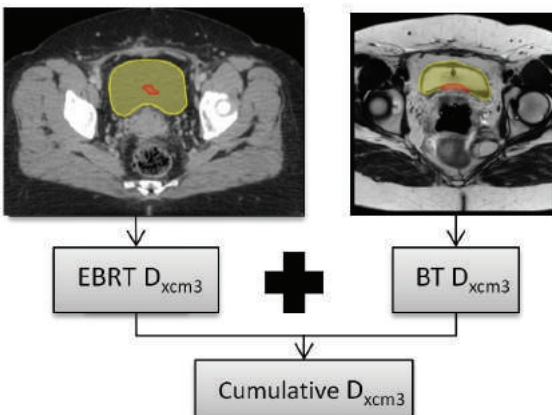


**Fig. 2** The cumulative  $D_{xcm3}$  in the bladder (yellow) is calculated using three methods.

A) For 3D addition with DIR,  $D_{xcm3}$  is calculated from the cumulative 3D dose.

B) For the uniform dose (UD) method, the  $D_{xcm3}$  is calculated in the BT structure (red) and added to the EBRT prescription dose.

C) For the overlapping high dose (OHD) method  $D_{xcm3}$  is calculated separately for EBRT (red) and BT (red) and then added to obtain the cumulative  $D_{xcm3}$ .

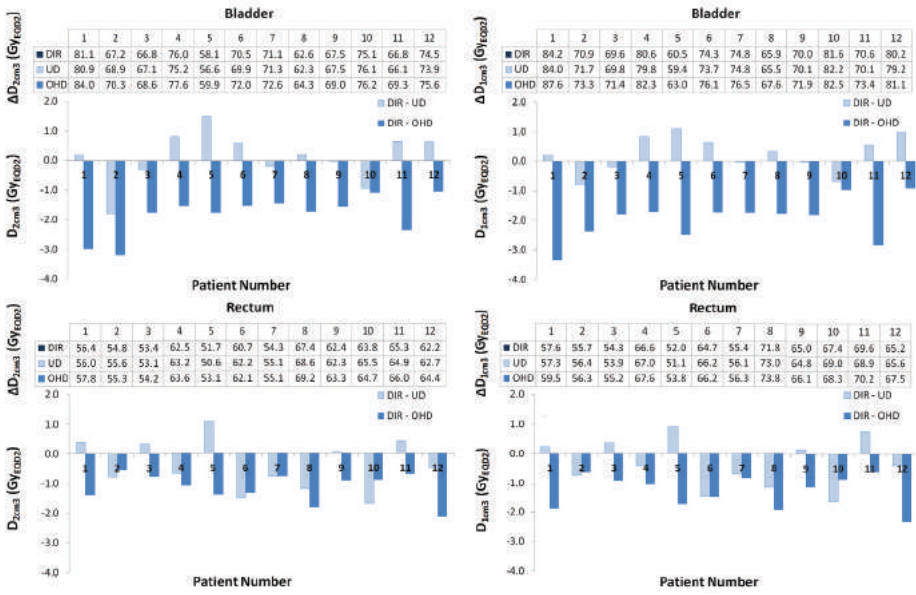


**Fig. 3** The planned cumulative  $D_{2cm3}$  and  $D_{1cm3}$  calculated with the DIR method, UD method and OHD method for bladder and rectum. For visualization, the difference in  $D_{2cm3}$  and  $D_{1cm3}$  of the DIR method with the UD method and OHD method ( $\Delta D_{2cm3}$  and  $\Delta D_{1cm3}$ ) are plotted.

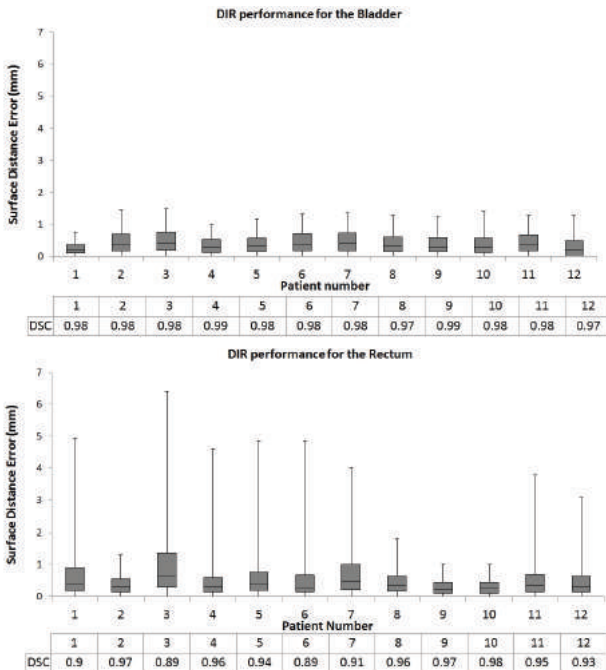


**Fig. 4** Boxplot of the surface distance errors with the 25<sup>th</sup>, 50<sup>th</sup>, 75<sup>th</sup> and 95<sup>th</sup> percentile for all patients in bladder and rectum.



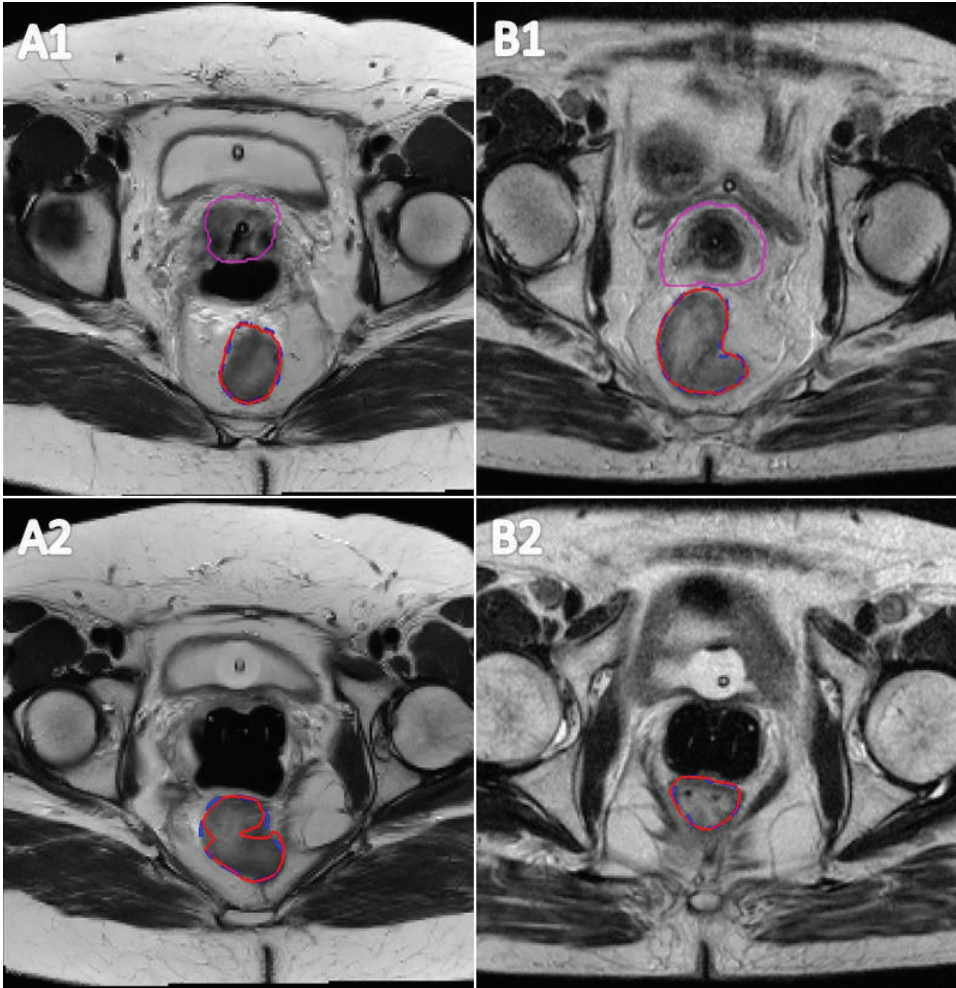


**Fig. 5** Axial view of the BT MRI where the propagated rectum contour (solid) is shown together with the reference contour (dashed). The contours are shown either close to the target (magenta) (patient 3: A1, patient 10: B1), or on different MR images located caudally (patient 3: A2, patient 10: B2).

## Discussion

The present study is the first to use structure-based DIR to evaluate cumulative DVH parameters in combined EBRT and BT treatment for cervical cancer for bladder and rectum. The results were compared to UD and OHD methods. The difference in cumulative  $D_{2\text{cm}^3}/D_{1\text{cm}^3}$  in the bladder and rectum was always  $<1.8 \text{ Gy}_{\text{EQD2}}$  (UD vs. DIR) and  $<3.3 \text{ Gy}_{\text{EQD2}}$  (OHD vs. DIR). The results of our study suggest that, even for highly conformal dose distributions (VMAT), EBRT dose distributions can be considered uniform in the rectum and bladder for evaluation of cumulative  $D_{2\text{cm}^3}/D_{1\text{cm}^3}$ .

The DIR method was used to benchmark assumptions made with other methods. By comparing DIR to UD, differences in  $D_{2\text{cm}^3}/D_{1\text{cm}^3}$  were always  $<1.8 \text{ Gy}_{\text{EQD2}}$ . This shows that planned EBRT dose distributions were indeed uniform at the location of the high dose volumes. The OHD method overestimated  $D_{2\text{cm}^3}/D_{1\text{cm}^3}$  with differences up to  $3.3 \text{ Gy}_{\text{EQD2}}$  in all cases as compared to DIR, showing that the high dose volumes did not overlap for the evaluated dose distributions of EBRT and BT, and that the worst case scenario did not occur.

The differences in cumulative  $D_{2\text{cm}^3}/D_{1\text{cm}^3}$  between DIR and the other two methods were relatively small. In a study by Georg et al.<sup>20</sup> the dose response for OARs in cervical cancer was modeled. The cumulative  $D_{2\text{cm}^3}/D_{1\text{cm}^3}$  were calculated using the UD method in the bladder and rectum for patients receiving EBRT and BT, and related to the incidence of late effects. For the cumulative dose values found in this study, the risk of late effects remained within 5-10%, regardless of dose differences between the methods of up to  $3.2 \text{ Gy}_{\text{EQD2}}$ . Since dose differences between the methods are not clinically relevant, DIR provides no added value and at the time of BT planning the UD method is sufficient for evaluation of cumulative  $D_{2\text{cm}^3}/D_{1\text{cm}^3}$  to predict organ toxicity.

DIR accuracy was evaluated by calculating the DSC and SDE distributions. Although a high DSC was reached in both organs, it was, on average, higher in the bladder (0.97) compared to the rectum (0.94). The SDE distribution showed that the distance between points on the matched contours was small after DIR (75<sup>th</sup> percentile  $<0.6/0.7 \text{ mm}$  for bladder/rectum) compared to the imaging resolution of the planning scans (CT =  $1.2 \times 1.2 \times 3 \text{ mm}^3$ , MRI =  $0.7 \times 0.7 \times 3.3 \text{ mm}^3$ ). Since EBRT doses were calculated with a  $3 \times 3 \times 3 \text{ mm}^3$  resolution, dose points warped at this precision or lower were considered reliable. For the worst bladder/rectum match, only 3%/5% of the points had an SDE  $> 3 \text{ mm}$ , showing that the DIR algorithm is able to match the bladder and rectum contours with high accuracy.

For the evaluation of  $D_{2\text{cm}^3}/D_{1\text{cm}^3}$ , it is relevant to know whether mismatches are located near the BT boost region. Detailed analysis showed that for the patient with the worst rec-

tum match, this mismatch was not near the target, but more caudally (Fig. 5).

However, implications for accumulated  $D_{2\text{cm}^3}/D_{1\text{cm}^3}$  are limited even if the mismatch is near the high dose region. As a result of both the large PTV margin and the planning aims, the variation of the EBRT dose near the BT high dose volumes in bladder and rectum is small, limiting the dose warping error to 3%.

Previous research already investigated 3D accumulated doses with rigid registration<sup>5</sup> and different DIR methods<sup>3,4,6,7</sup>. In these studies, the intensity values of the images were used to register planning images of EBRT and BT in gynecological cancer for dose warping. However, with structure-based DIR, it is possible to reach a higher DSC and better accuracy than with other DIR methods<sup>8,9</sup>. Additionally, registering the organs separately and assessing the dose only in the matched region further improves the accuracy of the match. In the aforementioned studies, the dose was propagated only once and evaluated for all organs, decreasing the dose summation accuracy. In addition, not all studies have extensively evaluated the accuracy of deformable registration. A potential limitation of our study is that the quality of the delineations is limited by the different imaging modalities, as well as the (axial) resolution of the images. Regardless of the differences in methods, our results are consistent with earlier studies using DIR that found variations  $<5\%$  for  $D_{2\text{cm}^3}/D_{1\text{cm}^3}$  between the methods. This shows that there is no clinically relevant difference between the DIR method, and the UD/OHD method.

For patients 1 and 5, the affected nodes could not be reached by BT and were therefore treated with an additional SIB. Small differences were found with the UD method ( $<1.5 \text{ Gy}_{\text{EQD2}}$ ). For the patients in our study, EBRT dose uniformity near the location of the BT boost was specifically addressed by setting a hotspot criterion during planning. When the boosted nodes are located closer to the target (e.g. obturator lymph nodes) care should be taken that the EBRT dose near the BT high dose region is still uniform. For the select group of patients where dose spillage from the SIB into the region of the BT boost cannot be avoided because the lymph nodes are very close to the BT boost, DIR might have added value over the UD method.

It should be noted that the value of DSC and SDE as accuracy metrics is limited. Using structure-based DIR, a high DSC is typically reached since the optimization strives to increase the overlap of reference structure and propagated structure. Similarly, the SDE does not measure voxel-to-voxel agreements, but solely provides information about the remaining distance between the structure surfaces. No information is provided about the accuracy within the organ. For the present study, however, this does not affect the results. The

bladder and rectum are hollow organs for which only the organ wall is clinically relevant, and DIR accuracy within the organ is not relevant. For non-hollow organs like the target, markers within the organ could be used to assess the registration accuracy.<sup>14,21</sup>

As of yet no anatomical landmarks were used to evaluate the DIR, since these are difficult to detect in bladder and rectum. A separate verification for this same algorithm using lipiodol markers on the bladder showed that there was a remaining error in marker distance in the bladder of 0.9-4.0 mm in bladder cancer patients, demonstrating that the algorithm performs well in the bladder.<sup>10</sup> However, no such study was done for the rectum. Since the results from our study show that the rectum match was worse, the deformation error is expected to be higher than in the bladder (>0.9-4.0 mm).

The effects of EBRT inter-fraction motion on the dose uniformity of bladder and rectum were not considered for these patients. As a result of the large PTV margin and the instructions to have a full bladder at the time of treatment, the BT high dose volumes were not expected to move out of the uniform part of the EBRT dose. For future investigations, we plan to investigate the feasibility of dose accumulation with DIR using the daily cone beam CT for patients treated using smaller margins.

### Conclusions

The DIR and OHD methods resulted in maximum differences of  $<3.3 \text{ Gy}_{\text{EQD2}}$  in  $D_{2\text{cm}^3}$  and  $D_{1\text{cm}^3}$  for the bladder and rectum, while the DIR and UD method resulted in differences  $<1.6 \text{ Gy}_{\text{EQD2}}$ . For the parameters under consideration, the DIR method provides no added value and the EBRT dose can be considered uniform both in bladder and rectum.

### Acknowledgements

This work was funded by Elekta Brachytherapy (II 250008).

## References

- [1] Bermudez A, Bhatla N, Leung E. Cancer of the cervix uteri. *Int J Gynaecol Obstet* 2015;131 Suppl:S88-95.
- [2] Pötter R, Haie-Meder C, Van Limbergen E, Barillot I, De Brabandere M, Dimopoulos J, et al. Recommendations from gynaecological (GYN) GEC ESTRO working group (II): concepts and terms in 3D image-based treatment planning in cervix cancer brachytherapy-3D dose volume parameters and aspects of 3D image-based anatomy, radiation physics, radiobiology. *Radiother Oncol* 2006;78:67–77.
- [3] Abe T, Tamaki T, Makino S, Ebara T, Hirai R, Miyaura K, et al. Assessing cumulative dose distributions in combined radiotherapy for cervical cancer using deformable image registration with pre-imaging preparations. *Radiat Oncol* 2014;9:293.
- [4] Hayashi K, Isohashi F, Akino Y, Wakai N, Mabuchi S, Suzuki O, et al. Estimation of the total rectal dose of radical external beam and intracavitary radiotherapy for uterine cervical cancer using the deformable image registration method. *J Radiat Res* 2015;56:546–52.
- [5] Van de Kamer JB, De Leeuw AAC, Moerland MA, Jürgenliemk-Schulz I-M. Determining DVH parameters for combined external beam and brachytherapy treatment: 3D biological dose adding for patients with cervical cancer. *Radiother Oncol* 2010;94:248–53.
- [6] Kim H, Huq MS, Houser C, Beriwal S, Michalski D. Mapping of dose distribution from IMRT onto MRI-guided high dose rate brachytherapy using deformable image registration for cervical cancer treatments: preliminary study with commercially available software. *J Contemp Brachytherapy* 2014;6:178–84.
- [7] Teo B-K, Bonner Millar LP, Ding X, Lin LL. Assessment of cumulative external beam and intracavitary brachytherapy organ doses in gynecologic cancers using deformable dose summation. *Radiother Oncol* 2015;115:195–202.
- [8] Jamema S V, Mahantshetty U, Andersen E, Noe KØ, Sørensen TS, Kallehauge JF, et al. Uncertainties of deformable image registration for dose accumulation of high-dose regions in bladder and rectum in locally advanced cervical cancer. *Brachytherapy* 2015;15:953–62.
- [9] Wognum S, Heethuis SE, Rosario T, Hoogeman MS, Bel A. Validation of deformable image registration algorithms on CT images of ex vivo porcine bladders with fiducial markers. *Med Phys* 2014;41:071916.
- [10] Wognum S, Bondar L, Zolnay AG, Chai X, Hulshof MCCM, Hoogeman MS, et al. Control over structure-specific flexibility improves anatomical accuracy for point-based deformable registration in bladder cancer radiotherapy. *Med Phys* 2013;40:021702.
- [11] Ryckman JM, Shelton JW, Waller AF, Schreiber E, Latifi K, Diaz R. Anatomic structure-based deformable image registration of brachytherapy

- implants in the treatment of locally advanced cervix cancer. *Brachytherapy* 2016; 15:584-92.
- [12] Andersen ES, Noe KØ, Sørensen TS, Nielsen SK, Fokdal L, Paludan M, et al. Simple DVH parameter addition as compared to deformable registration for bladder dose accumulation in cervix cancer brachytherapy. *Radiother Oncol* 2013;107:52–7.
- [13] International Commission on Radiation Units and Measurements. Prescribing, Recording, and Reporting Brachytherapy for Cancer of the Cervix (ICRU report 89). vol. 13. 2013.
- [14] Bondar L, Hoogeman M, Mens JW, Dhawtal G, de Pree I, Ahmad R, et al. Toward an individualized target motion management for IMRT of cervical cancer based on model-predicted cervix-uterus shape and position. *Radiother Oncol* 2011;99:240–5.
- [15] Vásquez Osorio EM, Hoogeman MS, Bondar L, Levendag PC, Heijmen BJM. A novel flexible framework with automatic feature correspondence optimization for nonrigid registration in radiotherapy. *Med Phys* 2009;36:2848.
- [16] Vásquez Osorio EM, Kolkman-Deurloo I-KK, Schuring-Pereira M, Zolnay A, Heijmen BJM, Hoogeman MS. Improving anatomical mapping of complexly deformed anatomy for external beam radiotherapy and brachytherapy dose accumulation in cervical cancer. *Med Phys* 2015;42:206–20.
- [17] Christensen GE, Johnson HJ. Consistent image registration. *IEEE Trans Med Imaging* 2001;20:568–82.
- [18] Dice LR. Measures of the Amount of Ecologic Association Between Species. *Ecology* 1945;26:297–302.
- [19] Bondar L, Hoogeman MS, Vásquez Osorio EM, Heijmen BJM. A symmetric nonrigid registration method to handle large organ deformations in cervical cancer patients. *Med Phys* 2010;37:3760.
- [20] Georg P, Lang S, Dimopoulos JCA, Dörr W, Sturdza AE, Berger D, et al. Dose-volume histogram parameters and late side effects in magnetic resonance image-guided adaptive cervical cancer brachytherapy. *Int J Radiat Oncol Biol Phys* 2011;79:356–62.
- [21] Ahmad R, Hoogeman MS, Bondar M, Dhawtal V, Quint S, De Pree I, et al. Increasing treatment accuracy for cervical cancer patients using correlations between bladder-filling change and cervix-uterus displacements: proof of principle. *Radiother Oncol* 2011;98:340–6.







# Chapter 5

Role of deformable image registration for delivered dose accumulation of adaptive external beam radiation therapy and brachytherapy in cervical cancer

L.E. van Heerden, J. Visser, C. Koedooder, C.R.N. Rasch, B.R. Pieters, A. Bel

Department of Radiation Oncology, Amsterdam UMC, University of Amsterdam, location AMC, Meibergdreef 9, 1105 AZ Amsterdam, The Netherlands

Published in: Journal of Contemporary Brachytherapy 2018;10:542–50

## **Abstract**

### ***Purpose***

Deformable image registration (DIR) can be used to accumulate the absorbed dose distribution of daily image-guided adaptive external beam radiation treatment (EBRT) and brachytherapy (BT). Since dose-volume parameter addition assumes a uniform delivered EBRT dose around the planned BT boost, the added value of DIR over direct addition was investigated for dose accumulation in bladder and rectum.

### ***Material and Methods***

For 10 patients (EBRT 46/46.2 Gy<sub>EQD2</sub>, EBRT+BT: D<sub>90</sub> 85-90 Gy<sub>EQD2</sub>, in equivalent dose in 2 Gy fractions) the actually delivered dose from adaptive volumetric-modulated arc therapy (VMAT)/intensity-modulated radiotherapy (IMRT) EBRT was calculated using the daily anatomy from the cone-beam computed tomography (CBCT) scans acquired prior to irradiation. The CBCT of the first EBRT fraction and the BT planning MRI were registered using DIR. The cumulative dose to the 2 cm<sup>3</sup> with the highest dose (D<sub>2cm<sup>3</sup></sub>) from EBRT and BT to the bladder and rectum was calculated and compared to direct addition assuming a uniform EBRT dose (UD).

### ***Results***

Differences (DIR-UD) in the total EBRT+BT dose ranged between -0.2–3.9 Gy<sub>EQD2</sub> (bladder) and -1.0–3.7 Gy<sub>EQD2</sub> (rectum). The total EBRT+BT dose calculated with DIR was at most 104% of the dose calculated with the UD method.

### ***Conclusions***

Differences between UD and DIR were small (<3.9 Gy<sub>EQD2</sub>). The dose delivered with adaptive VMAT/IMRT EBRT to bladder and rectum near the planned BT boost can be considered uniform for the evaluation of bladder/rectum D<sub>2cm<sup>3</sup></sub>.

## Introduction

Locally-advanced cervical cancer is treated with concurrent chemotherapy and radiotherapy. The standard of care for radiotherapy is external beam radiation treatment (EBRT) and a brachytherapy (BT) boost to the tumor area using an intracavitary/interstitial applicator. The recommended EBRT dose to the target is 45-50 Gy in 1.8-2.0 Gy/fraction,<sup>1</sup> with a BT boost up to a total dose of at least 90 Gy<sub>EQD<sub>2</sub></sub>, expressed as equivalent dose in 2 Gy fractions (EQD<sub>2</sub>), to at least 90% of the clinical target volume at high risk (CTV-HR). To avoid toxicity, the cumulative dose to the 2 cm<sup>3</sup> with the highest dose (D<sub>2cm<sup>3</sup></sub>) from EBRT and BT to the bladder and rectum should not exceed 90 Gy<sub>EQD<sub>2</sub></sub> and 75 Gy<sub>EQD<sub>2</sub></sub>, respectively,<sup>2,3</sup>

To evaluate the cumulative bladder and rectum D<sub>2cm<sup>3</sup></sub> of EBRT and BT, the International Commission on Radiation Units and Measurements (ICRU) recommends that the EBRT dose to the organs at risk should be considered uniform and equal to the prescription dose, meaning that the EBRT prescription dose and the BT dose-volume histogram (DVH) parameters can simply be added.<sup>4</sup> However, intensity-modulated radiotherapy (IMRT) and volumetric-modulated arc therapy (VMAT), as well as adaptive EBRT strategies such as plan-of-the-day strategies,<sup>5</sup> are being used increasingly to create highly conformal dose distributions (Fig. 1A). Possibly, the delivered dose from EBRT to OAR is non-uniform near the location of the planned BT boost, causing the estimated cumulative D<sub>2cm<sup>3</sup></sub> to be inaccurate at the time of brachytherapy planning. This might lead to errors in establishing the dose-response relationship. It should therefore be investigated whether it is preferable to sum the 3D dose distributions instead of using the uniform dose (UD) method.

When accumulating the total dose, deformable image registration (DIR) can be used to account for deformation due to differences in bladder and rectum filling and/or the presence of air, as well as the effect of the applicator on the position of the bladder and rectum. In earlier studies<sup>6-10</sup> the added value of DIR for the calculation of cumulative bladder and rectum D<sub>2cm<sup>3</sup></sub> was investigated and small differences (<5%) with the UD method were found. However, in these previous studies the planning images of BT and EBRT were registered and subsequently the planned EBRT dose was summed with the planned BT dose. At the time of BT planning, the delivered EBRT dose may deviate from planned dose due to daily positioning variability and daily variation in organ filling. Moreover, for clinical patients treated with a plan-of-the-day strategy the delivered EBRT dose near the location of the planned BT boost has not yet been investigated. A plan-of-the-day strategy in combination with smaller margins may lead to a non-uniform delivered EBRT dose to the BT high dose volumes.

The impact of EBRT dose non-uniformity in the planned BT high dose volumes has never been investigated before, while taking into account the daily interfraction motion during EBRT. In the present study we calculate the delivered EBRT dose for each fraction using the daily anatomy from the cone-beam computed tomography (CBCT) scan acquired prior to irradiation, and then sum the accumulated delivered EBRT dose to the planned BT 3D dose distribution.

The aim of the present study is therefore to evaluate, for an adaptive EBRT planning procedure, if it is necessary to account for EBRT dose non-uniformity with deformable image registration when evaluating the cumulative EBRT and BT dose in bladder and rectum.

## Materials and Methods

### *Patients, dose scheme and imaging*

In this study ten patients treated for locally-advanced cervical carcinoma (FIGO stages IIA-IVA) were investigated. The patients were treated with EBRT, receiving 46 Gy in daily fractions of 2 Gy (8 patients) or 46.2 Gy in 1.65 Gy fractions with a para-aortal boost up to 56 Gy in 2 Gy fractions (2 patients), and a BT boost. For patients treated with 46 Gy in 2 Gy fractions, five received an additional simultaneous-integrated boost (SIB) of 0.4 Gy per fraction to affected lymph nodes. These lymph nodes were located in the region between the aortic bifurcation above the internal/external iliac, and the dose to these nodes will not contribute to the BT boost region. All patients were treated according to a plan-of-the-day strategy.<sup>11</sup> Besides two planning CTs (i.e., full and empty bladder), all patients received CBCT imaging (Synergy platform, Elekta AB, Stockholm, Sweden) before irradiation. For both planning CTs, the corresponding primary CTVs (pCTVs), consisting of the gross tumor volume, cervix, corpus-uterus and upper part of the vagina, were registered using a structure-based DIR algorithm.<sup>12</sup> With the resulting deformation vector field, 1-3 patient-specific primary internal target volumes (pITVs) were generated. For each pITV, a primary planning target volume (PTV) was generated by enlarging the part of the pITV including the corpus-uterus with an 8 mm margin and the part of the pITV including the cervix and vagina with a margin of 8 mm, 8 mm and 13 mm in left–right, superior–inferior and anterior–posterior direction, respectively.<sup>11</sup>

A patient-specific plan library was defined by generating 1-3 plans corresponding to the different target volumes. Each treatment day the library plan best fitting the anatomy as observed on the pre-fraction CBCT image was selected.

EBRT was planned with volumetric modulated arc therapy (VMAT) for nine patients, and with intensity modulated radiation therapy (IMRT) for one patient. For all EBRT plans ( $46 \text{ Gy}_{\text{EQD2}}$ ,  $46 \text{ Gy}_{\text{EQD2}} + \text{SIB}$  or  $46.2 \text{ Gy}_{\text{EQD2}}$ ) the same bladder and rectum dose constraints were applied. For the target,  $\geq 99\%$  of the PTV should receive  $\geq 95\%$  of the prescription dose, with a conformity index ( $V_{95}/\text{PTV volume}$ )  $< 1.35$ . A hotspot criterion was used for bladder and rectum ( $D_{1\text{cm}^3} < 103\%$  of the prescription dose i.e.  $46 \text{ Gy}/46.2 \text{ Gy}$ ). The dose fall-off region from 45-22.5 Gy was aimed to be  $< 1.2 \text{ cm}$ .

For brachytherapy a dose of 24 Gy in pulse doses of 1 Gy every hour was delivered to the high-risk CTV ( $\text{CTV}_{\text{HR}}$ ) using the Utrecht CT/MR compatible applicator (Elekta, Veenendaal, The Netherlands) with vaginal ovoids and interstitial needles where needed for lateral coverage. Prior to the BT delivery,  $T_2$ -weighted Turbo Spin Echo MRI (in-plane resolution  $0.5 \times 0.5 \text{ mm}^2$ , slice thickness  $3.3 \text{ mm}$ ) was acquired on an Ingenia 3 T MRI scanner (Philips Healthcare, Best, The Netherlands).<sup>13</sup> BT planning was performed using Oncentra Brachy 4.5 (Elekta, Veenendaal, The Netherlands), using a library for applicator reconstruction. The plan was manually optimized aiming at a cumulative  $D_{90}$  (minimal dose received by 90% of the volume) of 90-95  $\text{Gy}_{\text{EQD2}}$  from EBRT and BT on the  $\text{CTV}_{\text{HR}}$ . To spare the bladder and rectum, the planned cumulative  $D_{2\text{cm}^3}$  from EBRT and BT should not exceed 90  $\text{Gy}_{\text{EQD2}}$  and 75  $\text{Gy}_{\text{EQD2}}$ , respectively. The radiotherapy techniques are described in Table 1 and typical planned EBRT and BT dose distributions are shown in Fig. 1 (A and B).

On the CT, CBCT and MRI scans, the bladder was delineated and the rectum was delineated from the rectosigmoid junction to the level of the anal sphincter. For EBRT, patients were instructed to have a full bladder daily, while a catheter was inserted for BT to guarantee a minimum bladder filling. No rectal management was applied for BT dose delivery.

### ***Study-specific daily dose calculation of external beam radiotherapy***

For all 10 patients, CBCTs of all fractions were available, in total 240 images. Accurate CBCT based dose calculation is difficult with the Elekta XVI imaging system used in this study because the Hounsfield Units (HU) numbers are not accurate. To enable daily dose distribution calculation, for all images CT HU numbers were mapped to CBCT images by registering the planning CT to CBCT images using DIR (Fig. 2).<sup>14</sup> For each pre-fraction CBCT image, the planning CT with accurate HU numbers was deformed to represent CBCT images using a B-spline deformable image registration based on intensity values (VelocityAI, version 3.1.0/3.2.0, Varian Medical Systems, Inc., Palo Alto, CA). Of the two available planning CT's (i.e., full and empty bladder), we selected the CT with the closest bladder volume to the daily anatomy of the CBCT for this step. Prior to the deformable

image registration a rigid registration was performed to match the bony anatomy. The deformable match was visually assessed to ensure that the body contours and the soft tissue matched sufficiently. The quality of CT-to-CBCT deformable registration in the pelvic area using the VelocityAI software was investigated previously and DIR results were reported to be accurate for dose calculation.<sup>15,16</sup>

Each daily selected plan was used to calculate the corresponding daily dose distribution.

### ***Deformable image registration for dose accumulation***

To accumulate the delivered EBRT dose and EBRT+BT dose the structure-guided DIR available in VelocityAI was used. This is a hybrid version of the B-spline DIR where a higher weight is assigned to voxels within the structure. Our method is similar to earlier described DIR strategies for dose accumulation.<sup>17,18</sup> To obtain DIR of sufficient quality, all delineated EBRT and BT images were converted into binary images before DIR, for bladder and rectum separately. Two registrations for each patient were created for bladder and rectum separately to improve the quality of each registration in the proximity of the evaluated organ.

First, all CBCT images were registered to the CBCT of the first fraction (CBCT1) using deformable image registration. A mapping was established to propagate delineated structures on each subsequent CBCT to CBCT1 scan. Next, the CBCT1 image was deformably registered to the BT planning MRI, to obtain a mapping of delineated structures on CBCT1 to the BT MRI.

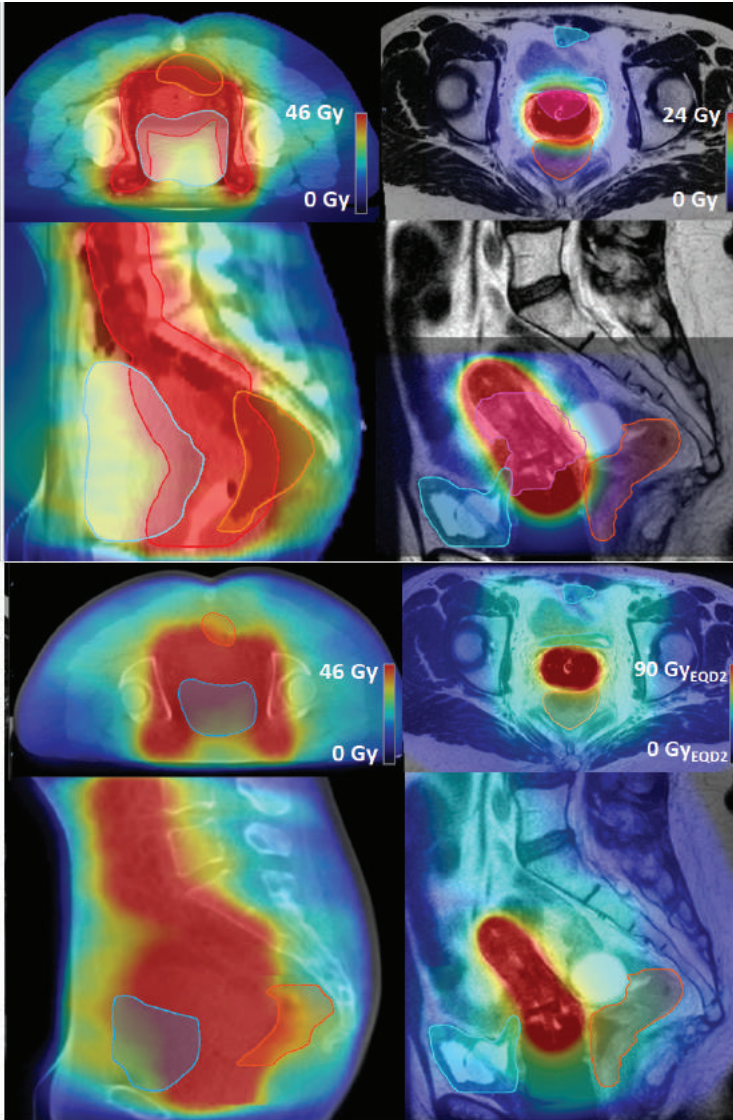


**Fig. 1** A, B: Axial (upper panel) and sagittal (lower panel) view of a patient CT/MRI with a color wash of the planned VMAT/BT dose. The VMAT dose is not uniform in the proximity of the bladder/rectum walls (blue/orange) closest to the target (red/pink). C: CBCT of the first fraction with the total delivered dose from EBRT accumulated using DIR for the bladder as described in this paper, D: MRI with the accumulated dose from EBRT and BT, which is calculated by summing the delivered VMAT and planned BT dose distribution.

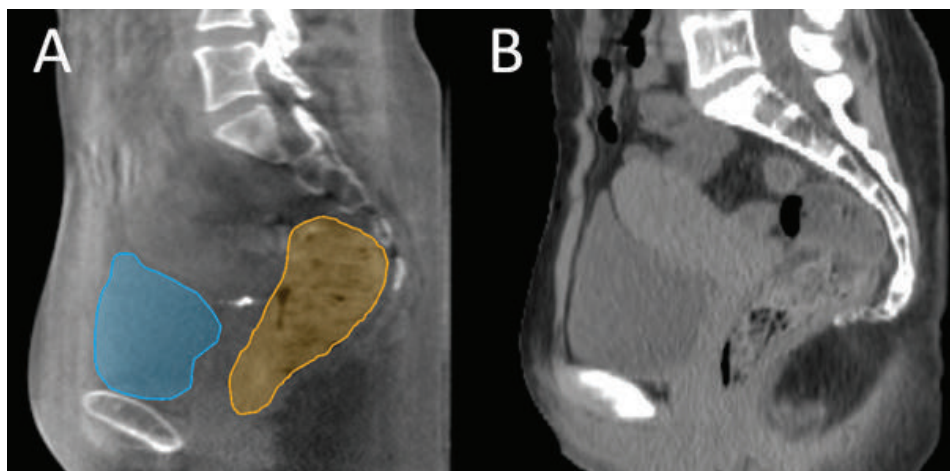


**Fig. 2** A: Sagittal view of a patient CBCT with the bladder/rectum delineations (blue/orange), B: The planning CT with accurate HU numbers deformed to the CBCT frame of reference.

**Table 1** Radiotherapy techniques for EBRT and PDR BT

	External Beam Radiation Therapy	Brachytherapy
<b>Treatment type</b>	VMAT/IMRT	PDR
<b>Treatment planning system</b>	Oncentra 4.3*	Oncentra Brachy 4.5*
<b>Dose calculation algorithm</b>	Collapsed Cone	Based on the TG-43 formalism
<b>Imaging</b>	CT images	T <sub>2</sub> -weighted Turbo Spin Echo MRI
<b>Scanner specification</b>	LightSpeed RT16 (GE, WI, USA)	Ingenia 3 T (Philips Healthcare, Best, The Netherlands)
<b>Imaging resolution (mm<sup>3</sup>)</b>	1.2 x 1.2 x 3	0.7 x 0.7 x 3.3
<b>Dose calculation grid size (mm<sup>3</sup>)</b>	3 x 3 x 3	1 x 1 x 1
<b>Planning aims</b>	PTV V <sub>95</sub> ≥99% Bladder V <sub>45Gy</sub> <40%; Rectum V <sub>40Gy</sub> <70%; Bladder + Rectum D <sub>1cm<sup>3</sup></sub> <103%	CTV <sub>HR</sub> D <sub>90</sub> 85-90 Gy <sub>EQD2</sub> Bladder/rectum D <sub>2cm<sup>3</sup></sub> <80/65 Gy <sub>EQD2</sub>

PTV: planning target volume;

CTV<sub>HR</sub>: clinical target volume at high risk;

D<sub>90</sub>: dose received by 90% of the volume;

V<sub>95</sub>: the percentage of the volume receiving ≥95% of the prescription dose;

V<sub>45Gy</sub> / V<sub>40Gy</sub>: the percentage of the volume receiving ≥45/40 Gy;

D<sub>2cm<sup>3</sup></sub> / D<sub>1cm<sup>3</sup></sub>: dose to the most irradiated 2 cm<sup>3</sup> / 1 cm<sup>3</sup>)

\*Elekta AB, Stockholm Sweden



### ***Dose accumulation***

For both organ-specific matches, the deformation vector fields (DVF) obtained with the CBCT-to-CBCT DIR were used to map all EBRT fraction doses to the CBCT1 frame of reference. This is the delivered dose distribution from all EBRT fractions (Fig. 2,C). The CBCT1-to-MRI DVF was used to map the delivered EBRT dose distribution and organ contours to the frame of reference of the planned BT dose distribution. Next, the EBRT and BT doses were converted to EQD<sub>2</sub> on a voxel-by-voxel level (Matlab R2014b, Mathworks Inc., MA), using LQ-model based equations with an  $\alpha/\beta$  value of 3 Gy for late OAR toxicity and a 1.5 hour repair half-time.<sup>19,20</sup> Finally, the EBRT and BT doses were summed to create the accumulated dose (Fig. 2, D). Fig. 3 shows a schematic overview of the workflow.

### ***Dosimetric data analysis***

Bladder and rectum D<sub>2cm3</sub> were acquired using VelocityAI. For the DIR method, D<sub>2cm3</sub> was calculated from the accumulated dose distributions for both rectum and bladder. For the UD method, the cumulative D<sub>2cm3</sub> was calculated by adding the planned dose of 46 Gy<sub>EQD2</sub>/46.2 Gy<sub>EQD2</sub> to the D<sub>2cm3</sub> from BT. For both methods, the mean and range of bladder and rectum D<sub>2cm3</sub> were calculated over all patients, as well as the difference in D<sub>2cm3</sub> (DIR-UD).

### ***DIR accuracy***

The Dice Similarity Coefficient (DSC) was used to compare propagated and reference contours.<sup>21</sup> DSC quantifies the spatial overlap of the matched bladder and rectum. Additionally, the surface distance error (SDE), i.e. the Euclidean distance between the reference and propagated contours, was determined for each bladder/rectum match.<sup>22,23</sup> Over all bladder/rectum matches, the mean DSC and range over all patients were calculated. The 25<sup>th</sup>, 50<sup>th</sup>, 75<sup>th</sup> and 100<sup>th</sup> percentile of the mean SDEs were calculated for all bladders/rectums.

## **Results**

### ***Cumulative DVH parameters***

The D<sub>2cm3</sub> mean and range for bladder and rectum are shown in Table 2. The difference range (DIR-UD) was -0.2 – 3.7% (-0.2 – 3.9 Gy<sub>EQD2</sub>) for bladder and -1.9 – 3.7% (-1.0 – 3.7 Gy<sub>EQD2</sub>) for rectum, meaning that the dose to the OARs calculated with DIR was at most 104% of the dose calculated with the UD method. Individual patient results can be found in Fig. 4.

**DIR accuracy**

For every patient the mean DSC over all bladder/rectum matches was calculated. For the bladder, the mean DSC was 0.96, ranging between 0.95-0.97 over all patients. The mean rectum DSC was 0.92(0.89-0.94).

For the bladder, the mean SDE over all registrations was 0.7 mm, ranging between 0.5-0.9 mm. For the rectum, the mean SDE was 0.9 mm (0.4-1.9 mm). Individual patient results are shown in Fig. 5. For the CBCT1-to-MRI registration, which was used to map the delivered EBRT dose distribution to the frame of reference of the planned BT dose distribution, the DSC ranged over all patients between 0.94-0.98 for bladder and for rectum between 0.89-0.92. The mean SDE varied for bladder between 0.3-0.7 mm and for the rectum between 1.0-1.9 mm.

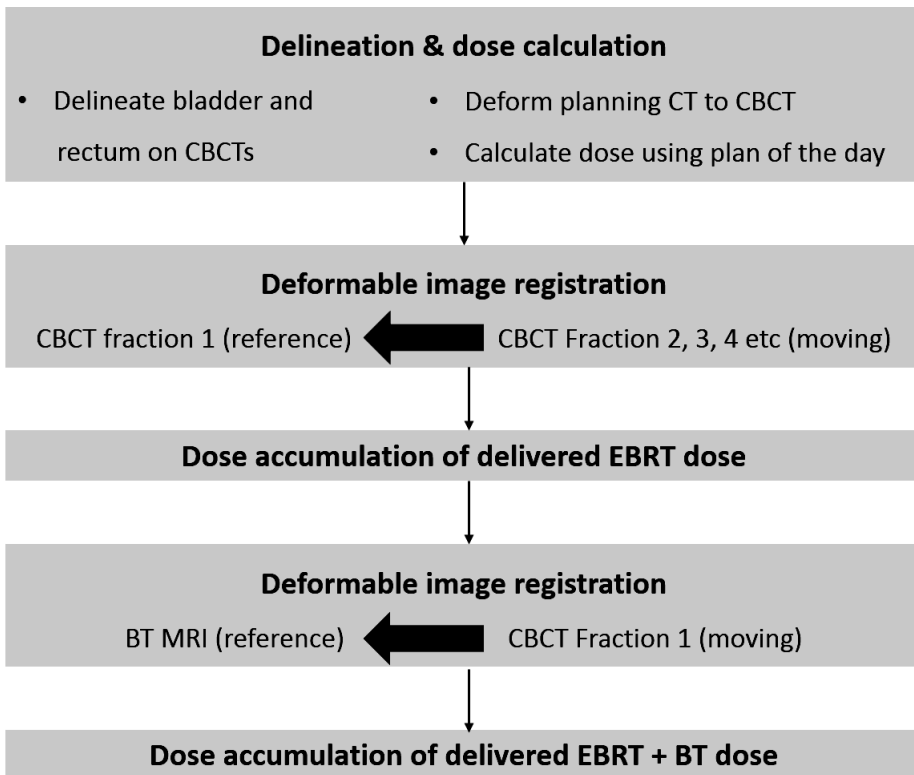


**Fig. 3** Schematic overview of the workflow for accumulating the EBRT+BT dose.

**Table 2** The mean and the range over all patients of the cumulative  $D_{2\text{cm}^3}$  calculated with the DIR method and the UD method, and the difference  $\Delta D_{2\text{cm}^3}$  (DIR-UD), in bladder and rectum.

Bladder		
Method	DIR Mean (Range)	Uniform dose Mean (Range)
$D_{2\text{cm}^3}(\text{Gy}_{\text{EQD2}})$	75.6(57.4;106.9)	74.5(56.6;103.2)
$\Delta D_{2\text{cm}^3}(\text{Gy}_{\text{EQD2}})$		-1.1(-3.7;0.2)
Rectum		
Method	DIR Mean (Range)	Uniform dose Mean (Range)
$D_{2\text{cm}^3}(\text{Gy}_{\text{EQD2}})$	63.2(50.6;74.7)	63.3(49.7;77.5)
$\Delta D_{2\text{cm}^3}(\text{Gy}_{\text{EQD2}})$		0.0(-2.8;1.0)

## Discussion

In the present study we investigated if it is necessary to account for non-uniformity of the dose from adaptive EBRT with deformable image registration when evaluating the cumulative bladder and rectum  $D_{2\text{cm}^3}$  from EBRT and BT at the time of BT planning. This is to our knowledge the first study to estimate the delivered dose from EBRT and to compare the  $D_{2\text{cm}^3}$  from the accumulated EBRT and BT 3D dose distribution to the UD method for patients treated with a plan-of-the-day strategy. For the total EBRT+BT dose, small differences were found between UD and DIR ( $\Delta D_{2\text{cm}^3} < 3.9 \text{ Gy}_{\text{EQD2}}$ ).

There are many uncertainties related to brachytherapy planning for cervical cancer.<sup>24,25</sup> Delineation uncertainty, inter- and intrafraction motion and applicator reconstruction uncertainty because of e.g. image distortions are major contributors to the total uncertainty for the estimation of the total radiotherapy dose.<sup>26,27</sup> Calculation of the accumulated dose to bladder and rectum with the ICRU formalism<sup>20</sup> may lead to additional uncertainty, since it assumes that the delivered EBRT dose is uniform. In this paper we accumulated the dose from EBRT and BT using DIR while taking into account interfraction motion between EBRT fractions. Since we found small differences between the DIR and UD method, this study shows that using the ICRU formalism leads to small additional uncertainty for the estimated total EBRT and BT dose.

In previous studies the dose effect relationship for late side effects was determined for bladder and rectum using the UD method.<sup>28,29</sup> Regardless of whether UD or DIR was used to

calculate  $D_{2\text{cm}^3}$ , in our study the risk remained within 5-10% for nine out of ten patients. For one patient, the cumulative bladder dose exceeded the dose limit of  $90 \text{ Gy}_{\text{EQD2}}$  and was as high as  $103 \text{ Gy}_{\text{EQD2}}$ , since the bladder wall was part of the target. For another patient, the rectum dose was relatively high, with a value of  $74.6 \text{ Gy}_{\text{EQD2}}$ . Still, the risk of side effects remained within 11-14% with DIR or UD. Based on these results we conclude that DIR provides no added value over the UD method for the evaluation of bladder/rectum  $D_{2\text{cm}^3}$  in order to predict organ toxicity.

For dose warping purposes it is desirable to obtain high voxel-to-voxel correspondence after DIR. With our current methods, we did not directly investigate the voxel-to-voxel correspondence, and the DIR method used for dose accumulation was not validated using ground truth data. After DIR, we found a high DSC (bladder: 0.96, rectum: 0.92) and small mean SDE (bladder: 0.7 mm, rectum: 0.9 mm) for both bladder and rectum. For the evaluation of  $D_{2\text{cm}^3}$ , it is relevant to know whether mismatches are located near the BT boost region. Visual assessment showed that for all registrations the contours were overlapping near the BT boost. The mean SDE distribution showed that for all registrations the distance between points on the matched contours was small after DIR ( $<1.9 \text{ mm}$ ) compared to the imaging resolution of the planning scans ( $\text{CT} = 1.2 \times 1.2 \times 3 \text{ mm}^3$ ,  $\text{MRI} = 0.7 \times 0.7 \times 3.3 \text{ mm}^3$ ). Since EBRT doses were calculated with a  $3 \times 3 \times 3 \text{ mm}^3$  resolution, dose points warped at this precision or lower were considered reliable. Moreover, since the EBRT dose is uniform near the high dose volumes of brachytherapy the impact of mismatches after DIR is limited. For bladder and rectum  $D_{2\text{cm}^3}$  the difference between the values calculated with the UD and DIR method were indeed small. We therefore conclude that the DIR performance was sufficiently accurate for accumulating the bladder and rectum  $D_{2\text{cm}^3}$ .

## Deformable dose addition of delivered EBRT and planned BT

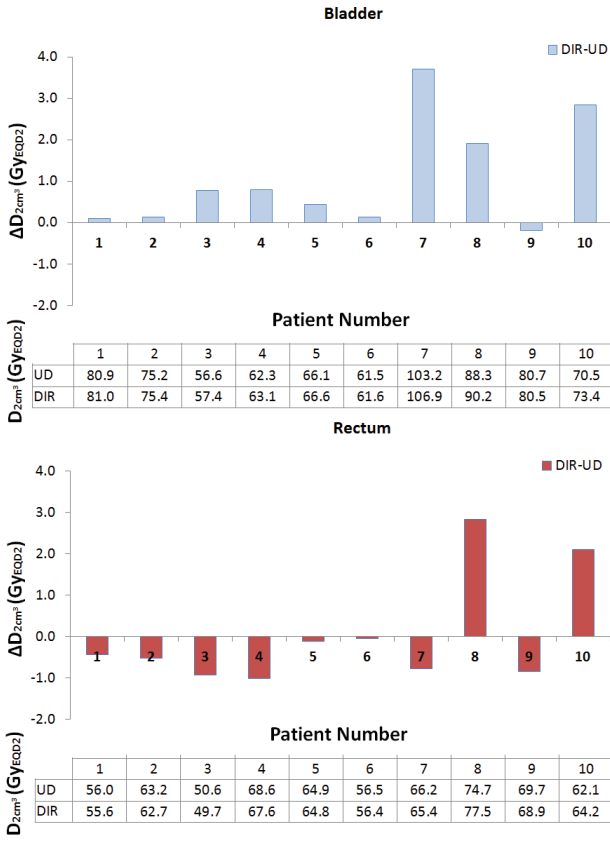


**Fig. 4** The cumulative  $D_{2cm^3}$  calculated with the DIR and UD method for bladder and rectum. For visualization, the difference in  $D_{2cm^3}$  of the DIR method with the UD method ( $\Delta D_{2cm^3}$ ) is plotted.

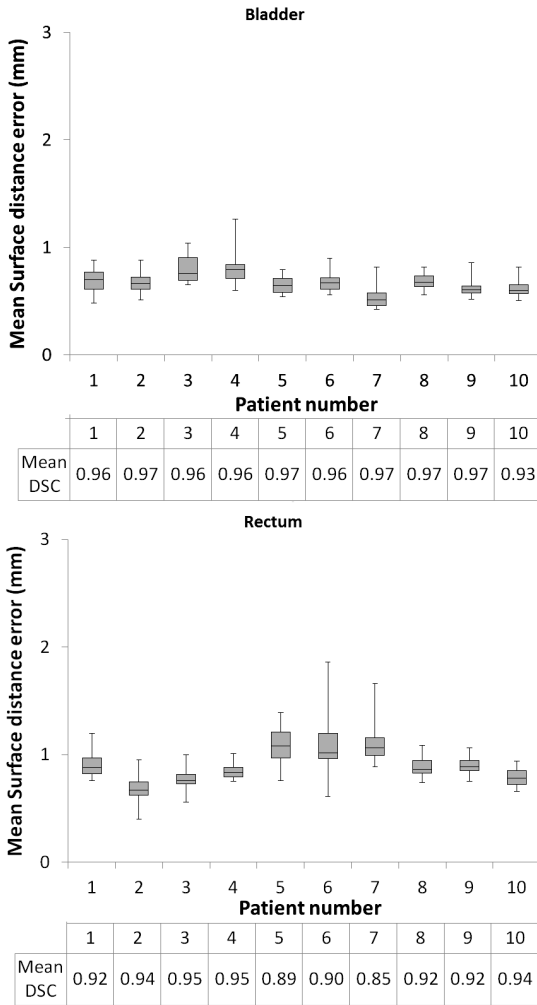


**Fig. 5** Boxplot of the mean surface distance errors with the 25<sup>th</sup>, 50<sup>th</sup>, 75<sup>th</sup> and 100<sup>th</sup> percentile over all fractions, for all patients in bladder and rectum. The table shows the mean Dice Similarity coefficient (DSC) over all fractions.

Patients in this study were treated with smaller margins than for conventional VMAT/IMRT cervix plans to increase organ at risk sparing. Our results show that the EBRT dose near the BT boost can be considered uniform even when a conformal plan-of-the-day strategy is used. For patient treated at our facility with the currently available conformal treatment planning strategies, it is therefore not necessary to accumulate the bladder and rectum dose of EBRT and BT with DIR at the time of brachytherapy planning. Recently, planning strategies have been developed to create even more conformal EBRT dose distributions such as for proton therapy<sup>30</sup> or online MRI guidance.<sup>31</sup> It may be necessary to use DIR when accumulating the dose from EBRT and BT in these cases.

The small differences we found between the DIR and UD method are not unexpected, since for all patients a hotspot criterion ( $D_{1\text{cm}^3} < 103\%$  of the prescription dose) was used. When such a criterion is not used, the delivered EBRT dose near the planned BT boost may be non-uniform, and DIR may have added value over the UD method.

Four out of the ten patients were treated with an additional SIB boost to pathological lymph nodes. For these patients the difference between DIR and UD was also small. Possibly for patients receiving a SIB boost special care needs to be taken during EBRT planning to avoid a non-uniform dose near the planned BT high dose volumes, such as the hotspot criterion used in this study.

In our previous study<sup>8</sup> differences between the DIR and UD method for the planned EBRT dose were investigated without considering the effect of interfraction motion between EBRT fractions and plan selection. Four patients from this previous study were also analyzed in this study. For the delivered EBRT dose calculated in our present study, differences between DIR and UD were up to 2.5 times larger than for the planned EBRT dose. Regardless whether the delivered or planned EBRT dose was investigated, the risk of late side effects remained within 5-10% for these patients.

A limitation of this study is the use of CBCT delineations to guide DIR. Due to the low contrast and imaging artifacts CBCT images may be less suitable for delineations than CT or MRI. Both for bladder<sup>32</sup> and rectum<sup>33,34</sup> the inter-observer variation is small on CBCT, showing these structures can be recognized and delineated on CBCT.

In this study the effects of intrafraction motion during EBRT were not incorporated in the estimation of the delivered EBRT dose. In a previous study<sup>35</sup> intrafraction motion during EBRT was studied for cervical cancer using bladder and rectum delineations of pre- and postfraction CBCT scans. The change in rectum volume during one fraction was negligible, but the average bladder volume changed by on average 62 cm<sup>3</sup>. However, in this study the time interval between the pre- and postfraction scan was 20.8 min, while in our institute the time interval is less than 7 min. The dosimetric impact of intrafraction motion during EBRT is therefore limited for bladder and rectum.

### Acknowledgements

This work was funded by Elekta Brachytherapy (II 250008).

## References

- [1] Bermudez A, Bhatla N, Leung E. Cancer of the cervix uteri. *Int J Gynaecol Obstet* 2015;131 Suppl:S88-95.
- [2] Georg P, Pötter R, Georg D, Lang S, Dimopoulos JCA, Sturdza AE, et al. Dose effect relationship for late side effects of the rectum and urinary bladder in magnetic resonance image-guided adaptive cervix cancer brachytherapy. *Int J Radiat Oncol Biol Phys* 2012;82:653–7.
- [3] Mazon R, Fokdal LU, Kirchheiner K, Georg P, Jastaniyah N, Šegedin B, et al. Dose–volume effect relationships for late rectal morbidity in patients treated with chemoradiation and MRI-guided adaptive brachytherapy for locally advanced cervical cancer: Results from the prospective multicenter EMBRACE study. *Radiother Oncol* 2016;120:412–9.
- [4] Pötter R, Haie-Meder C, Van Limbergen E, Barillot I, De Brabandere M, Dimopoulos J, et al. Recommendations from gynaecological (GYN) GEC ESTRO working group (II): concepts and terms in 3D image-based treatment planning in cervix cancer brachytherapy-3D dose volume parameters and aspects of 3D image-based anatomy, radiation physics, radiobiology. *Radiother Oncol* 2006;78:67–77.
- [5] van de Schoot AJAJ, de Boer P, Visser J, Stalpers LJA, Rasch CRN, Bel A. Dosimetric advantages of a clinical daily adaptive plan selection strategy compared with a non-adaptive strategy in cervical cancer radiation therapy. *Acta Oncol* 2017;56:667–74.
- [6] Abe T, Tamaki T, Makino S, Ebara T, Hirai R, Miyaura K, et al. Assessing cumulative dose distributions in combined radiotherapy for cervical cancer using deformable image registration with pre-imaging preparations. *Radiat Oncol* 2014;9:293.
- [7] Hayashi K, Isohashi F, Akino Y, Wakai N, Mabuchi S, Suzuki O, et al. Estimation of the total rectal dose of radical external beam and intracavitary radiotherapy for uterine cervical cancer using the deformable image registration method. *J Radiat Res* 2015;56:546–52.
- [8] van Heerden LE, Houweling AC, Koedooder C, van Kesteren Z, van Wieringen N, Rasch CRN, et al. Structure-based deformable image registration: Added value for dose accumulation of external beam radiotherapy and brachytherapy in cervical cancer. *Radiother Oncol* 2017;123:319–24.
- [9] Kim H, Huq MS, Houser C, Beriwal S, Michalski D. Mapping of dose distribution from IMRT onto MRI-guided high dose rate brachytherapy using deformable image registration for cervical cancer treatments: preliminary study with commercially available software. *J Contemp Brachytherapy* 2014;6:178–84.
- [10] Teo B-K, Bonner Millar LP, Ding X, Lin LL. Assessment of cumulative external beam and intracavitary brachytherapy organ doses in gynecologic cancers using deformable dose summation. *Radiother Oncol* 2015;115:195–202.



- [11] van de Schoot AJAJ, de Boer P, Visser J, Stalpers LJA, Rasch CRN, Bel A. Dosimetric advantages of a clinical daily adaptive plan selection strategy compared with a non-adaptive strategy in cervical cancer radiation therapy. *Acta Oncol* 2017;56:667–74.
- [12] Vásquez Osorio EM, Hoogeman MS, Bondar L, Levendag PC, Heijmen BJM. A novel flexible framework with automatic feature correspondence optimization for nonrigid registration in radiotherapy. *Med Phys* 2009;36:2848.
- [13] van Heerden LE, van Kesteren Z, Gurney-Champion OJ, Houweling AC, Koedooder K, Rasch CRN, et al. Image distortions on a plastic interstitial CT/MR brachytherapy applicator at 3 T MRI and their dosimetric impact. *Int J Radiat Oncol* 2017.
- [14] Veiga C, McClelland J, Moinuddin S, Lourenço A, Ricketts K, Annkah J, et al. Toward adaptive radiotherapy for head and neck patients: Feasibility study on using CT-to-CBCT deformable registration for “dose of the day” calculations. *Med Phys* 2014;41:031703.
- [15] Stanley N, Glide-Hurst C, Kim J, Adams J, Li S, Wen N, et al. Using patient-specific phantoms to evaluate deformable image registration algorithms for adaptive radiation therapy. *J Appl Clin Med Phys* 2013;14:4363.
- [16] Onozato Y, Kadoya N, Fujita Y, Arai K, Dobashi S, Takeda K, et al. Evaluation of On-Board kV Cone Beam Computed Tomography–Based Dose Calculation With Deformable Image Registration Using Hounsfield Unit Modifications. *Int J Radiat Oncol* 2014;89:416–23.
- [17] Kadoya N, Miyasaka Y, Yamamoto T, Kuroda Y, Ito K, Chiba M, et al. Evaluation of rectum and bladder dose accumulation from external beam radiotherapy and brachytherapy for cervical cancer using two different deformable image registration techniques. *J Radiat Res* 2017;56:1–9.
- [18] Hayashi K, Isohashi F, Akino Y, Wakai N, Mabuchi S, Suzuki O, et al. Estimation of the total rectal dose of radical external beam and intracavitary radiotherapy for uterine cervical cancer using the deformable image registration method. *J Radiat Res* 2015;56:546–52.
- [19] International Commission on Radiation Units and Measurements. Prescribing, Recording, and Reporting Brachytherapy for Cancer of the Cervix (ICRU report 89). vol. 13. 2013.
- [20] Pötter R, Haie-Meder C, Van Limbergen E, Barillot I, De Brabandere M, Dimopoulos J, et al. Recommendations from gynaecological (GYN) GEC ESTRO working group (II): concepts and terms in 3D image-based treatment planning in cervix cancer brachytherapy-3D dose volume parameters and aspects of 3D image-based anatomy, radiation physics, radiobiology. *Radiother Oncol* 2006;78:67–77.
- [21] Dice LR. Measures of the Amount of Ecologic Association Between Species. *Ecology* 1945;26:297–302.
- [22] Bondar L, Hoogeman MS, Vásquez Osorio EM, Heijmen BJM. A symmetric

- nonrigid registration method to handle large organ deformations in cervical cancer patients. *Med Phys* 2010;37:3760.
- [23] Wognum S, Heethuis SE, Rosario T, Hoogeman MS, Bel A. Validation of deformable image registration algorithms on CT images of ex vivo porcine bladders with fiducial markers. *Med Phys* 2014;41:071916.
- [24] Kirisits C, Rivard MJ, Baltas D, Ballester F, De Brabandere M, van der Laarse R, et al. Review of clinical brachytherapy uncertainties: analysis guidelines of GEC-ESTRO and the AAPM. *Radiother Oncol* 2014;110:199–212.
- [25] Nesvacil N, Tanderup K, Lindegaard JC, Pötter R, Kirisits C. Can reduction of uncertainties in cervix cancer brachytherapy potentially improve clinical outcome? *Radiother Oncol* 2016;120:390–6.
- [26] Hellebust TP, Tanderup K, Lervåg C, Fidarova E, Berger D, Malinen E, et al. Dosimetric impact of interobserver variability in MRI-based delineation for cervical cancer brachytherapy. *Radiother Oncol* 2013;107:13–9.
- [27] Nesvacil N, Tanderup K, Hellebust TP, De Leeuw A, Lang S, Mohamed S, et al. A multicentre comparison of the dosimetric impact of inter- and intra-fractional anatomical variations in fractionated cervix cancer brachytherapy. *Radiother Oncol* 2013;107:20–5.
- [28] Georg P, Pötter R, Georg D, Lang S, Dimopoulos JCA, Sturdza AE, et al. Dose effect relationship for late side effects of the rectum and urinary bladder in magnetic resonance image-guided adaptive cervix cancer brachytherapy. *Int J Radiat Oncol Biol Phys* 2012;82:653–7.
- [29] Mazon R, Fokdal LU, Kirchheiner K, Georg P, Jastaniyah N, Šegedin B, et al. Dose–volume effect relationships for late rectal morbidity in patients treated with chemoradiation and MRI-guided adaptive brachytherapy for locally advanced cervical cancer: Results from the prospective multicenter EMBRACE study. *Radiother Oncol* 2016;120:412–9.
- [30] van de Schoot AJAJ, de Boer P, Crama KF, Visser J, Stalpers LJA, Rasch CRN, et al. Dosimetric advantages of proton therapy compared with photon therapy using an adaptive strategy in cervical cancer. *Acta Oncol* 2016;55:892–9.
- [31] Kerkhof EM, Raaymakers BW, van der Heide UA, van de Bunt L, Jürgenliemk-Schulz IM, Lagendijk JJW. Online MRI guidance for healthy tissue sparing in patients with cervical cancer: An IMRT planning study. *Radiother Oncol* 2008;88:241–9.
- [32] Nishioka K, Shimizu S, Kinoshita R, Inoue T, Onodera S, Yasuda K, et al. Evaluation of inter-observer variability of bladder boundary delineation on cone-beam CT. *Radiat Oncol* 2013;8:185.
- [33] Foroudi F, Haworth A, Pangehel A, Wong J, Roxby P, Duchesne G, et al. Inter-observer variability of clinical target volume delineation for bladder cancer using CT and cone beam CT. *J Med Imaging Radiat Oncol* 2009;53:100–6.
- [34] Lütgendorf-Caucig C, Fotina I, Stock M, Pötter R, Goldner G, Georg D.

Feasibility of CBCT-based target and normal structure delineation in prostate cancer radiotherapy: Multi-observer and image multi-modality study. *Radiother Oncol* 2011;98:154–61.

- [35] Heijkoop ST, Langerak TR, Quint S, Mens JWM, Zolnay AG, Heijmen BJM, et al. Quantification of intra-fraction changes during radiotherapy of cervical cancer assessed with pre- and post-fraction Cone Beam CT scans. *Radiother Oncol* 2015;117:536–41.



# Chapter 6

Dose warping uncertainties for the accumulated rectal wall dose  
in cervical cancer brachytherapy

L.E. van Heerden, N. van Wieringen, C. Koedooder, C.R.N. Rasch,  
B.R. Pieters, A. Bel

Department of Radiation Oncology, Amsterdam UMC, University of Amsterdam, location AMC, Meibergdreef 9, 1105 AZ Amsterdam, The Netherlands

Published in: *Brachytherapy* 2018;17:449–55

## **Abstract**

### ***Purpose***

Structure-based deformable image registration (DIR) can be used to calculate accumulated dose volume histogram (DVH) parameters for cervical cancer brachytherapy (BT). The purpose of this study is to investigate dose warping uncertainties for the accumulated dose to the 2 cm<sup>3</sup> receiving the highest dose ( $D_{2\text{cm}^3}$ ) in the rectal wall, using a physically realistic model describing rectal wall deformation.

### ***Methods***

For ten patients, treated with Magnetic Resonance Imaging (MRI)-guided Pulsed-dose rate BT (two times 24 x 0.75 Gy, given in two applications BT1 and BT2), the planning images were registered with structure-based DIR. The resulting transformation vectors were used to accumulate the total rectum dose from brachytherapy. To investigate the dose warping uncertainty a physically realistic model (PRM) describing rectal deformation was used. For point pairs on  $\text{rectum}_{\text{BT1}}$  and  $\text{rectum}_{\text{BT2}}$  that were at the same location according to the PRM, the dose for BT1 and BT2 was added ( $D_{\text{PRM}}$ ) and compared to the DIR accumulated dose ( $D_{\text{DIR}}$ ) in the BT2 point. The remaining distance after DIR between corresponding point pairs, defined as the residual distance, was calculated.

### ***Results***

For points within the  $D_{2\text{cm}^3}$  volume, more than 75% was part of the  $D_{2\text{cm}^3}$  volume according to both PRM and DIR. The absolute dose difference was  $<7.3 \text{ Gy}_{\text{EQD2}}$ , and the median (95<sup>th</sup> percentile) of the residual distance was 8.7(22) mm.

### ***Conclusions***

DIR corresponded with the PRM for on average 75% of the  $D_{2\text{cm}^3}$  volume. Local absolute dose differences and residual distances were large. Care should therefore be taken with DIR for dose warping purposes in brachytherapy.

## Introduction

Locally-advanced cervical cancer is commonly treated with concurrent chemotherapy and radiotherapy. The radiation treatment consists of external beam radiotherapy (EBRT) combined with a brachytherapy (BT) boost in multiple applications to the tumor area. After each BT implantation the 3D dose distribution is calculated using image-guided treatment planning. Planning aims include a recommended dose to 90% of the high-risk clinical target volume (CTV<sub>HR</sub>) from EBRT and BT of 90-95 Gy<sub>EQD2</sub>, expressed as equivalent dose in 2 Gy fractions (EQD<sub>2</sub>).<sup>1</sup> The dose to the most irradiated 2 cm<sup>3</sup> of the rectum (D<sub>2cm<sup>3</sup></sub>), which is associated with rectal toxicity, should not exceed 75 Gy<sub>EQD2</sub>.<sup>2,3</sup>

It is recommended by the International Commission on Radiation Units and Measurements (ICRU) to assume that the high dose volumes are at the same location on the rectal wall for the evaluation of the cumulative rectum D<sub>2cm<sup>3</sup></sub> of multiple BT applications, meaning that the DVH parameters can simply be added.<sup>1</sup> With the ICRU formalism, D<sub>2cm<sup>3</sup></sub> is possibly overestimated, which may lead to errors in establishing the dose-response relationship in the rectum. To avoid overestimating the cumulative D<sub>2cm<sup>3</sup></sub>, it may be preferable to sum the 3D dose distributions instead.

When summing the total dose it is necessary to use deformable image registration (DIR) to account for rectal deformation due to differences in filling and/or the presence of air and the effect of the applicator on the position of the rectum. Earlier studies investigated the added value of DIR when calculating cumulative rectal D<sub>2cm<sup>3</sup></sub> and they found small differences (<10%) with direct addition of the D<sub>2cm<sup>3</sup></sub>.<sup>4-7</sup> Because of the DIR related uncertainty, they concluded that there was limited benefit of dose accumulation with DIR over direct addition of DVH parameters.

Indeed, little is known about the reliability of DIR for accumulation of the BT dose in the rectum. Jamema et al. analyzed uncertainties when accumulating the BT dose in the rectum, by comparing intensity-based to structure-based matching.<sup>6</sup> They found that dose accumulation based on structure-based matching is more reliable than intensity-based matching since intensity-based DIR led to implausible deformation and a systematic underestimation of the dose. Dose accumulation accuracy may improve further when the matching is performed based on a physically realistic model that includes an estimate of the biomechanical properties, since such properties are not taken into account in the structure-based DIR. As of yet, no studies have investigated the dose warping uncertainties for accumulated BT doses through landmark identification. Such anatomical landmarks cannot be identified through visual assessment on BT planning images (CT/anatomical MRI).

We propose to investigate uncertainties for dose accumulation based on structure-based matching by identifying corresponding point pairs on the rectum wall using a model describing rectal deformation.

The purpose of this study is therefore to accumulate the total brachytherapy dose to the rectal wall using structure-based deformable image registration and to investigate dose warping uncertainties using a physically realistic model describing rectal deformation.

## Materials and Methods

### *Patients*

Ten cervical cancer patients treated with EBRT (45-50 Gy in 1.8-2.0 Gy/fraction) and a pulsed-dose rate BT boost, delivered in two applications BT1 and BT2 of 18 Gy each in pulse doses of 75 cGy every hour, were included in this study. EBRT was planned with volumetric modulated arc therapy. For brachytherapy an intrauterine device with ovoids and if needed interstitial needles was used. The time interval between the BT applications was <2 weeks. The planning aim was a cumulative  $D_{90}$  of 90-95  $Gy_{EQD2}$  from EBRT and BT on the  $CTV_{HR}$ . To spare the rectum, the planned cumulative  $D_{2cm^3}$  from EBRT and the BT applications should not exceed 75  $Gy_{EQD2}$ . Prior to the BT delivery,  $T_2$ -weighted Turbo Spin Echo MRI (voxel size: 0.5x0.5x3.3 mm<sup>3</sup>) was acquired on an Ingenia 3 T MRI scanner (Philips Healthcare, Best, The Netherlands).<sup>8</sup> On the MRI scans, the rectum was delineated from the rectosigmoid junction to the level of the anal sphincter. Rectum volumes at the time of BT1 and BT2 are described in Table 1. BT planning was performed using Oncentra Brachy 4.5 (Elekta, Veenendaal, The Netherlands), using a library for applicator reconstruction, after which the plan was manually optimized. Typical dose distributions are shown in Fig. 1.

### *Implementation of the physically realistic model*

We used a physically realistic model (PRM) describing rectal deformation to localize corresponding point pairs on the rectum wall, because there is a lack of corresponding anatomical landmarks that can be distinguished on the BT planning MRI.<sup>9,10</sup> The principles of the PRM were previously described by Meijer et al.<sup>11</sup> and Hoogeman et al.<sup>12</sup> This model was already used to quantify rectum displacements<sup>12,13</sup> and to relate dose surface maps to toxicity.<sup>14,15</sup>



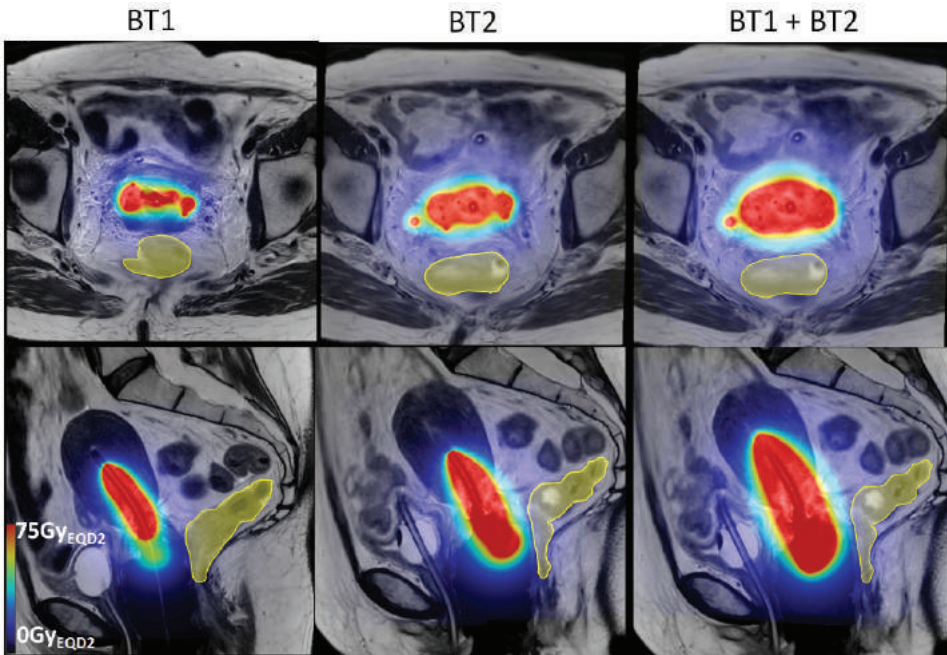


**Fig. 1** Axial (top row) and sagittal view (bottom row) of the patient MRI with a color wash of the planned dose from BT1 (left), BT2 (middle) and the dose from BT1 and BT2, accumulated using structure-based deformable image registration as described in this paper (right). The rectum is shown in yellow.

The model is based on physiological characteristics of the rectum.<sup>11,12,16</sup> The rectum is attached on the dorsal side to the sacrum by the mesorectum. The rectum wall has an inner lining of circular smooth muscle which will stretch and elongate with increased rectal filling. This stretching, which is assumed to always be perpendicular to the central axis, is accompanied by an overall narrowing of the rectum wall. Due to this trade-off between rectal wall thickness and stretching of the rectum muscularis, the amount of tissue in the rectal wall is constant in every intersection perpendicular to the central axis. Since displacements along the length of the axis can be neglected, the central axes of the rectum of BT1 and BT2 ( $\text{rectum}_{\text{BT1}}$ ,  $\text{rectum}_{\text{BT2}}$ ) are assumed to be fixed in length.

The central axes were constructed using a minimum distance field as described by Zhou et al.<sup>17</sup>, to find for each lateral plane the voxel with the shortest distance to the boundary (Matlab R2014b, Mathworks Inc., MA) (Fig. 2). Subsequently, the axis was smoothed using a moving average filter with a span of 0.5 cm.

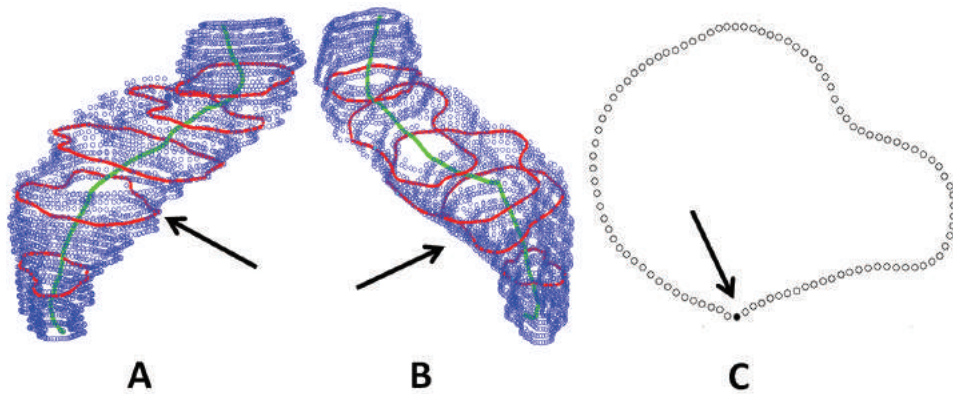


**Fig. 2** View from the left side (A), and the right side (B) of the rectum point cloud (blue), with the central axis (green), and the 5 intersection curves describing the planes orthogonal to the central axis (red). C) The curve indicated by the arrows in A and B. 100 points were evenly distributed over the curve. The filled dot and arrow indicates the most dorsal point.

For both  $\text{rectum}_{\text{BT1}}$  and  $\text{rectum}_{\text{BT2}}$ , orthogonal planes were constructed at 5 evenly spaced positions on the axis. For areas of high curvature in the rectum, the planes might intersect. To avoid intersecting planes, only 5 planes were constructed and the planes were rotated away from each other if the local curvature of the central axes exceeded a fixed maximum. Next, 100 points were evenly distributed over the intersection curve of each plane with the rectal wall. It was assumed that the rectum is fixed at the dorsal side. This fixed dorsal point was point 1 and it was found by sampling the point on the intersection curve for which the left-right coordinate was closest to that of the central axis. All corresponding point pairs were stored to be used for the DIR evaluation.

### ***Deformable image registration & dose accumulation***

The dose from BT1 and BT2 was accumulated in  $\text{EQD}_2$  using DIR to take into account rectal deformation. First, the BT doses were converted to  $\text{EQD}_2$  on a voxel-by-voxel level using LQ-model based equations with an  $\alpha/\beta$  value of 3 Gy for late rectal toxicity and a 1.5 hour repair half-time.<sup>1,18</sup>

The Feature-Based Deformable Registration (FBDR) tool, available in a research version of Oncentra Brachy was used for structure-based DIR with the BT1 as the reference frame. The DIR algorithm in the FBDR tool is directly derived from the symmetric unidirectional thin plate spline robust point matching algorithm.<sup>10,19,20</sup> The delineated rectums were converted to 3D surface meshes, and a mapping was established to propagate elements on the

surface of  $\text{rectum}_{\text{BT1}}$  to the surface of  $\text{rectum}_{\text{BT2}}$ .

To evaluate the DIR accuracy, the Dice coefficient<sup>21</sup> was calculated between the propagated (BT1) and reference (BT2) contours as well the mean surface distance error, which is the Euclidean distance between the reference and propagated contours. Finally, the transformation vectors were used to deform the BT1 dose distribution and the BT1 and BT2 doses were summed voxel-by-voxel (Fig. 1, right panel).

**DIR accuracy in the rectal wall**

The point pairs defined with the PRM were used to quantify uncertainties in the accumulated DIR dose. For corresponding points on  $\text{rectum}_{\text{BT1}}$  and  $\text{rectum}_{\text{BT2}}$  the dose of BT1 and BT2 was added ( $D_{\text{PRM}}$ ) and compared to the DIR accumulated dose ( $D_{\text{DIR}}$ ) in the BT2 point. Additionally the remaining distance after DIR between corresponding points, which is defined as the residual distance, was calculated (Fig. 3).

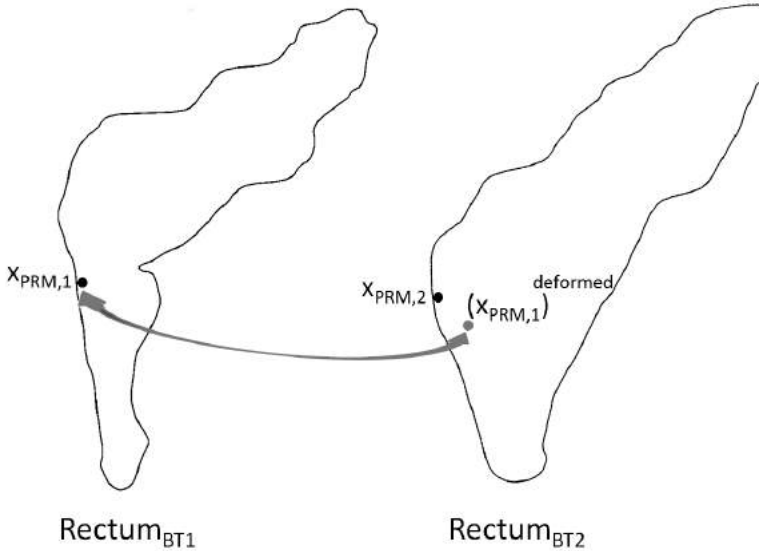


**Fig. 3** Corresponding point pair on the rectum of BT1 and BT2 ( $x_{\text{PRM},1}$  and  $x_{\text{PRM},2}$ ) localized using the PRM. For this point pair,  $D_{\text{PRM}}$  and  $D_{\text{DIR}}$  are calculated according to:

$$D_{\text{PRM}} = D_{\text{BT1}}(x_{\text{PRM},1}) + D_{\text{BT2}}(x_{\text{PRM},2}) \text{ and } D_{\text{DIR}} = D_{\text{BT1}}^{\text{deformed}}(x_{\text{PRM},2}) + D_{\text{BT2}}(x_{\text{PRM},2}).$$

The dose difference is  $D_{\text{PRM}} - D_{\text{DIR}}$ . The residual distance (RD) is the Euclidean distance between  $x_{\text{PRM},2}$  and the deformed point  $x_{\text{PRM},1}$ :  $\text{RD} = |x_{\text{PRM},1}^{\text{deformed}} - x_{\text{PRM},2}|$ .

For BT, the high dose regions in the rectum are most relevant. Therefore, only those point pairs for which  $D_{DIR}$  was  $\geq D_{2cm^3}^{ICRU}$  were considered in the rest of the analysis. The  $D_{2cm^3}^{ICRU}$  was calculated by adding  $D_{2cm^3}$  from BT1 to  $D_{2cm^3}$  from BT2, according to the ICRU formalism.  $D_{2cm^3}^{ICRU}$  was used as a threshold, because this is a conservative estimate of the cumulative  $D_{2cm^3}$  since it assumes the high dose volumes are overlapping. The analysis was done in this way to avoid analyzing points outside the  $D_{2cm^3}$  volume.

We calculated the average  $D_{PRM}$  and  $D_{DIR}$  for all patients and compared these values. For every patient the 25<sup>th</sup>, 50<sup>th</sup>, 75<sup>th</sup> and 95<sup>th</sup> percentiles of the absolute dose difference

( $|D_{DIR} - D_{PRM}|$ ) and the 25<sup>th</sup>, 50<sup>th</sup>, 75<sup>th</sup> and 95<sup>th</sup> percentiles of the residual distance were calculated. For both the absolute dose difference and residual distance, the 50<sup>th</sup> and 95<sup>th</sup> percentile over all patients was determined.

Points within the 2 cm<sup>3</sup> volume receiving the highest dose should be correctly identified, meaning that DIR is in agreement with PRM about which points are part of the  $D_{2cm^3}$  volume. For the points under consideration, this was investigated by calculating the average percentage for which  $D_{PRM} \geq D_{2cm^3}^{ICRU}$  over all patients.

## Results

The Dice coefficient after DIR was between 0.95-0.97 and the mean surface distance error was between 0.2-0.7 mm, showing that after DIR the rectum contours were overlapping. Over all patients, on average 11% of the PRM points were within the volume for which  $D_{DIR}$  was  $\geq D_{2cm^3}^{ICRU}$ , and the mean(range) of the number of points was 56(22-81). Only these point pairs are considered in the following results.

Averaged over all patients, the mean  $D_{DIR}$  was 1.3 Gy<sub>EQD2</sub> higher than the mean  $D_{PRM}$ , with differences ranging between (-3.5)-4.9 Gy<sub>EQD2</sub>. For 9 out of 10 patients, the mean  $D_{PRM}$  was smaller than the mean  $D_{DIR}$ .

For the median absolute dose difference, values varied over all patients between 0.6-4.9 Gy<sub>EQD2</sub>, while the 95<sup>th</sup> percentile varied between 1.4-7.3 Gy<sub>EQD2</sub> (Fig. 4). For all patients combined, 50% of the absolute dose differences was  $< 2.2$  Gy<sub>EQD2</sub> and 95% of the absolute dose differences was  $< 5.8$  Gy<sub>EQD2</sub>. The residual distance varied between 1.5-33 mm (Fig. 5). For all calculated residual distance values, 50% was  $< 8.7$  mm and 95% was  $< 23$  mm.  $D_{PRM}$  was  $\geq D_{2cm^3}^{ICRU}$  for 75% of the points under consideration, meaning that DIR and PRM were in agreement that these points were part of the  $D_{2cm^3}$  volume.

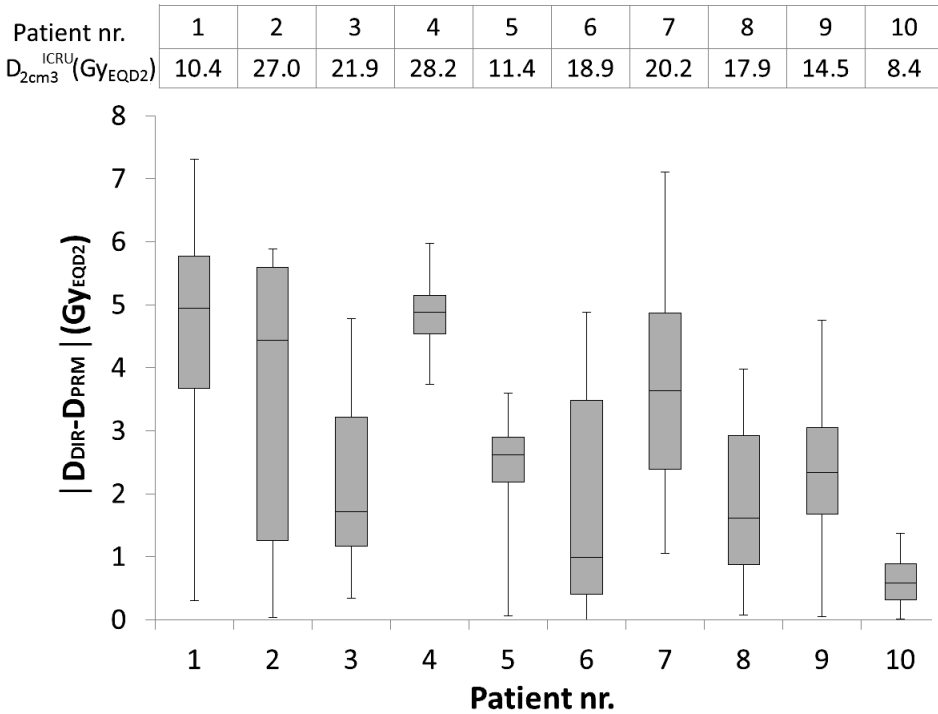


**Fig. 4** Boxplot of the absolute dose difference calculated for corresponding points within the  $D_{2\text{cm}^3}$  volume for all patients, with the median and the 25th and 75th percentiles. The whiskers show the minimum and the 95th percentile. The table shows the  $D_{2\text{cm}^3}^{\text{ICRU}}$ , which is the cumulative  $D_{2\text{cm}^3}$  of both applications, calculated with the ICRU formalism.

## Discussion

This is the first study to use a physically realistic model that describes rectal deformation to investigate local dose warping uncertainties for the brachytherapy rectum dose accumulated with structure-based DIR. We used the physically realistic model to locate points on the rectal wall. For points within the  $2\text{ cm}^3$  receiving the highest dose, dose differences could be as high as  $7.3\text{ Gy}_{\text{EQD2}}$ , and the median residual distance after DIR was  $8.7\text{ mm}$ . For the points under consideration, more than 75% was part of the  $D_{2\text{cm}^3}$  volume according to both PRM and DIR. Our results show that due to large local uncertainties dose accumulation with this structure-based DIR algorithm is problematic for doses that have steep gradients such as in brachytherapy.



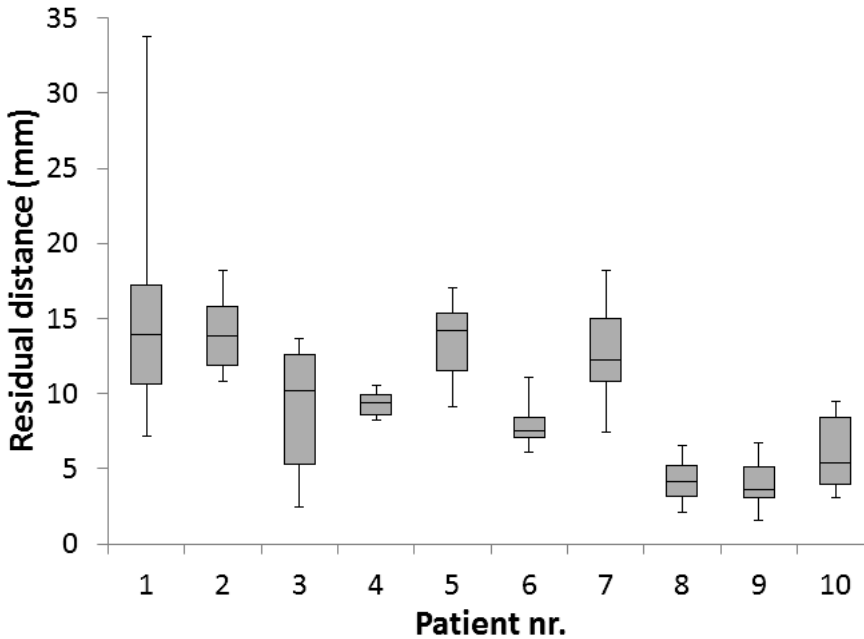


**Fig. 5** Boxplot of the residual distance after DIR between corresponding points within the  $D_{2cm^3}$  volume for all patients, with the median and the 25<sup>th</sup> and 75<sup>th</sup> percentile. The whiskers show the minimum and the 95<sup>th</sup> percentile.

There are many uncertainties related to cervical cancer brachytherapy.<sup>22,23</sup> Inter- and intra-fraction motion and delineation uncertainties are major contributors to the total uncertainty in estimation of the delivered dose.<sup>24,25</sup> Calculation of accumulated dose from BT using the ICRU formalism is another source of uncertainty, since it may lead to a systematic overestimation of the delivered dose. However, our results show that using DIR to calculate cumulative DVH parameters will introduce large new uncertainties.

Structure-based DIR was used in this study to accumulate BT dose in the rectum. The choice of DIR algorithm is important, because the quality of the registration depends strongly on the DIR performance. According to Jamema et al.<sup>6</sup>, who compared structure-based and intensity-based DIR for 3D accumulated  $D_{2cm^3}$ , structure-based DIR is the best choice for DIR-based dose accumulation in the rectum. Compared to earlier studies<sup>5,7</sup> high Dice coefficients ( $>0.95$ ) and low mean residual distances ( $<0.7$  mm) were achieved in this study with structure-based DIR, showing that the rectum contours were matched with high accuracy.

We narrowed down our results to the dose difference and residual distance of only those point pairs for which  $D_{PRM}$  was  $\geq D_{2cm^3}^{ICRU}$ , since DVH parameters of the high dose volumes are commonly reported for rectum in BT. Although 500 points were sampled at different positions on the rectal wall, only a small selection (11%) was relevant for this study. These points were predominantly located at the more caudal region of the rectum, which is near the region of the BT boost. Since points were localized in planes over the entire rectal surface, the method explained in this study could be used to evaluate accumulated doses for different dose schemes, such as fractionated EBRT, by including more points. However, this was beyond the scope of this study.

For the points under consideration the mean  $D_{DIR}$  was on average  $1.3 \text{ Gy}_{EQD2}$  higher than the mean  $D_{PRM}$ . This is as expected, since the high dose area obtained by PRM might not be the same as obtained by DIR. For one patient, PRM overestimated the mean dose to the  $D_{2cm^3}$  volume. For this patient, the true minimum within the volume was possibly not found, since only 22 points were included in the analysis.

The absolute dose difference for individual points could be as high as  $7.3 \text{ Gy}_{EQD2}$ , while the median absolute dose difference over all patients was  $2.2 \text{ Gy}_{EQD2}$ , and the 95<sup>th</sup> percentile of the residual distance was 23 mm. This shows that locally uncertainties can be large. The impact of these uncertainties on the  $D_{2cm^3}$  is unclear. This could be evaluated by calculating  $D_{2cm^3}$  using the PRM and then compare this to  $D_{2cm^3}$  calculated with DIR, but this is not possible with the method used in this study. 75% of the points were identified as part of the  $D_{2cm^3}$  volume by both PRM and DIR, meaning that the points were merely redistributed by DIR within the  $D_{2cm^3}$  volume. Thus the location of the  $D_{2cm^3}$  volume in the DIR accumulated dose is similar to the location of the  $D_{2cm^3}$  volume in the real dose.

For patient 1 the 95<sup>th</sup> percentile of the residual distance was as high as 33 mm. Visual inspection showed that a high overlap of the rectum contours was achieved near the high dose area (Fig. 6). However, this was the patient with the largest absolute ( $48 \text{ cm}^3$ ) and relative volume difference (Volume BT2 / volume BT1 : 2.09) between rectum 1 and rectum 2 (see Table 1). This indicates a large difference in rectal filling which may have affected the quality of the registration.

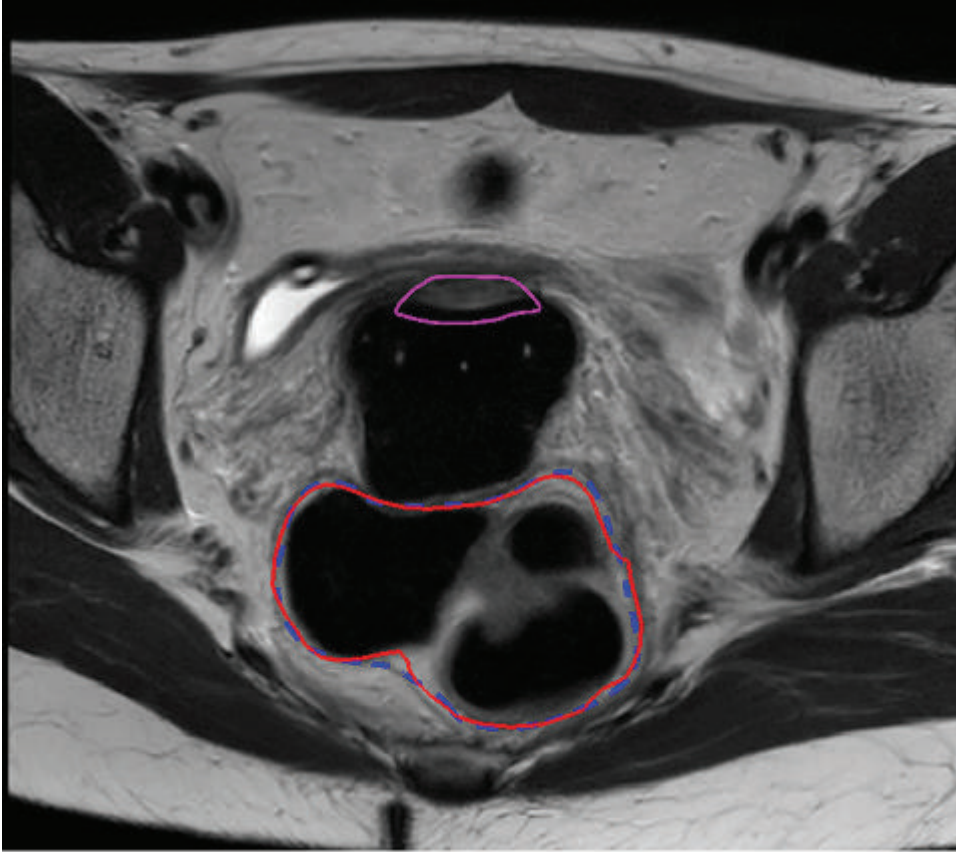


**Fig. 6** Axial view of the BT MRI of patient 1 where the propagated rectum contour (solid) is shown together with the reference contour (dashed). The contours are shown close to the target (magenta).

There are no other studies which investigate brachytherapy dose uncertainties in the rectum in corresponding point pairs on the rectum wall, so it is not possible to directly compare the dose uncertainties we found. For the residual distance, Nassef et al.<sup>26</sup> investigated uncertainties in accumulated rectum dose from EBRT using the daily CBCTs, for prostate cancer. In a numerical phantom of the female pelvis, they defined surface points on the rectum, and found mean landmark errors of 2.4 mm on the rectal wall. Vasquez-Osorio et al.<sup>10</sup> defined landmarks near the cervix-uterus, bladder and in the mesorectum and reported the mean error (3.4 mm) of all these landmarks for MRI registration using the same DIR algorithm as this study. These values were smaller than the median residual distance of 8.7 mm



found in this study. However, in the mentioned studies landmarks over the whole rectum or near the rectum were included, as well as landmarks near other structures, while in our study we evaluated only points in the  $D_{2\text{cm}^3}$  volume of the rectum.

	Rectum Mean (Range)
BT1 volume (cm <sup>3</sup> )	45 (28;90)
BT2 volume (cm <sup>3</sup> )	47 (27;83)
BT1 – BT2   Volume difference   (cm <sup>3</sup> )	16 (0.9;48)
Volume BT2 / volume BT1	1.12 (0.47;2.09)

**Table 1** The mean and the range over all patients of the rectum volume at the time of brachytherapy application 1 and 2 (BT1, BT2), and the absolute difference between the BT volumes, as well as the ratio.

The evaluated points were all located on the rectal surface, while the  $D_{2\text{cm}^3}$  volume could partly be filling. According to Wachter-Gerstner et al.<sup>27</sup> and Olszewska et al.<sup>28</sup>, the  $D_{2\text{cm}^3}$  calculated from the DVH of the external contour is a good estimate of rectal wall dose. Thus our method is adequate to determine dose errors in the  $D_{2\text{cm}^3}$  volume.

In this study we did not investigate dose warping uncertainties for EBRT-BT dose accumulation. Residual distances between registered EBRT and BT rectums will likely be comparable to the BT-BT registrations reported in this study, since in our institute for EBRT and BT the same pretreatment instructions apply to control the rectal filling and therefore the rectal volumes will be similar. Yet, even though geometrical errors will be large, dose errors for EBRT-to-BT accumulation will be small for the patients included in this study. For EBRT a planning aim was used for the rectum ( $D_{1\text{cm}^3} < 103\%$  of the prescription dose) to ensure a uniform dose. We focused on errors for the BT-to-BT dose accumulation, because the BT dose has high gradients and voxel-to-voxel correspondence of DIR is more important for a non-uniform dose. An extensive DIR analysis of the local errors in EBRT-to-BT accumulation would be interesting when more conformal EBRT planning strategies with smaller margins are used.

The PRM includes assumptions based on physiological characteristics of the rectum. However plausible these assumptions, a limitation of this study is that the PRM was not validated for point-to-point consistency. We could not identify anatomical points on the rectum wall on the planning MRI to check the model. It could be argued that for points located on



the caudal side of the rectum, the point-to-point consistency is worse than for dorsal points. In the model we assume isotropic expansion away from the most dorsal point. For caudally located point pairs, the position will be more affected by local non-isotropic expansions of the rectum, such as gas bubbles.

An earlier study by Meijer et al. showed that EBRT DVHs of the rectal wall constructed using the PRM and of the delineated rectal wall were comparable. Future work should look into such an analysis of the PRM validity using visible landmarks as has already been done for DIR in the bladder.<sup>29</sup> Other future studies could accumulate the total brachytherapy dose to the rectal wall using the PRM and compare accumulated DVH parameters to the direct addition method.

### **Conclusions**

For a large part (75%) of the  $D_{2\text{cm}^3}$  volume, DIR corresponded with PRM. Within the  $D_{2\text{cm}^3}$  volume, absolute dose differences were large ( $<7.3 \text{ Gy}_{\text{EQD2}}$ ), as well as the median residual distance (8.7 mm). Care should therefore be taken for dose accumulation with this DIR algorithm for doses that have steep gradients such as in brachytherapy.

### **Acknowledgements**

This work was funded by Elekta Brachytherapy (II 250008). The authors are grateful to dr. Joost Schillings from Elekta Brachytherapy for his help with the FBDR tool.

## References

- [1] Pötter R, Haie-Meder C, Van Limbergen E, Barillot I, De Brabandere M, Dimopoulos J, et al. Recommendations from gynaecological (GYN) GEC ESTRO working group (II): concepts and terms in 3D image-based treatment planning in cervix cancer brachytherapy-3D dose volume parameters and aspects of 3D image-based anatomy, radiation physics, radiobiology. *Radiother Oncol* 2006;78:67–77.
- [2] Georg P, Pötter R, Georg D, Lang S, Dimopoulos JCA, Sturdza AE, et al. Dose effect relationship for late side effects of the rectum and urinary bladder in magnetic resonance image-guided adaptive cervix cancer brachytherapy. *Int J Radiat Oncol Biol Phys* 2012;82:653–7.
- [3] Mazon R, Fokdal LU, Kirchheiner K, Georg P, Jastaniyah N, Šegedin B, et al. Dose–volume effect relationships for late rectal morbidity in patients treated with chemoradiation and MRI-guided adaptive brachytherapy for locally advanced cervical cancer: Results from the prospective multicenter EMBRACE study. *Radiother Oncol* 2016;120:412–9.
- [4] Abe T, Tamaki T, Makino S, Ebara T, Hirai R, Miyaura K, et al. Assessing cumulative dose distributions in combined radiotherapy for cervical cancer using deformable image registration with pre-imaging preparations. *Radiat Oncol* 2014;9:293.
- [5] Flower E, Do V, Sykes J, Dempsey C, Holloway L, Summerhayes K, et al. Deformable image registration for cervical cancer brachytherapy dose accumulation: Organ at risk dose–volume histogram parameter reproducibility and anatomic position stability. *Brachytherapy* 2017;16:387–92.
- [6] Jamema S V, Mahantshetty U, Andersen E, Noe KØ, Sørensen TS, Kallehauge JF, et al. Uncertainties of deformable image registration for dose accumulation of high-dose regions in bladder and rectum in locally advanced cervical cancer. *Brachytherapy* 2015;15:953–62.
- [7] Sabater S, Andres I, Sevillano M, Berenguer R, Machin-Hamalainen S, Arenas M. Dose accumulation during vaginal cuff brachytherapy based on rigid/deformable registration vs. single plan addition. *Brachytherapy* 2014;13:343–51.
- [8] van Heerden LE, Gurney-Champion OJ, van Kesteren Z, Houweling AC, Koedooder C, Rasch CRN, et al. Quantification of image distortions on the Utrecht interstitial CT/MR brachytherapy applicator at 3T MRI. *Brachytherapy* 2016;15:118–26.
- [9] Torkzad MR, Pählman L, Glimelius B. Magnetic resonance imaging (MRI) in rectal cancer: a comprehensive review. *Insights Imaging* 2010;1:245–67.
- [10] Vásquez Osorio EM, Kolkman-Deurloo I-KK, Schuring-Pereira M, Zolnay A, Heijmen BJM, Hoogeman MS. Improving anatomical mapping of complexly deformed anatomy for external beam radiotherapy and brachytherapy dose accumulation in cervical cancer. *Med Phys* 2015;42:206–20.

- [11] Meijer GJ, van den Brink M, Hoogeman MS, Meinders J, Lebesque J V. Dose–wall histograms and normalized dose–surface histograms for the rectum: a new method to analyze the dose distribution over the rectum in conformal radiotherapy. *Int J Radiat Oncol* 1999;45:1073–80.
- [12] Hoogeman MS, van Herk M, de Bois J, Muller-Timmermans P, Koper PCM, Lebesque J V. Quantification of local rectal wall displacements by virtual rectum unfolding. *Radiother Oncol* 2004;70:21–30.
- [13] Nijkamp J, Pos FJ, Nuver TT, de Jong R, Remeijer P, Sonke J-J, et al. Adaptive Radiotherapy for Prostate Cancer Using Kilovoltage Cone-Beam Computed Tomography: First Clinical Results. *Int J Radiat Oncol* 2008;70:75–82.
- [14] Heemsbergen WD, Hoogeman MS, Hart GAM, Lebesque J V., Koper PCM. Gastrointestinal toxicity and its relation to dose distributions in the anorectal region of prostate cancer patients treated with radiotherapy. *Int J Radiat Oncol* 2005;61:1011–8.
- [15] Wortel RC, Witte MG, van der Heide UA, Pos FJ, Lebesque J V., van Herk M, et al. Dose–surface maps identifying local dose–effects for acute gastrointestinal toxicity after radiotherapy for prostate cancer. *Radiother Oncol* 2015;117:515–20.
- [16] Baxter NN, Burnstein MJ. *Treatment of colorectal cancer*. Elsevier; 2014.
- [17] Zhou SM, Marks LB, Tracton GS, Sibley GS, Light KL, Maguire PD, et al. A new three-dimensional dose distribution reduction scheme for tubular organs. *Med Phys* 2000;27:1727–31.
- [18] International Commission on Radiation Units and Measurements. *Prescribing, Recording, and Reporting Brachytherapy for Cancer of the Cervix (ICRU report 89)*. vol. 13. 2013.
- [19] Bondar L, Hoogeman M, Mens JW, Dhawtal G, de Pree I, Ahmad R, et al. Toward an individualized target motion management for IMRT of cervical cancer based on model-predicted cervix-uterus shape and position. *Radiother Oncol* 2011;99:240–5.
- [20] Vásquez Osorio EM, Hoogeman MS, Bondar L, Levendag PC, Heijmen BJM. A novel flexible framework with automatic feature correspondence optimization for nonrigid registration in radiotherapy. *Med Phys* 2009;36:2848.
- [21] Dice LR. Measures of the Amount of Ecologic Association Between Species. *Ecology* 1945;26:297–302.
- [22] Kirisits C, Rivard MJ, Baltas D, Ballester F, De Brabandere M, van der Laarse R, et al. Review of clinical brachytherapy uncertainties: analysis guidelines of GEC-ESTRO and the AAPM. *Radiother Oncol* 2014;110:199–212.
- [23] Nesvacil N, Tanderup K, Lindegaard JC, Pötter R, Kirisits C. Can reduction of uncertainties in cervix cancer brachytherapy potentially improve clinical outcome? *Radiother Oncol* 2016;120:390–6.
- [24] Hellebust TP, Tanderup K, Lervåg C, Fidarova E, Berger D, Malinen E, et al. Dosimetric impact of interobserver variability in MRI-based delineation for

- cervical cancer brachytherapy. *Radiother Oncol* 2013;107:13–9.
- [25] Nesvacil N, Tanderup K, Hellebust TP, De Leeuw A, Lang S, Mohamed S, et al. A multicentre comparison of the dosimetric impact of inter- and intra-fractional anatomical variations in fractionated cervix cancer brachytherapy. *Radiother Oncol* 2013;107:20–5.
- [26] Nassef M, Simon A, Cazoulat G, Duménil A, Blay C, Lafond C, et al. Quantification of dose uncertainties in cumulated dose estimation compared to planned dose in prostate IMRT. *Radiother Oncol* 2016.
- [27] Wachter-Gerstner N, Wachter S, Reinstadler E, Fellner C, Knocke TH, Wambersie A, et al. Bladder and rectum dose defined from MRI based treatment planning for cervix cancer brachytherapy: comparison of dose-volume histograms for organ contours and organ wall, comparison with ICRU rectum and bladder reference point. *Radiother Oncol* 2003;68:269–76.
- [28] Olszewska AM, Saarnak AE, de Boer RW, van Bunningen BN, Steggerda MJ. Comparison of dose-volume histograms and dose-wall histograms of the rectum of patients treated with intracavitary brachytherapy. *Radiother Oncol* 2001;61:83–5.
- [29] Wognum S, Heethuis SE, Rosario T, Hoogeman MS, Bel A. Validation of deformable image registration algorithms on CT images of ex vivo porcine bladders with fiducial markers. *Med Phys* 2014;41:071916.



# Chapter 7

General discussion

Brachytherapy planning and treatment delivery are associated with a number of uncertainties and there is major concern in the brachytherapy community on the clinical consequences of possible errors due to these uncertainties.<sup>1,2</sup> This thesis focused on the impact of uncertainties on the cumulative 3D dose distribution in multimodality radiotherapy for cervical cancer, particularly those related to image distortions (chapter 2 and 3) and dose accumulation uncertainties (chapters 4 to 6).

In chapter 2 and 3, image distortions for brachytherapy planning on 3 T magnetic resonance (MR) images were evaluated. We described an MRI-only method to quantify image distortions on the planning images (chapter 2). Our results showed that uncertainties in the total planned brachytherapy dose due to image distortions were limited, thereby proving that accurate applicator reconstruction is possible on images acquired with a 3 T MRI scanner. Following up on these results, the dosimetric implications of these image distortions were investigated in patients and found to be clinically insignificant in chapter 3. Based on these studies, we concluded that 3 T MRI can safely be implemented in the clinical brachytherapy procedure.

In chapters 4, 5 and 6 we evaluated an approach to accumulate the 3D dose distribution using deformable image registration. We investigated the added value of non-rigid registration for the evaluation of cumulative external beam radiotherapy (EBRT) and brachytherapy (BT) dose volume histogram (DVH) parameters, for both the planned (chapter 4) and delivered EBRT dose (chapter 5). For the summation of EBRT and BT doses in the various OARs, dose differences between simple DVH parameter addition and 3D dose addition with deformable image registration were small. Even for patients treated using a plan-of-the-day strategy, the delivered EBRT dose near the planned BT boost could be considered uniform for the evaluation of bladder/rectum dose. With the current planning strategies, dose addition with DIR is not necessary and simple addition of DVH parameters is an adequate method to assess the toxicity in bladder and rectum from EBRT and BT.

Non-rigid registration could also be used for the accumulation of the total radiotherapy dose from multiple BT fractions. In chapter 6, we investigated uncertainties related to deformable image registration when accumulating the dose to the rectum of multiple brachytherapy fractions. We showed that, due to incorrect registration, dose addition with DIR is problematic for doses that have steep gradients such as brachytherapy doses. This chapter will discuss the results presented in chapters 2-6 and we will present an outlook for future research



### ***Contouring and anatomical variation***

Compared to applicator reconstruction errors and dose accumulation errors, contouring and anatomical variations are more important contributors to the total uncertainty in delivered BT dose.<sup>3,4</sup> Earlier investigations have shown that errors in applicator reconstruction could lead to an average change of 5% in expected  $D_{2\text{cm}^3}$  for bladder and rectum and 4% in  $D_{90}$  for the target per mm displacement of the applicator.<sup>5</sup> Dose accumulation errors stemming from incorrect assumptions could lead to an over- or underestimation of the cumulative dose delivered with combined EBRT and BT. According to Hellebust et al. the dosimetric impact of contouring variation is 9% for the target and 5-11% for OAR.<sup>6</sup> A multi-center study by Nesvacil et al. showed that intra-application anatomical variations could lead to dose differences of 10% for the target and 24% for OAR.<sup>3</sup> The latter can be substantial over 24 h of PDR brachytherapy. A study by de Leeuw et al. showed that intra-application motion over 22 h of PDR brachytherapy could lead to an increase of 12 Gy<sub>EQD2</sub> in bladder  $D_{2\text{cm}^3}$ .<sup>7</sup>

In this thesis we did not take the impact of contouring variation or anatomical variation into account. Compared to the contouring and anatomical variation, the uncertainties described in this thesis resulted in a negligible change in expected outcome, while large dose uncertainties of 20-30% due to intra-application motion can lead to differences in the dose response curves of >5%.<sup>8</sup> For patients treated at our institute the effects of inter-application motion can be ignored, since a new plan was created for every application based on re-imaging after implantation.

The impact of dose variations on expected outcome depends on the prescribed dose level to the target structure or OAR. Uncertainties will have more impact for doses which are close to the planning constraint or for doses which are in the steep part of the dose-response curve.<sup>2,4</sup> Target doses are usually in the flat part of the tumor response curves, and expected tumor control is robust to uncertainties. Even large variations of 20% in the target dose had negligible impact on the tumor control probability. The largest effort in reducing uncertainties should therefore be for the OAR, while care should be taken to maintain a high tumor control.<sup>2</sup>

### ***Uncertainties related to image distortions***

For brachytherapy, MRI-guided dose planning and applicator reconstruction is recommended by the ICRU due to the superior soft-tissue contrast compared to ultrasound and CT.<sup>9</sup> Incorrect applicator reconstruction can lead to dose errors up of 1 Gy per 1 mm shift.<sup>5</sup> In the first two chapters we described MRI distortions of the applicator due to main magnetic field ( $B_0$ ) inhomogeneity. A  $B_0$  map was used to quantify the displacements using the

bandwidth of clinical scans. Our work shows that at a field strength of 3 T it is possible to perform accurate applicator reconstruction, because the image distortions are small (<0.8 mm).

In previous research, quality assurance of applicators was performed in patients by comparing an undistorted CT image to the distorted MR image using rigid registration.<sup>10,11</sup> With the methods described in chapters 2 and 3 the expected distortions can be quantified directly from the  $B_0$  map using the MR imaging sequence characteristics. As a result, it is not necessary to acquire a CT scan for applicator reconstruction only, resulting in a reduced patient burden as well as lower cost for the hospital and a lower radiation dose for patients. This technique may be applied irrespective of the applicator used. Acquisition of  $B_0$  maps should therefore become a standard part of the quality assurance (QA) procedure for brachytherapy planning with MRI.

Higher magnetic field strengths might benefit brachytherapy planning by facilitating the use of functional MR imaging. Cervical tumor delineation may improve by combining functional MR imaging with anatomical MRI scans, as has been demonstrated for prostate cancer.<sup>12</sup> It should be noted, however, that functional imaging uses a shorter bandwidth than the clinical bandwidth we investigated. Since the severity of image distortions increases with shorter bandwidths, this may hamper tumor delineation. A recent study investigated geometric distortions on diffusion weighted images of cervical cancer brachytherapy patients with the applicator in situ, and they reported distortions as large as 9 mm.<sup>13</sup> Unless geometric distortions can be reduced, functional imaging for brachytherapy planning remains problematic.

It should be noted that our research was limited to image distortions on the plastic Utrecht interstitial CT/MR applicator of Elekta commonly used in the clinic.<sup>14-16</sup> Other types of applicators are also available for cervical cancer brachytherapy.<sup>10,11,17</sup> Some of these applicators are partly made of metal for which larger artifacts can be expected, and these were not investigated. In addition, we did not quantify the  $B_0$  induced geometric distortions outside a region of interest which contained the intrauterine device, the ovoids as well as tissue. Geometric distortion on tissue outside of this region of interest may impact DVH parameters, since planning decisions are made based on organs delineations. Since geometric distortion was less than 1 mm for tissue within the region of interest, we expect that the impact of geometric distortion outside of this region of interest will be limited.

### ***Dose accumulation uncertainties***

Volumetric assessment of the dose and reporting of dose volume histogram (DVH) param-

eters is recommended by the Fédération Internationale de Gynécologie et d'Obstétrique (FIGO).<sup>18,19</sup> Because DVH parameters do not convey 3D information, it could be beneficial to investigate the total 3D dose distribution when assessing the effect of uncertainties. Deformable image registration (DIR) can be used to account for changes in anatomy and to construct deformation vector fields with which doses can be accumulated in the same frame of reference. This method shall henceforth be referenced to as *deformable dose accumulation*. Assessment of the 3D delivered dose distribution could improve the estimation of dose response relationships. Additionally, planning decisions can be based on an estimation of the previously delivered 3D dose distribution.

It depends on the type of organ and DVH parameter to be assessed if deformable dose addition can be expected to have added value, as well as on the planning and treatment protocol. Due to increased survival, cervical cancer radiotherapy is moving towards increased OAR sparing, attempting to reduce late toxicities to the bladder, rectum, sigmoid, bowel and vagina. We focused on dose accumulation for bladder and rectum. Based on the cumulative DVH parameters, we concluded that the planned dose from EBRT can be considered uniform near the location of the brachytherapy boost. This means that at least for bladder and rectum it is not necessary to accumulate the dose from EBRT and BT with DIR and that it is accurate enough for the current clinical practice to just assume the prescription dose was delivered to the OAR. The same was shown for the delivered dose from EBRT. Thus, using the ICRU formalism leads to small additional uncertainty for the estimated total dose of EBRT and BT. Additionally, for patients treated with an adaptive planning strategy during EBRT we did not see a difference between DVH parameters calculated with the ICRU formalism and with deformable dose accumulation. This means that the ICRU recommendations about dose summation regarding EBRT still need to be followed.

Assessment of cumulative  $D_{2\text{cm}^3}$  from multiple brachytherapy fractions might benefit from deformable dose accumulation. However, there is the risk of introducing new errors due to incorrect deformable registration. For brachytherapy doses with high gradients this could lead to large errors. In this thesis we used a structure-guided DIR algorithm to register the bladder and rectum contours, and then used the resulting vector fields to accumulate the 3D brachytherapy dose. Our results show that at least for this deformable registration algorithm the expected errors on relevant OAR DVH parameters can be as large as 8 Gy. For the target, it is even more difficult to register with high quality with this algorithm, because inside the structure there will be large voxel-to-voxel errors. In a study by Jamema et al. deformable dose accumulation was compared to direct addition for bladder and rectum  $D_{2\text{cm}^3}$  and an average deviation of 2.4% and 5.0% for the total brachytherapy dose was

found, for bladder and rectum, respectively.<sup>20</sup> It is difficult to predict the extent of uncertainties stemming from incorrect deformable image registration, while uncertainties due to simple parameter addition are small compared to the other uncertainties in brachytherapy planning which were discussed previously. In the research described in this thesis, effects of anatomical movement between PDR pulses, or intra-application motion, on the estimated brachytherapy dose were not taken into account, nor were contouring variations. Intra-application motion may be substantial for PDR treatment since the treatment time is approximately 24 hours. Deformable dose accumulation, as well as simple parameter addition, could either underestimate or overestimate the delivered  $D_{2\text{cm}^3}$  from multiple BT fractions, since the volume that receives the highest dose from brachytherapy may move either closer or farther away from the planned brachytherapy boost. Therefore, deformable dose accumulation should be avoided for brachytherapy until better methods are available.

Deformable dose accumulation in other OARs such as the sigmoid, bowel and the vagina were not analyzed, while moderate toxicity has been reported for vagina.<sup>21–23</sup> Acute gastro-intestinal toxicity is a common side effect of radiotherapy, and possibly doses to the sigmoid and bowel may be predictive.<sup>24</sup> As opposed to the bladder and rectum, it is to be expected for the sigmoid that the EBRT dose is not uniform and equal to the prescription dose near the brachytherapy boost. Unfortunately, the DIR method we applied in this thesis focuses on minimizing the distance between closest points on the contour and is therefore unsuitable for curved structures such as the sigmoid. The sigmoid registration could be improved by incorporating a biomechanical model in the deformable registration algorithm describing the motility of (part of) the bowel, but creating a model to predict bowel motility is difficult.<sup>25,26</sup> Efforts have been made to quantify bowel motility using deformable registration of dynamic in vivo MRI data sets.<sup>26,27</sup> However, dynamic MRI is not performed during the brachytherapy procedure, and the motion pattern that is captured at another time might not be representative of the motion pattern during brachytherapy. As of yet, no studies investigating bowel motility during radiotherapy have been published.

To assess the toxicity to OAR from combined EBRT and BT, typical DVH parameters to consider are the doses to small volumes which will receive a high dose, such as the  $D_{2\text{cm}^3}$ .<sup>28,29</sup> In this thesis, the effect of deformable dose accumulation was only investigated for bladder or rectum  $D_{2\text{cm}^3}$  and  $D_{1\text{cm}^3}$ . Since DVH parameters for high dose volumes are calculated based on the dose to a very small volume, dose accumulation with DIR could improve the estimation of this parameter. However, incorrect DIR will have a large impact on the estimated dose, as we show in chapter 6. Other parameters that we could have considered are the mean dose and parameters in the form of  $V_d$ , the volume receiving a dose  $d$ . These

parameters are also used to assess organ toxicity in combined EBRT and BT.<sup>9</sup> With the dose accumulation method used in this thesis, dose voxels are only warped within the contours of the organ. Therefore, the mean dose will not be any different whether simple parameter addition is used or deformable dose accumulation. In general, for estimation of the mean dose not much benefit can be expected of deformable dose accumulation.<sup>9</sup> For parameters describing the dose to a volume, it depends on the size of the volume if deformable dose accumulation can be expected to improve the estimation of the parameter. Similarly to high dose volume parameters such as the  $D_{2\text{cm}^3}$ , potential errors in DIR will have a large effect on volume parameters describing a small volume within a structure.

Although dose accumulation may improve estimation of specific DVH parameters, it is associated with large uncertainties. This is both the case for accumulating EBRT and BT doses in the sigmoid, and for accumulating BT doses of multiple fractions in the rectum (chapter 6). Unfortunately, when the uncertainties due to dose accumulation with DIR are limited, it is not necessary, as is the case for the accumulated EBRT and BT bladder and rectum dose.

Therefore we conclude that for the present imaging techniques and treatment techniques there is no reason to deviate from the ICRU recommendations concerning dose summation.

### ***Implications of this research for future cervical cancer radiotherapy***

In the near future, radiotherapy can be delivered with a higher precision now that technologies such as MR-guided external beam radiotherapy are becoming available. With high precision techniques delivery uncertainties are reduced, which will lead to a smaller planning margins and more conformal planned EBRT doses. The ICRU assumption that the EBRT dose is uniform near the OARs will then need to be re-evaluated. However, to warp doses with a steep gradient it is necessary to develop more reliable deformable image registration algorithms. Possibly, models can be developed for deformable image registration that take into account biomechanical properties. Verification of the model used in the registration is necessary, for example with anatomical landmarks or fiducial markers. 3 T MRI can be used for applicator reconstruction and the acquisition of  $B_0$  maps should become a standard part of the QA for brachytherapy planning with MRI.

This thesis focused on a combined modality radiotherapy approach for cervical cancer, in which brachytherapy was an essential part of the treatment. We expect our results to remain relevant, since this treatment strategy has proven to be very effective with high survival rates. With the combined treatment, the edges of the target volume receive a dose of at least 85-90 Gy<sub>EDD2</sub>, but a central region receives a very high dose of >120 Gy<sub>EQD2</sub>. A more

conformally planned EBRT field may have the benefit of reducing dose to OAR close to the target, but this does not mean that this type of EBRT boost can replace the brachytherapy. It may be dangerous to exclude brachytherapy from the treatment, because the high local control may be obtained due to the high dose delivered to the central region of the target.<sup>30,31</sup> Earlier studies have shown that reducing or omitting brachytherapy results in poorer survival rates and higher complication rates.<sup>32,33</sup> Therefore, it is to be expected that brachytherapy will remain an essential part of the radiation treatment and that assessing the total 3D dose from the whole treatment will become an even more important topic in the future.

## References

- [1] Kirisits C, Rivard MJ, Baltas D, Ballester F, De Brabandere M, van der Laarse R, et al. Review of clinical brachytherapy uncertainties: analysis guidelines of GEC-ESTRO and the AAPM. *Radiother Oncol* 2014;110:199–212.
- [2] Nesvacil N, Tanderup K, Lindegaard JC, Pötter R, Kirisits C. Can reduction of uncertainties in cervix cancer brachytherapy potentially improve clinical outcome? *Radiother Oncol* 2016;120:390–6.
- [3] Nesvacil N, Tanderup K, Hellebust TP, De Leeuw A, Lang S, Mohamed S, et al. A multicentre comparison of the dosimetric impact of inter- and intra-fractional anatomical variations in fractionated cervix cancer brachytherapy. *Radiother Oncol* 2013;107:20–5.
- [4] Tanderup K, Nesvacil N, Pötter R, Kirisits C. Uncertainties in image guided adaptive cervix cancer brachytherapy: impact on planning and prescription. *Radiother Oncol* 2013;107:1–5.
- [5] Tanderup K, Hellebust TP, Lang S, Granfeldt J, Pötter R, Lindegaard JC, et al. Consequences of random and systematic reconstruction uncertainties in 3D image based brachytherapy in cervical cancer. *Radiother Oncol* 2008;89:156–63.
- [6] Hellebust TP, Tanderup K, Lervåg C, Fidarova E, Berger D, Malinen E, et al. Dosimetric impact of interobserver variability in MRI-based delineation for cervical cancer brachytherapy. *Radiother Oncol* 2013;107:13–9.
- [7] De Leeuw AAC, Moerland MA, Nomden C, Tersteeg RHA, Roesink JM, Jürgenliemk-Schulz IM. Applicator reconstruction and applicator shifts in 3D MR-based PDR brachytherapy of cervical cancer. *Radiother Oncol* 2009;93:341–6.
- [8] Nesvacil N, Tanderup K, Lindegaard JC, Pötter R, Kirisits C. Can reduction of uncertainties in cervix cancer brachytherapy potentially improve clinical outcome? *Radiother Oncol* 2016;120:390–6.
- [9] International Commission on Radiation Units and Measurements. Prescribing, Recording, and Reporting Brachytherapy for Cancer of the Cervix (ICRU report 89). vol. 13. 2013.
- [10] Haack S, Nielsen SK, Lindegaard JC, Gelineck J, Tanderup K. Applicator reconstruction in MRI 3D image-based dose planning of brachytherapy for cervical cancer. *Radiother Oncol* 2009;91:187–93.
- [11] Kim Y, Muruganandham M, Modrick JM, Bayouth JE. Evaluation of artifacts and distortions of titanium applicators on 3.0-tesla MRI: Feasibility of titanium applicators in MRI-guided brachytherapy for gynecological cancer. *Int J Radiat Oncol Biol Phys* 2011;80:947–55.
- [12] Groenendaal G, Moman MR, Korporaal JG, van Diest PJ, van Vulpen M, Philippens MEP, et al. Validation of functional imaging with pathology for tumor delineation in the prostate. *Radiother Oncol* 2010;94:145–50.
- [13] Haack S, Kallehauge JF, Jespersen SN, Lindegaard JC, Tanderup K, Pedersen

- EM. Correction of diffusion-weighted magnetic resonance imaging for brachytherapy of locally advanced cervical cancer. *Acta Oncol* 2014;53:1073–8.
- [14] Jürgenliemk-Schulz IM, Tersteeg RJHA, Roesink JM, Bijmolt S, Nomden CN, Moerland MA, et al. MRI-guided treatment-planning optimisation in intracavitary or combined intracavitary/interstitial PDR brachytherapy using tandem ovoid applicators in locally advanced cervical cancer. *Radiother Oncol* 2009;93:322–30.
- [15] Nomden CN, de Leeuw AAC, Moerland MA, Roesink JM, Tersteeg RJHA, Jürgenliemk-Schulz IM. Clinical Use of the Utrecht Applicator for Combined Intracavitary/Interstitial Brachytherapy Treatment in Locally Advanced Cervical Cancer. *Int J Radiat Oncol* 2012;82:1424–30.
- [16] Shi D, He M-Y, Zhao Z-P, Wu N, Zhao H-F, Xu Z-J, et al. Utrecht Interstitial Applicator Shifts and DVH Parameter Changes in 3D CT-based HDR Brachytherapy of Cervical Cancer. *Asian Pac J Cancer Prev* 2015;16:3945–9.
- [17] Lang S, Nesvacil N, Kirisits C, Georg P, Dimopoulos JCA, Federico M, et al. Uncertainty analysis for 3D image-based cervix cancer brachytherapy by repetitive MR imaging: Assessment of DVH-variations between two HDR fractions within one applicator insertion and their clinical relevance. *Radiother Oncol* 2013;107:26–31.
- [18] Haie-Meder C, Pötter R, Van Limbergen E, Briot E, De Brabandere M, Dimopoulos J, et al. Recommendations from Gynaecological (GYN) GEC-ESTRO Working Group (I): concepts and terms in 3D image based 3D treatment planning in cervix cancer brachytherapy with emphasis on MRI assessment of GTV and CTV. *Radiother Oncol* 2005;74:235–45.
- [19] Pötter R, Haie-Meder C, Van Limbergen E, Barillot I, De Brabandere M, Dimopoulos J, et al. Recommendations from gynaecological (GYN) GEC ESTRO working group (II): concepts and terms in 3D image-based treatment planning in cervix cancer brachytherapy-3D dose volume parameters and aspects of 3D image-based anatomy, radiation physics, radiobiology. *Radiother Oncol* 2006;78:67–77.
- [20] Jamema S V, Mahantshetty U, Andersen E, Noe KØ, Sørensen TS, Kallehauge JF, et al. Uncertainties of deformable image registration for dose accumulation of high-dose regions in bladder and rectum in locally advanced cervical cancer. *Brachytherapy* 2015;15:953–62.
- [21] Kirchheiner K, Fidarova E, Nout RA, Schmid MP, Sturdza A, Wiebe E, et al. Radiation-induced morphological changes in the vagina. *Strahlentherapie Und Onkol* 2012;188:1010–9.
- [22] Kirchheiner K, Nout RA, Tanderup K, Lindegaard JC, Westerveld H, Haie-Meder C, et al. Manifestation Pattern of Early-Late Vaginal Morbidity After Definitive Radiation (Chemo)Therapy and Image-Guided Adaptive Brachytherapy for Locally Advanced Cervical Cancer: An Analysis From the EMBRACE Study. *Int J Radiat Oncol* 2014;89:88–95.
- [23] Kirchheiner K, Nout RA, Lindegaard JC, Haie-Meder C, Mahantshetty U,



- Segedin B, et al. Dose–effect relationship and risk factors for vaginal stenosis after definitive radio(chemo)therapy with image-guided brachytherapy for locally advanced cervical cancer in the EMBRACE study. *Radiother Oncol* 2016;118:160–6.
- [24] Limkin EJ, Dumas I, Rivin del Campo E, Chargari C, Maroun P, Annède P, et al. Vaginal dose assessment in image-guided brachytherapy for cervical cancer: Can we really rely on dose-point evaluation? *Brachytherapy* 2016;15:169–76.
- [25] Du P, Paskaranandavadivel N, Angeli TR, Cheng LK, O’Grady G. The virtual intestine: in silico modeling of small intestinal electrophysiology and motility and the applications. *Wiley Interdiscip Rev Syst Biol Med* 2016;8:69–85.
- [26] Menys A, Hamy V, Makanyanga J, Hoad C, Gowland P, Odille F, et al. Dual registration of abdominal motion for motility assessment in free-breathing data sets acquired using dynamic MRI. *Phys Med Biol* 2014;59:4603–19.
- [27] Odille F, Menys A, Ahmed A, Punwani S, Taylor SA, Atkinson D. Quantitative assessment of small bowel motility by nonrigid registration of dynamic MR images. *Magn Reson Med* 2012;68:783–93.
- [28] Georg P, Lang S, Dimopoulos JCA, Dörr W, Sturdza AE, Berger D, et al. Dose-volume histogram parameters and late side effects in magnetic resonance image-guided adaptive cervical cancer brachytherapy. *Int J Radiat Oncol Biol Phys* 2011;79:356–62.
- [29] Kirisits C, Pötter R, Lang S, Dimopoulos J, Wachter-Gerstner N, Georg D. Dose and volume parameters for MRI-based treatment planning in intracavitary brachytherapy for cervical cancer. *Int J Radiat Oncol* 2005;62:901–11.
- [30] Al Feghali KA, Elshaikh MA. Why brachytherapy boost is the treatment of choice for most women with locally advanced cervical carcinoma? *Brachytherapy* 2016;15:191–9.
- [31] Tanderup K, Eifel PJ, Yashar CM, Pötter R, Grigsby PW. Curative Radiation Therapy for Locally Advanced Cervical Cancer: Brachytherapy Is NOT Optional. *Int J Radiat Oncol* 2014;88:537–9.
- [32] Lanciano RM, Won M, Coia LR, Hanks GE. Pretreatment and treatment factors associated with improved outcome in squamous cell carcinoma of the uterine cervix: A final report of the 1973 and 1978 patterns of care studies. *Int J Radiat Oncol* 1991;20:667–76.
- [33] Logsdon MD, Eifel PJ. FIGO IIIB squamous cell carcinoma of the cervix: an analysis of prognostic factors emphasizing the balance between external beam and intracavitary radiation therapy. *Int J Radiat Oncol* 1999;43:763–75.



# Summary

## Multi-modality radiotherapy in cervical cancer: impact on the 3D dose distribution

Cervical cancer is the fourth most common cancer in the world, and the sixth most common in the Netherlands with 847 new cases in 2016. For locally-advanced cervical cancer, concurrent radiotherapy and chemotherapy is the standard of care. The radiation treatment typically combines external beam radiotherapy (EBRT) with a magnetic resonance image (MRI)-guided brachytherapy (BT) boost to the tumor area in one or multiple applications using an intracavitary/interstitial applicator with needles if needed. Many uncertainties affect the estimated cumulative 3D dose distribution from combined radiotherapy, leading to errors in the expected tumor control and normal tissue complication probability. This thesis focuses on uncertainties related to MRI distortions and on dose accumulation uncertainties for the combined dose of EBRT and BT.

Brachytherapy planning may benefit from high field MRI because of increased signal to noise and the possibility to obtain functional images. However, high field scanners ( $>1.5$  T) are associated with increased image distortion due to inhomogeneity in the main magnetic field ( $B_0$ ). Geometric uncertainties near the applicator could lead to an incorrect reconstruction of the applicator, which leads to uncertainties in the dose distribution and the delivery of unintended dose to the OARs. **Chapter 2** describes an MRI-only method to quantify these distortions. MR images of the Utrecht Interstitial CT/MR applicator at a field strength of 3 T were acquired of a phantom suspending the applicator in water and in four patients. The MR-only method comprised 1) measuring a map of the  $B_0$  inhomogeneity and calculating the displacements, and 2) matching the cross section of the intrauterine device on scans acquired using opposing readout directions. According to the  $B_0$  field map method, the displacement of the Utrecht applicator in the phantom and in the patients was smaller than the pixel size (0.75 mm) of the  $T_2$ -weighted turbo spin echo (TSE) scans in our clinical scanning protocols. The results of our study therefore suggested that for the Utrecht applicator patient movement has a larger impact on treatment uncertainty than susceptibility artifacts.

This work was extended in **chapter 3**. For eleven cervical cancer patients the dosimetric implications of image distortions caused by  $B_0$  inhomogeneity at 3 T MRI were quantified. Using the MRI-only method, we found that displacements of the applicator on  $T_2$ -weighted TSE scans were small ( $<0.75$  mm) and that the dosimetric impact was limited. Combined with **chapter 2**, the results of **chapter 3** indicate that the uncertainty related to image distortions from  $B_0$  inhomogeneity at 3 T has a limited impact on the dose distribution and that accurate reconstruction of the plastic Utrecht Interstitial CT/MR applicator with plastic needles can be performed at 3 T MRI in clinical practice.

To evaluate the cumulative bladder and rectum dose of EBRT and BT, the International Commission on Radiation Units and Measurements (ICRU) recommends that the EBRT dose to the organs at risk should be considered uniform and equal to the prescription dose. This means that the EBRT prescription dose and the BT dose-volume histogram (DVH) parameters can simply be added, denoted as the uniform dose (UD) method. However, intensity-modulated radiotherapy (IMRT) and volumetric-modulated arc therapy (VMAT), as well as adaptive EBRT strategies such as plan-of-the-day strategies, are being used increasingly to create highly conformal dose distributions. Possibly, the delivered dose from EBRT to OAR is non-uniform near the location of the planned BT boost, causing the estimated cumulative dose the  $2\text{ cm}^3$  volume with the highest planned dose ( $D_{2\text{cm}^3}$ ) to be inaccurate at the time of brachytherapy planning. Alternatively, a number of previous investigations evaluated cumulative doses by assuming overlapping high dose volumes for both treatments, denoted as the overlapping high dose (OHD) method. **Chapter 4** describes an investigation of the accumulated planned BT and EBRT 3D doses by calculating cumulative DVH parameters in the bladder and rectum using structure-based DIR. This was compared to the UD and OHD method. The UD method provided a better estimate of bladder and rectum  $D_{2\text{cm}^3}/D_{1\text{cm}^3}$  than the OHD method. For the planned EBRT and BT dose distribution, there was no added value of DIR since differences with direct addition methods were not clinically significant. We concluded that planned EBRT dose distributions can be considered uniform in bladder and rectum for brachytherapy planning purposes.

At the time of BT planning, the delivered EBRT dose may vary from planned dose due to daily positioning variability and daily variation in organ filling. In **chapter 5** we describe a study in which we accumulated the delivered dose distribution of EBRT and the planned BT dose distribution using DIR. All patients were treated with a plan-of-the-day strategy. For ten patients the delivered VMAT/IMRT EBRT dose was calculated using the daily anatomy from the CBCT scans acquired prior to irradiation. The CBCT of the first EBRT fraction and the BT planning MRI were registered using DIR. Cumulative bladder/rectum  $D_{2\text{cm}^3}$

from EBRT and BT was calculated and compared to the UD method. The total EBRT+BT dose calculated with DIR was at most 104% of the dose calculated with the UD method and differences between UD and DIR were small ( $<3.9 \text{ Gy}_{\text{EQD2}}$ , in biologically equivalent dose in 2 Gy per fraction). Based on the results of this study, we concluded that even for patient treated with a plan-of-the-day strategy, the delivered EBRT dose near the planned BT boost can be considered uniform for the evaluation of bladder/rectum  $D_{2\text{cm}^3}$ .

For the evaluation of the cumulative rectum dose of multiple BT applications the ICRU recommends to assume that the high dose volumes are at the same location on the rectal wall, meaning that the DVH parameters planned for each application can simply be added. To avoid an inaccurate estimation of the cumulative dose, it may be preferable to sum the 3D dose distributions using DIR. However, little is known about the reliability of DIR for accumulation of the BT dose in the rectum. The BT dose distribution typically has a very steep dose distribution, and low registration accuracy may therefore impact dose accumulation accuracy. In **chapter 6** we investigated dose warping uncertainties in the rectal wall. For ten patients treated with BT the planning images were registered with structure-based DIR. The resulting transformation vectors were used to accumulate the total rectum dose from brachytherapy. A physically realistic model (PRM) describing rectal deformation was used to investigate the dose warping uncertainty. For point pairs on  $\text{rectum}_{\text{BT1}}$  and  $\text{rectum}_{\text{BT2}}$  that were at the same location according to the PRM, the dose for BT1 and BT2 was added ( $D_{\text{PRM}}$ ) and compared to the DIR accumulated dose ( $D_{\text{DIR}}$ ) in the BT2 point. Although DIR corresponded with the PRM for on average 75% of the  $D_{2\text{cm}^3}$  volume, local absolute dose differences and residual distances were large. Our results showed that dose accumulation with this structure-based DIR algorithm is problematic for doses that have steep gradients such as brachytherapy doses.

In **chapter 7** we discuss the consequences of our results for cervical cancer radiotherapy. We state that it is safe to use 3 T MRI scanners for applicator reconstruction during brachytherapy planning since the dosimetric implications of  $B_0$  inhomogeneity induced distortions are limited. For currently available plans, there is no added value of deformable image registration for the evaluation of cumulative EBRT and BT DVH parameters. When adding up the brachytherapy doses of multiple applications, DIR may have added value, but errors were shown to be large for a currently available structure-based DIR algorithm.

With the advent of novel techniques, such as MRI-guided radiotherapy, assessing the 3D dose distribution will become more important. For these new techniques with a high gradient dose distribution, it may be necessary to evaluate the cumulative dose using DIR. How-

ever, for the accumulation of 3D dose distributions with very steep gradients new DIR algorithms/strategies need to be developed that take into account biomechanical properties.

# Samenvatting

## Gecombineerde radiotherapie voor baarmoederhalskanker: invloed op de 3D-dosisverdeling

Baarmoederhalskanker staat op de vierde plaats wereldwijd van de meest voorkomende vormen van kanker. In Nederland staat het op de zesde plaats met 846 nieuwe gevallen in 2016. De behandeling van lokaal gevorderd cervix carcinoom bestaat uit een combinatie van radiotherapie en chemotherapie. Uitwendige radiotherapie wordt gecombineerd met een extra dosis met brachytherapie op de tumor. De brachytherapie wordt gepland op magnetic resonance imaging (MRI) scans. Er wordt een intracavitair/interstitiële applicator ingebracht, waarbij naalden kunnen worden gebruikt om tot een optimale dosisverdeling te komen. Onzekerheden in de totale afgeleverde dosis van uitwendige radiotherapie en brachytherapie kunnen leiden tot een lagere tumor dosis en tot complicaties in het gezonde weefsel. In deze thesis hebben we twee oorzaken van onzekerheid onderzocht: vervormingen op de MR beelden en het optellen van de totale dosis van zowel uitwendige radiotherapie als brachytherapie.

Het gebruik van MRI scanners met een hoge veldsterkte zou kunnen leiden tot een kwaliteitsverbetering van de behandelingsplannen van brachytherapie, omdat deze een hogere signaal-ruisverhouding bieden en bij hogere veldsterkte functionele imaging mogelijk is. Een hogere veldsterkte ( $>1.5$  T) gaat echter vaak samen met vervormingen van het beeld ten gevolge van de inhomogeniteit van het magnetisch veld in de scanner ( $B_0$ ). Beeldvervalsingen nabij de applicator kunnen ertoe leiden dat de reconstructie van de applicator op MR beelden incorrect is. In **Hoofdstuk 2** beschrijven we een methode waarbij we alleen MR beelden gebruiken om deze beeldvervalsingen te bepalen. We maakten MR beelden van de Utrecht interstitiële CT/MRI applicator bij een MRI veldsterkte van 3 T, in een fantoom dat gevuld was met water. We herhaalden deze meting in vier patiënten met baarmoederhalskanker. Onze MRI-meting bestond uit 1) het meten van een kaart van de inhomogeniteit van het  $B_0$ -veld, waaruit de lokale verplaatsing kon worden berekend, en 2) een rigide registratie van de doorsnedes van de intra-uteriene staaf. Voor deze laatste stap gebruikten we scans die met een tegengestelde MRI-uitlees-gradiënt zijn gemaakt. Volgens

de  $B_0$ -kaart waren in het fantoom en in patiënten lokale verplaatsingen op en nabij de applicator kleiner dan de pixelgrootte (0.75 mm) van de  $T_2$ -gewogen turbo spin echo (TSE) scans van het klinische scan protocol. Hieruit concludeerden we dat voor deze applicator susceptibiliteitsartefacten nauwelijks invloed hebben op de reconstructie-onzekerheid in vergelijking met patiëntbeweging.

In **Hoofdstuk 3** hebben we elf patiënten met hetzelfde MRI protocol gescand. Het doel van deze studie was de dosimetrische implicaties van beeldvervalsingen door  $B_0$ -inhomogeniteit op 3 T-MRI te onderzoeken. Lokale verplaatsingen van de applicator op  $T_2$ -gewogen scans waren klein ( $<0.75$  mm) en hadden weinig invloed op de dosis. De resultaten beschreven in hoofdstuk 2 en 3 laten zien dat beeldvervalsingen door  $B_0$ -inhomogeniteit op 3 T nauwelijks invloed hadden op de dosisverdeling. We concluderen hieruit dat het mogelijk is in de kliniek de plastic Utrecht interstitiële CT/MRI applicator met plastic naalden te reconstrueren voor 3 T-MRI.

Voor het berekenen van de cumulatieve blaas en rectum dosis van uitwendige radiotherapie en brachytherapie adviseert de International Commission on Radiation Units and Measurements (ICRU) aan te nemen dat de dosisverdeling van uitwendige radiotherapie uniform is en gelijk aan de voorgeschreven dosis. Uit deze aannames volgt dat de prescriptie-dosis van uitwendige radiotherapie en de dose-volume histogram (DVH) parameters van brachytherapie simpelweg bij elkaar op kunnen worden geteld. Deze methode wordt hier aangeduid als de Uniforme Dosis (UD) methode. Tegenwoordig worden vaak intensiteits-gemoduleerde radiotherapie en adaptieve plan-strategieën gebruikt voor uitwendige radiotherapie, hetgeen leidt tot een dosisverdeling die veel strakker de vorm van het doelgebied volgt. Daardoor is het mogelijk dat de afgeleverde dosis van uitwendige radiotherapie op de gezonde organen niet langer uniform is in de buurt van geplande brachytherapieboost. Dit zou ervoor kunnen zorgen dat de UD methode leidt tot fouten in de geschatte cumulatieve  $D_{2\text{cm}^3}$  ten tijde van de brachytherapieplanning. In een aantal eerdere studies is de cumulatieve dosis berekend door aan te nemen dat de het volume met de hoogste dosis overlapt voor uitwendige radiotherapie en brachytherapie, de Overlappende Hoge Dosis (OHD) methode. In **Hoofdstuk 4** is de geplande totale dosis berekend voor blaas en rectum met behulp van structuur-gebaseerde deformeerbare beeldregistratie (DBR). We vergeleken dit met de UD en OHD methode. Hier bleek uit dat de UD methode de beste afschatting maakte van de  $D_{2\text{cm}^3}/D_{1\text{cm}^3}$  in blaas en rectum, vergeleken met de OHD methode. Omdat er geen verschil is tussen DBR en methodes waarbij direct wordt opgeteld concludeerden we dat het voor de geplande dosis van uitwendige radiotherapie en brachytherapie niet nodig is om structuur-gebaseerde DBR te gebruiken voor het berekenen van de cumulatieve dosis.



De geleverde uitwendige radiotherapie dosis verschilt mogelijk van de geplande dosis door variatie in de dagelijkse positionering en orgaanbeweging. In **Hoofdstuk 5** wordt beschreven hoe we de geleverde dosis van uitwendige radiotherapie en de geplande dosis van brachytherapie hebben opgeteld met behulp van DBR. Alle patiënten in deze studie werden behandeld met een adaptieve plan-van-de-dag strategie. Voor alle tien patiënten berekenden we de geleverde dosis van uitwendige radiotherapie met behulp van de CBCT scans van elke fractie. De CBCT van de eerste fractie en de MRI waarop de brachytherapieboost werd gepland werden geregistreerd met behulp van DBR. De cumulatieve blaas/rectum  $D_{2\text{cm}3}$  van uitwendige radiotherapie en brachytherapie werden berekend en vervolgens vergeleken met de UD methode. De totale dosis van uitwendige radiotherapie en brachytherapie berekend met DBR was hooguit 104% van de UD berekende dosis, en verschillen tussen UD en DBR waren klein ( $<3.9 \text{ Gy}_{\text{EQD2}}$ , in biologisch equivalente dosis in 2 Gy per fractie). De conclusie van deze studie was dat, ook voor patiënten bestraald met een plan-van-dag, de geleverde dosis van uitwendige radiotherapie in de buurt van de geplande brachytherapieboost uniform is.

Voor het optellen van de doses van meerdere brachytherapie-applicaties adviseert de ICRU aan te nemen dat hoge-dosisvolumes binnen de rectale wand op dezelfde plek zitten voor elke applicatie. Dit betekent dat geplande DVH-parameters van elke applicatie direct opgeteld kunnen worden. Om fouten in de cumulatieve dosis te vermijden is het mogelijk beter om de 3D-dosisverdelingen op te tellen. Er is echter weinig bekend over de betrouwbaarheid van DBR wanneer het gebruikt wordt voor het optellen van de dosis van brachytherapie in het rectum. De dosisverdeling van brachytherapie wordt gekenmerkt door een hoge gradiënt, waardoor fouten in de registratie een grote impact kunnen hebben op de nauwkeurigheid van de dosisoptelling. In **Hoofdstuk 6** onderzochten we onzekerheden bij het vervormen van de dosis in de rectale wand voor patiënten die met twee brachytherapie-applicaties worden behandeld. Voor elke applicatie werd een nieuw behandelingsplan gemaakt. Voor tien patiënten werden de beelden, gemaakt voor de behandelingsplanning, geregistreerd met behulp van structuur-gebaseerde DBR. De transformatie matrix werd vervolgens gebruikt om de totale rectumdosis van brachytherapie op te tellen. De onzekerheid in het optellen van de doses werd onderzocht met behulp van een model dat vervorming van de rectumwand beschrijft (het rectum model of RM). Voor puntparen op  $\text{rectum}_{\text{BT1}}$  en  $\text{rectum}_{\text{BT2}}$  die op dezelfde locatie lagen volgens het RM, werd de punt dosis opgeteld ( $D_{\text{RM}}$ ) en vergeleken met de dosis die was opgeteld met behulp van DBR ( $D_{\text{DBR}}$ ). Het  $D_{2\text{cm}3}$  volume van RM en DBR overlapte voor 75%, maar absolute dosis verschillen tussen RM en DBR waren groot. Uit onze resultaten bleek dat dit structuur-gebaseerde

registratiealgoritme beter niet gebruikt kan worden om de dosis op te tellen voor doses met een hoge gradiënt, zoals de dosis van brachytherapie.

In **Hoofdstuk 7** hebben we onze resultaten besproken in het kader van radiotherapie voor baarmoederhalskanker. Uit onze resultaten volgt dat het veilig is om 3 T-MRI scanners te gebruiken voor reconstructie van de applicator tijdens het plannen van de brachytherapie, omdat de  $B_0$ -inhomogeniteit nauwelijks effect op de dosis heeft bij deze veldsterkte. Met de huidige planningstechnieken is het niet nodig om DBR te gebruiken bij het optellen van dosisverdelingen van uitwendige radiotherapie en brachytherapie. Het zou kunnen dat DBR wel nodig is voor het optellen van de dosis van meerdere brachytherapie-applicaties, maar in deze thesis hebben we voor een structuur-gebaseerde deformeerbare beeldregistratie-algoritme laten zien dat onzekerheden te groot zijn.

Met de komst van nieuwe technieken zoals MRI-gestuurde radiotherapie zal het belangrijker worden om de 3D-dosisverdeling te evalueren. Deze dosisverdelingen worden gekenmerkt door een hoge gradiënt met een sterke afval van de hoge dosis buiten het doelgebied. Hierdoor zal het mogelijk nodig zijn om de totale dosis te evalueren met behulp van DBR. Om dosisverdelingen met een hoge gradiënt op een correcte manier op te tellen, moeten nieuwe deformeerbare beeldregistratie-algoritmes worden ontwikkeld op basis van de beschikbare biomechanische informatie.

# List of Publications

## List of Publications

### *Peer reviewed scientific articles*

Crezee J, van Leeuwen CM, Oei AL, **van Heerden LE**, Bel A, Stalpers LJA, Ghadjar P, Franken NAP, Kok HP. Biological modelling of the radiation dose escalation effect of regional hyperthermia in cervical cancer. *Radiat Oncol* 2016;11:14.

**van Heerden LE**, Gurney-Champion OJ, van Kesteren Z, Houweling AC, Koedooder C, Rasch CRN, Pieters BR, Bel A. Quantification of image distortions on the Utrecht interstitial CT/MR brachytherapy applicator at 3T MRI. *Brachytherapy* 2016;15:118–26.

**van Heerden LE**, Houweling AC, Koedooder C, van Kesteren Z, van Wieringen N, Rasch CRN, Pieters BR, Bel A. Structure-based deformable image registration: Added value for dose accumulation of external beam radiotherapy and brachytherapy in cervical cancer. *Radiother Oncol* 2017;123:319–24. 3.015.

**van Heerden LE**, van Kesteren Z, Gurney-Champion OJ, Houweling AC, Koedooder C, Rasch CRN, Pieters BR, Bel A. Image Distortions on a Plastic Interstitial Computed Tomography/Magnetic Resonance Brachytherapy Applicator at 3 Tesla Magnetic Resonance Imaging and Their Dosimetric Impact. *Int J Radiat Oncol* 2017;99:710–8.

**van Heerden LE**, van Wieringen N, Koedooder C, Rasch CRN, Pieters BR, Bel A. Dose warping uncertainties for the accumulated rectal wall dose in cervical cancer brachytherapy. *Brachytherapy* 2018;17:449–55.

**van Heerden LE**, Visser J, Koedooder C, Rasch CRN, Pieters BR, Bel A. Role of deformable image registration for delivered dose accumulation of adaptive external beam radiation therapy and brachytherapy in cervical cancer. *J Contemp Brachytherapy* 2018;10:542–50.

### *Conference abstracts*

**van Heerden LE**, Gurney-Champion OJ, Van Kesteren Z, Pieters BR, Bel A. OC-0093: Quantification of deformations on 3T MRI for the Utrecht Interstitial CT/MR brachytherapy applicator. *Radiother Oncol* 2015;115:S47.

van Wieringen N, **van Heerden LE**, Gurney-Champion OJ, van Kesteren Z, Houweling AC,

Pieters BR, Bel A. SU-E-J-216: A Sequence Independent Approach for Quantification of MR Image Deformations From Brachytherapy Applicators. *Med Phys* 2015;42:3315–3315.

**van Heerden LE**, Houweling AC, Koedooder C, van Kesteren Z, Rasch CRN, Pieters BR, Bel A. Potential Added Value of Structure-Based Deformable Image Registration for Dose Accumulation in External Beam Radiotherapy and Brachytherapy in Cervical Cancer. *Brachytherapy* 2016;15:S36.

**van Heerden LE**, Gurney-Champion OJ, van Kesteren Z, Houweling AC, Koedooder C, Rasch CRN, Pieters BR, Bel A. In Vivo Quantification of Image Distortions on The Utrecht Interstitial CT/MR Brachytherapy Applicator at 3T MRI. *Brachytherapy* 2016;15:S152.

**van Heerden LE**, Van Wieringen N, Koedooder C, Rasch CRN, Pieters BR, Bel A. OC-0360: Dose warping uncertainties for the cumulative rectal wall dose from brachytherapy in cervical cancer. *Radiother Oncol* 2017;123:S192–3.

**van Heerden LE**, Visser J, Koedooder C, Rasch CRN, Pieters BR, Bel A. OC-0174: Deformable image registration for dose accumulation of adaptive EBRT and BT in cervical cancer. *Radiother Oncol* 2018;127:S91.

## PhD portfolio

Name PhD student: Laura Elisabeth van Heerden  
AMC department: Radiation Oncology  
Research school: AMC Graduate School for Medical Sciences  
PhD period: October 2013 – October 2017  
Promotor: Prof. dr. C.R.N. Rasch  
Copromotores: Dr. A. Bel  
Dr. B.R. Pieters

1 ECTS = 28 hours

<b>PhD training</b>	<b>Year</b>	<b>Workload (ECTS)</b>
<i>General courses</i>		
Practical biostatistics	2013	1.1
The AMC world of science	2013	0.7
Scientific writing in English for publication	2013	1.5
<i>Specific courses</i>		
ESTRO course Basic treatment planning	2014	1.5
NvvO course Basic Oncology	2014	1.5
ESTRO course Basic clinical radiobiology	2014	1.5
ESTRO pre-meeting course Adaptive Brachytherapy Strategies	2015	0.4
ESTRO pre-meeting course Medical Physics aspects of particle therapy	2017	0.4

Pre-meeting workshop 6th World Congress of Brachytherapy	2016	0.4
<i>Other courses</i>		
Medical lessons for clinical physicist in training	2014	0.4
Masterclass Spinoza Professor Peter Hoskin	2014	0.3
<i>International conferences</i>		
ESRO 3 <sup>rd</sup> Forum, Barcelona, Spain	2015	1.0
6th World Congress of Brachytherapy, San Francisco, USA	2016	1.0
ESTRO 36, Vienna, Austria	2017	1.0
ESTRO 37, Barcelona, Spain	2018	1.0
<i>National and regional events</i>		
OOA student retreats	2014-2015	2.0
Scientific Days for Radiotherapy Physicists	2013-2017	1.5
GCOA research day, NKI-AvL	2014	0.1
Amsterdam Regional Radiotherapy Evening lectures	2014-2017	0.5
IQ Signal lectures (AMC, VUmc, NKI-AvL)	2016	0.2
<i>Institutional scientific meetings</i>		
Physics staff meetings	2013-2017	
Multidisciplinary staff meetings	2013-2017	
Research meetings	2015-2017	

## *Presentations*

<i>Comparison of the effect of rigid and structure guided deformable registration on the cumulative EBRT and brachytherapy dose for cervical cancer</i> – Oral presentation at the Medical Physicist Meeting, Department of Radiation Oncology, AMC, the Netherlands	2015	0.5
<i>Quantification of deformations on 3T MRI for the Utrecht Interstitial CT/MR brachytherapy applicator</i> - Oral presentation at the 3rd ESTRO Forum, Barcelona, Spain	2015	0.5
<i>Quantification of image distortion on 3T MRI for the Utrecht Interstitial CT/MR brachytherapy applicator</i> – Oral presentation at the Scientific Day for Radiotherapy Physicists, UMCU, the Netherlands	2015	0.5
<i>Quantification of deformations on 3T MRI for the Utrecht Interstitial Fletcher brachytherapy applicator</i> – Poster presentation at the OOA PhD Student Retreat, Renesse, the Netherlands	2015	0.5
<i>Structure-based deformable image registration: added value for dose accumulation of external beam radiotherapy and brachytherapy in cervical cancer?</i> – Oral presentation at the Medical Physicist Meeting, Department of Radiation Oncology, AMC, the Netherlands	2016	0.5
<i>Dose warping uncertainties for the cumulative rectal wall dose from brachytherapy in cervical cancer</i> – Oral presentation at the Multidisciplinary Meeting, Department of Radiation Oncology, AMC, the Netherlands	2016	0.5
<i>Potential Added Value of Structure-Based Deformable Image Registration for Dose Accumulation in External Beam Radiotherapy and Brachytherapy in Cervical Cancer</i> - Snap oral presentation at the 6th World Congress of Brachytherapy	2016	0.5
<i>In Vivo Quantification of Image Distortions on The Utrecht Interstitial CT/MR Brachytherapy Applicator at 3T MRI</i> - Poster presentation at the 6th World Congress of Brachytherapy	2016	0.5

<i>Quantification of dose warping uncertainty for accumulation of the total rectal wall dose from multiple brachytherapy applications in cervical cancer</i> – Oral presentation at the OOA PhD Student Retreat, Renesse, the Netherlands	2016	0.5
<i>Dose warping uncertainties for the cumulative rectal wall dose from brachytherapy in cervical cancer</i> - Oral presentation for the Institute Quantivision Conference	2017	0.5
<i>Dose warping uncertainties for the cumulative rectal wall dose from brachytherapy in cervical cancer</i> - Oral presentation at ESTRO 36, Vienna, Austria	2017	0.5
<i>Dose warping uncertainties for the cumulative rectal wall dose from brachytherapy in cervical cancer</i> – Oral presentation at the Scientific Day for Radiotherapy Physicists, UMCU, the Netherlands	2017	
<i>Dose accumulation of adaptive external beam radiation therapy and brachytherapy in cervical cancer</i> – Oral presentation at the Scientific Day for Radiotherapy Physicists, UMCU, the Netherlands	2017	0.5
<i>Dose accumulation of adaptive external beam radiation therapy and brachytherapy in cervical cancer</i> – Oral presentation at ESTRO 37, Barcelona, Spain	2018	0.5



<b>Teaching and supervising</b>	<b>Year</b>	<b>Workload (ECTS)</b>
L. Gelling, Graduation project, bachelor student Physics from University of Amsterdam	2014	1.0
D. Kelder, Graduation project, bachelor student of Medische Beeldvorming en radiotherapeutische Technieken from Fontys Paramedische hogeschool, The Netherlands	2016	1.0
A. Heijdra, Graduation project, bachelor student of Medische Beeldvorming en radiotherapeutische Technieken from Fontys Paramedische hogeschool, The Netherlands	2016	1.0
<b>Parameters of Esteem</b>	<b>Year</b>	
Junior Brachytherapy Travel grant	2017	
Best Presentation Award, Institute Quantivision Conference	2017	

## Curriculum Vitae

Laura van Heerden was born on March 14<sup>th</sup> in Amsterdam, the Netherlands. She attended the Barlaeus Gymnasium in Amsterdam. She graduated in 2007, after which she started with the bachelor program “Physics and Astronomy” at the University of Amsterdam. After obtaining her bachelor’s degree in 2011, she continued with the master program “Physics”, where she followed the track “Physics of Life and Health”. Her master research project was performed at the radiology department at the Academic Medical Center in Amsterdam. She investigated the feasibility of diffusion tensor imaging of the carotid artery. In 2013, she obtained his master’s degree, after which she started as a PhD student at the department of radiation oncology at the Academic Medical Center. Here, she studied uncertainties in combined radiotherapy for cervical cancer. During her 4 years at the Academic Medical Center, she investigated image distortions on MRI and dose accumulation uncertainties. Her work resulted in this thesis, entitled “Multi-modality radiotherapy in cervical cancer: impact on the 3D dose distribution”. Since the winter of 2017, Laura works as a postdoctoral researcher at Erasmus Medical Center in Rotterdam. She is currently working on electromagnetic tracking for pretreatment dwell-position verification in pelvic brachytherapy.



## Dankwoord

Het promotieonderzoek kent veel leuke momenten, maar ook een aantal hobbels op je pad. Gelukkig zijn er mensen die je onderweg helpen en begeleiden. Ik wil hier een moment nemen om mijn dank te uiten.

Ten eerste wil ik mijn promotor Coen bedanken. Coen, ik heb je ervaren als een betrokken promotor, die tijd en aandacht had voor zijn promotiestudenten. Tijdens de maandelijkse meetings heb ik veel aan je scherpe opmerkingen gehad, maar je wist ook groter te denken wanneer ik zelf vooral met de kleinere details van het huidige onderzoek bezig was.

Arjan, bedankt voor de samenwerking, ik heb erg veel van je geleerd. Bij onze wekelijkse meetings bespraken we uiteraard inhoudelijke zaken, maar je had ook aandacht voor het persoonlijke. Door dit wekelijkse steunpunt heb ik mijn promotie als smooth sailing ervaren. Ook buiten onze wekelijkse meeting kon ik altijd aankloppen voor hulp en feedback, en je maakte zelfs in je vakanties tijd om manuscripten van opmerkingen te voorzien. Ik keek elk jaar uit naar de jaarlijkse barbecues en dit was goede manier om met de hele fysica bij elkaar te komen.

Bradley, jij ook bedankt dat je mijn co-promotor wilt zijn. Je zorgde dat je altijd aanwezig kon zijn bij de maandelijkse meeting of bij proefpraatjes voor conferenties, maar ik kon ook daarbuiten langskomen. Je hebt me erg geholpen bij mijn zoektocht naar klinisch relevante onderzoeksvragen. Je suggestie om naar de World Congress of Brachytherapy te gaan was een gouden tip: ik heb er nieuwe contacten en inspiratie voor verder onderzoek aan overgehouden.

Daarnaast wil ik ook mijn andere co-auteurs bedanken. Kees, bedankt dat je zo vaak aanwezig was bij het maandelijkse overleg, ik heb ruim kunnen profiteren van je ervaring in de brachytherapie. Ook bedankt voor al je tips om een wetenschappelijke tekst coherent en makkelijk leesbaar te maken. Anette, ik heb veel aan je adviezen gehad. Je opmerking, dat de zoektocht naar een goede deformable image registratie methode meer dan een jaar ging kosten, was even schrikken, maar het heeft uiteindelijk beter onderzoek opgeleverd. Niek en Jorrit, bedankt voor de hulp bij het uitvoeren van mijn onderzoek en dat jullie mijn co-auteurs wilden zijn.

Uiteraard wil ook de rest van de klinisch fysici, klinisch fysisch medewerkers, artsen en onderzoekers bedanken voor hun opmerkingen en hulp. In het bijzonder wil ik de laboranten van de brachytherapie bedanken. Jullie hebben altijd heel geduldig mijn vragen

beantwoord en het was ook prettig samenwerken ten tijde van de patient metingen op de MRI. Hierbij werkte ik ook veel met Zdenko samen. Zdenko, voor mij ben jij een man met veel rollen: co-auteur, vriend en nu ook paranimf. Heel erg bedankt voor je samenwerking en advies bij het onderzoeken en schrijven. De kopjes koffie en etentjes bij jou thuis hebben de afgelopen 4 jaar verrijkt. Oliver, ook jij bent een co-auteur en vriend, mede door jou heb ik ontdekt dat ook voor de wetenschap geldt: samen is beter dan alleen. Ook wil ik graag Jan Sijbrands bedanken. Jan, bedankt dat je je zo hebt ingezet bij het ontwikkelen en bouwen van twee meetfantomen. Ik heb het AMC beter leren kennen doordat je mij op sleeptouw nam naar o.a. de 3D printers. Ik heb het erg leuk gevonden mee te kijken in de werkplaats terwijl we luisterden naar Queen.

Other PhD students, thank you for all the great moments. The weekly research meetings were a good way to catch up with everybody's research and to find common solutions. I greatly enjoyed all the drinks as well as the dance moves at the ESTRO. Kleopatra and Peng, it has been great to start all together with you, I wish you all the best in the rest of your careers. I am happy that we are still keeping in touch even after our AMC time ended. Peter, wij hebben in de cervix 'groep' ook fijn samengewerkt. Bedankt voor je idee voor de voorkant van het boekje.

Inger-Karine, bedankt dat ik door kon in de brachytherapie bij het Erasmus Medisch Centrum in Rotterdam en dat je nu in mijn commissie wilt zitten.

Dit onderzoek is uitgevoerd in samenwerking met Elekta Brachytherapy. Ik wil in het bijzonder Yuri bedanken en Joost voor zijn hulp bij het onderzoek met FBDR tool.

Ilja, we waren al vrienden toen ik begon als PhD-student. Het was super een vriendin zo dichtbij te hebben, en door onze kopjes koffie en wandelingen is het AMC heel snel een fijne plek geworden. Dat je nu mijn paranimf bent laat zien hoe betrokken je altijd bent gebleven.

Lieve papa en mama, zonder al jullie steun was het nooit gelukt en ik hoop dat jullie dit ook een leuke dag hebben gevonden. Bij moeilijke momenten was er sowieso altijd een stevig vangnet, en ik wil hierbij dan ook mijn broers en schoonfamilie bedanken.

Maar de belangrijkste bewaar ik voor het laatst. Lieve Jim, ten eerste bedankt voor je hulp bij het voorbereiden van de drukproef. Als 'grote' wetenschapper had je dit allemaal al een keer meegemaakt en herkende je elke typische PhD-student stress: of het nu ging om tegevallende resultaten of papers die terug gestuurd werden, je wist me gerust te stellen dat we hier allemaal last van hadden. Zonder jou zou ik het niet gered hebben, en ik draag het boekje daarom aan je op. Bedankt voor al je steun en liefde.